NASA TECHNICAL NOTE

NASA TN D-8157

NASA TN D-8157 e.1

COMPARISON OF A LINEAR AND A NONLINEAR WASHOUT FOR MOTION SIMULATORS UTILIZING OBJECTIVE AND SUBJECTIVE DATA FROM CTOL TRANSPORT LANDING APPROACHES

Russell V. Parrish and Dennis J. Martin, Jr.

Langley Research Center
Hampton, Va. 23665

NATIONAL AERONAUTICS AND SPACE ADMINISTRATION • WASHINGTON, D. C. • JUNE 1976

1. Report No. NASA TN D-8157	2. Government Accession No.	3. Recipient's Catalog No.
4. Title and Subtitle COMPARISON OF A LINEAR AND A NONLINEAR WASHOUT FOR MOTION SIMULATORS UTILIZING OBJECTIVE AND SUBJECTIVE DATA FROM CTOL TRANSPORT LANDING APPROACHES		5. Report Date June 1976 6. Performing Organization Code
7. Author(s) Russell V. Parrish and Dennis J. Martin, Jr.		8. Performing Organization Report No. L-10593
9. Performing Organization Name and Address NASA Langley Research Center Hampton, Va. 23665		10. Work Unit No. 504-09-41-01 11. Contract or Grant No.
12. Sponsoring Agency Name and Address National Aeronautics and Space Administration Washington, D.C. 20546		13. Type of Report and Period Covered Technical Note 14. Sponsoring Agency Code

15. Supplementary Notes

Dennis J. Martin, Jr.: Electronic Associates, Inc., Hampton, Va.

16. Abstract

Objective and subjective data gathered in the process of comparing a linear and a nonlinear washout for motion simulators reveal that there is no difference in the pilot-performance measurements used during instrument-landing-system (ILS) approaches with a Boeing 737 conventional take-off and landing (CTOL) airplane between fixed-base, linear-washout, and nonlinear-washout operations. However, the subjective opinions of the pilots reveal an important advance in motion-cue presentation. The advance is not in the increased cue available over a linear filter for the same amount of motion base travel but rather in the elimination of false rotational rate cues presented by linear filters.

17. Key Words (Suggested by Author(s)) Landing approach Washout system Coordinated washout Motion-cue evaluation	18. Distribution Statement Unclassified – Unlimited Subject Category 05		
19. Security Classif. (of this report) Unclassified	20. Security Classif. (of this page) Unclassified	21. No. of Pages 81	22. Price* $4.75

*For sale by the National Technical Information Service, Springfield, Virginia 22161

COMPARISON OF A LINEAR AND A NONLINEAR WASHOUT FOR MOTION SIMULATORS UTILIZING OBJECTIVE AND SUBJECTIVE DATA FROM CTOL TRANSPORT LANDING APPROACHES

Russell V. Parrish and Dennis J. Martin, Jr.*
Langley Research Center

SUMMARY

Objective and subjective data gathered in the process of comparing a linear and a nonlinear washout for motion simulators reveal that there is no difference in the pilot-performance measurements used during instrument-landing-system (ILS) approaches with a Boeing 737 conventional take-off and landing (CTOL) airplane between fixed-base, linear-washout, and nonlinear-washout operations. However, the subjective opinions of the pilots reveal an important advance in motion-cue presentation. The advance is not in the increased cue available over a linear filter for the same amount of motion base travel but rather in the elimination of false rotational rate cues presented by linear filters.

INTRODUCTION

Two methods of providing motion cues to a moving-base six-degree-of-freedom airplane simulation are currently available at the Langley Research Center. A linear method, essentially Schmidt and Conrad's coordinated washout (refs. 1 and 2), is documented in reference 3; and a nonlinear method, coordinated adaptive washout, is documented in references 4 and 5.

A comparison of the two methods has been made in which each method was applied to a Boeing 737 conventional take-off and landing (CTOL) airplane by using the Langley visual-motion simulator (refs. 6 and 7). The evaluation process consisted of the collection of objective and subjective data from 135 simulated instrument-landing-system (ILS) approaches, as well as subjective data from standard maneuvering about straight-and-level flight for specific motion-cue evaluation.

This paper will present both the objective and subjective results of this study, although the intended emphasis is on the subjective results, which indicate a significant advance in motion-cue presentation. The significant advancement is not in the increased

*Electronic Associates, Inc., Hampton, Va.

cue available over a linear filter for the same amount of motion-base travel (ref. 5) but rather in the elimination of false rotational cues presented by linear filters.

SYMBOLS

Measurements and calculations were made in U.S. Customary Units. They are presented herein in the International System of Units (SI) with the equivalent values given parenthetically in the U.S. Customary Units.

A,B,C main effects in analysis of variance

AB,AC,BC two factor interactions in analysis of variance

ABC three factor interaction in analysis of variance

A_1,A_2,A_3 acceleration lead parameters for translational channel lag compensation, sec^2

a_1,a_2,a_3 damping parameters for second-order translational washout filters, rad/sec

B_1,B_2,B_3 velocity lead parameters for translational channel lag compensation, sec

b_1,b_2,b_3 frequency parameters for second-order translational washout filters, rad/sec^2

b_x,b_y coefficients for position penalties in cost functions, per sec^4

b_ψ coefficient for yaw-position penalty in cost function, per sec^2

C_1,C_2,C_3 translational acceleration braking parameters, per sec

$\bar{c}$ mean aerodynamic chord, m (ft)

c_x,c_y coefficients for velocity penalties in cost functions, per sec^2

DPR scale factor, deg/rad

d_x,d_y damping parameters for second-order translational washouts, per sec

e_x,e_y frequency parameters for second-order translational washouts, per sec^2

e_ψ parameter for first-order yaw washout, per sec

$f^*_{c,x}, f^*_{c,y}$ body-axis longitudinal and lateral accelerations at centroid location after low-pass filtering, m/sec^2 (ft/sec^2)

$f_{c,z}$ body-axis vertical acceleration (referenced about 1g) at centroid location after high-pass filtering, m/sec^2 (ft/sec^2)

$f_{i,x}, f_{i,y}, f_{i,z}$ inertial-axis translational acceleration commands prior to translational washout, m/sec^2 (ft/sec^2)

$f^*_{i,x}, f^*_{i,y}$ inertial-axis specific-force error signals, m/sec^2 (ft/sec^2)

$f'_{i,x}, f'_{i,y}, f'_{i,z}$ components in inertial axis of filtered body-axis vertical acceleration at centroid location, m/sec^2 (ft/sec^2)

$f''_{i,z}$ artificial yaw-error signal, m/sec^2 (ft/sec^2)

$f_{s,x}, f_{s,y}$ body-axis longitudinal and lateral acceleration at centroid location, m/sec^2 (ft/sec^2)

$f_{s,z}$ body-axis vertical acceleration (referenced about 1g) at centroid location, m/sec^2 (ft/sec^2)

f_x, f_y, f_z airplane body-axis translational accelerations, m/sec^2 (ft/sec^2)

$f_{z,c}$ body-axis vertical acceleration at centroid location, m/sec^2 (ft/sec^2)

G_1 glide-slope error gain

g gravitational constant, m/sec^2 (ft/sec^2)

h altitude, m (ft)

h_c commanded altitude, m (ft)

h_o height of airplane center of gravity at touchdown, m (ft)

K_0 heading error gain

K_1 gain parameter of roll flight-director filter

K_2 damping parameter of roll flight-director filter, deg/sec

K_3 frequency parameter of roll flight-director filter, deg/sec

$K_{c,1}, K_{c,2}, K_{c,3}, K_{c,4}, K_{c,5}$ coefficients for initial-condition penalties in cost functions, per sec

$K_{x,1}, K_{y,1}, K_{x,3}, K_{y,3}$ gain parameters, sec^3/m^2 (sec^3/ft^2)

$K_{x,2}, K_{y,2}$ gain parameters, sec^6/m^4 (sec^6/ft^4)

K_y yaw-damper gain

K_β yaw-damper parameter, per sec

K_ψ yaw gain parameter, sec^2

k_p, k_q, k_r scaling parameters for angular rates

$k_{p,T,1}, k_{q,T,1}, k_{r,1}$ parameters of signal-shaping network, per m (per ft)

$k_{p,T,2}, k_{q,T,2}, k_{r,2}$ parameters of signal-shaping network, sec

$k_{p,T,3}, k_{q,T,3}, k_{r,3}$ parameters of signal-shaping network, per sec

$k_{z,1}, k_{z,2}$ gain parameters of vertical channel high-pass filter

$k_{\theta,1}, k_{\theta,2}$ gain parameters of longitudinal channel low-pass filter

$k_{\phi,1}, k_{\phi,2}$ gain parameters of lateral channel low-pass filter

$k_{\psi,l}, k_{\theta,l}, k_{\phi,l}$ lead parameters for rotational channel lag compensation, sec

$\mathscr{L}(A,B)$ operator equal to $\begin{cases} \text{sgn}(A,B) & \text{when } |A| > B \\ A & \text{when } |A| \leq B \end{cases}$

L_y localizer error rate limit, deg/sec

L_ϕ flight-director roll limit, deg/sec

p,q,r body-axis angular velocity commands, rad/sec

p',q',r' body-axis angular tilt velocity, rad/sec

p'',q'',r'' scaled body-axis aircraft angular velocities, rad/sec

p_a,q_a,r_a body-axis aircraft angular velocities, rad/sec

$p_{x,1},p_{x,3},p_{y,1},p_{y,3}$ adaptive parameters, position limited

$p_{x,2},p_{y,2}$ adaptive parameters, position limited, sec/m (sec/ft)

$p'_{x,1},p'_{y,1},p'_{x,3},p'_{y,3}$ adaptive parameters, rate limited

$p'_{x,2},p'_{y,2}$ adaptive parameters, rate limited, sec/m (sec/ft)

$\dot{p}''_{x,1},\dot{p}''_{y,1},\dot{p}''_{x,3},\dot{p}''_{y,3}$ adaptive-parameter rates, per sec

$\dot{p}''_{x,2},\dot{p}''_{y,2}$ adaptive-parameter rates, per m (per ft)

$p'_{x,1}(o),p'_{y,1}(o),p'_{x,3}(o),p'_{y,3}(o)$ initial conditions on adaptive parameters, rate limited

$p'_{x,2}(o),p'_{y,2}(o)$ initial conditions on adaptive parameters, rate limited, sec/m (sec/ft)

p_ψ adaptive yaw parameter, position limited

p'_ψ adaptive yaw parameter, rate limited

$\dot{p}''_\psi$ adaptive-yaw-parameter rate, per sec

$p'_{\psi}(o)$ initial condition on adaptive yaw parameter, rate limited

R range from runway, m (ft)

R_x,R_y,R_z centroid location with respect to center of gravity, m (ft)

S_1 pitch input to pitch flight director, deg

S_2 output of first-order pitch input lag, deg

S_x,S_y scale factors on $f_{s,x},f_{s,y}$

s Laplace operator

t time, sec

t_o starting time for roll flight-director operation

Δt time step size, sec

V_ℓ velocity limit, m/sec (ft/sec)

W_x,W_y angular-rate weighting coefficient, m^2/sec^2 (ft^2/sec^2)

x,y,z commanded inertial translational position of motion simulator, m (ft)

$\hat{x},\hat{y},\hat{z}$ commanded translational positions after compensation, m (ft)

x_{LF},y_{LF},z_{LF} scale factors on position limits

$\ddot{x}_b,\ddot{y}_b,\ddot{z}_b$ intermediate inertial-axis translational acceleration commands, m/sec^2 (ft/sec^2)

x_d,y_d,z_d inertial-axis translational position commands, m (ft)

x_ℓ,y_ℓ,z_ℓ inertial-axis position limits for translational channels, m (ft)

x_ℓ Earth-axis longitudinal coordinate of airplane center of gravity, m (ft)

x_o longitudinal coordinate of runway touchdown point, m (ft)

x_p, y_p, z_p coordinates of pilot's station with respect to center of gravity in body-axis system, m (ft)

$x_{p,c}, y_{p,c}, z_{p,c}$ coordinates of centroid location with respect to pilot's station in body-axis system, m (ft)

x_r x-distance of airplane center of gravity from runway, m (ft)

y_b distance behind runway touchdown point of localizer-beam origin, m (ft)

y_ℓ Earth-axis lateral coordinate of airplane center of gravity, m (ft)

y_o lateral coordinate of runway touchdown point, m (ft)

y_r y-distance of airplane center of gravity from runway, m (ft)

y_1, y_2 yaw-damper states

z_{neut} actuator extension for selected neutral point, m (ft)

β sideslip angle, rad

γ_c commanded glide-slope angle, deg

δ_a aileron-deflection angle, rad

δ_e elevator-deflection angle, rad

δ_r rudder-deflection angle, rad

$\delta_{R,y}$ yaw-damper contribution to rudder command, rad

δ_T throttle position, deg

ϵ_h vertical glide-slope error, m (ft)

ϵ_y localizer error, deg

$\epsilon_{y,\ell}$ rate-limited localizer error, deg

$\epsilon_{y,l}$ localizer-error lag, deg

ϵ_{γ} glide-slope error, deg

ϵ_{ψ} heading error, deg

$\epsilon_{\psi,1}$ scaled heading error, deg

θ_a actual airplane pitch angle, deg

θ_c commanded pitch angle, deg

θ_s pitch-command signal, deg

$\xi_{z,1}$ damping parameter for vertical channel high-pass filter

ξ_{θ},ξ_{ϕ} damping parameters of low-pass filters

τ yaw-damper parameter

ϕ_a actual airplane roll angle, deg

ϕ_c commanded roll angle, deg

ϕ_f roll flight director filter input, deg

ϕ_i intermediate roll-command angle, deg

ϕ_s roll-command signal, deg

$\phi_1,\dot{\phi}_1,\ddot{\phi}_1$ variables of roll flight-director filter, deg

ψ,θ,ϕ commanded inertial angular position of motion simulator, rad

$\hat{\psi},\hat{\theta},\hat{\phi}$ commanded angular positions after compensation, rad

ψ_a actual airplane heading, deg

$\dot{\psi}_a,\dot{\theta}_a,\dot{\phi}_a$ airplane angular velocities, rad/sec

ψ_c commanded heading, deg

$\dot{\psi}_T, \dot{\theta}_T, \dot{\phi}_T$ commanded inertial tilt rates, rad/sec

$\omega_{n,z,1}$ frequency parameter of vertical channel high-pass filter, rad/sec

$\omega_{n,\theta}, \omega_{n,\phi}$ frequency parameters of low-pass filters, rad/sec

Subscript:

meas measurement by instrument mounted on motion simulator

A dot over a variable indicates the time derivative of that variable.

THE FUNDAMENTAL DIFFERENCE

Figure 1 illustrates the fundamental difference in terms of motion cues between a linear filter and a nonlinear adaptive filter for the first-order filter case. The difference is anomalous rate cue presented by the linear filter as the pulse input in rate returns to zero. This false cue is most evident for pulse-type inputs and disappears as the input becomes sinusoidal. Thus, the fundamental difference between the linear and nonlinear filters varies dependent upon the responsiveness of the vehicle and the pilot's input in each axis, but not upon the parameter values of the linear filter.

Figure 2 presents a comparison of the linear and nonlinear washouts as applied to a simulation of a Boeing 737 conventional take-off and landing (CTOL) airplane for an aileron pulse input. Washout responses for typical pilot inputs in all axes will be presented later. As shown in figure 2, the linear washout represents the roll acceleration well (ignoring the scaling), while presenting the false cue in rotational rate. The nonlinear washout practically ignores the acceleration reversal (Time = 8 seconds) in order to eliminate the false rate cue. The importance of presenting the rotational rate cue properly rather than the rotational acceleration cue will be demonstrated in the comparison of the two washouts for roll inputs.

THE WASHOUT CIRCUITRY

The adapted version of Schmidt and Conrad's linear-coordinated washout circuitry used in this study is shown in figure 3 in block-diagram form. The detailed equations are presented in appendix A. The function of the circuitry is to represent the translational accelerations and the rotational rates of the simulated airplane while constraining

the motion commands to be within the hardware capabilities. The concept of this coordinated washout circuitry is to represent longitudinal and lateral translational cues by utilizing both translational and rotational motions and to obtain rotational washout through elimination of the false gravitational g cues that would be induced by a rotational movement.

The selection of the parameters for the washout circuitry began with employment of the values suggested in figure A.7 of reference 2. A representative "worst case" instrument-landing-system (ILS) approach was made with the fixed-base simulator, and the resulting translational accelerations and rotational rates were placed on tape. The tape was then used iteratively to drive the motion software for parameter variation.

Initial modification of the parameters was made to constrain the motions to remain within the motion limits of the hardware. Further modification of the parameters to improve the fidelity of the motion cues, in terms of time-history comparisons of airplane motion cues (simulated flight data) plotted against washout commands to represent these cues, was then made.

Final determination of the linear-washout parameters was then made based on the subjective opinions of three participating research pilots, and these parameter values are presented in table I. The major emphasis of this portion of the parameter-selection process fell on the roll channel parameters and is discussed in reference 8. The importance of the roll motion in the overall simulation is to be elaborated on later.

The nonlinear-washout method used in this study, coordinated adaptive washout, is shown in figure 4 in block-diagram form. The detailed equations are presented in appendix B. The concept of the nonlinear washout is similar to that of the linear circuitry, with the major differences being that the washout is carried out in the inertial reference frame rather than in the body-axis system, and employs nonlinear adaptive filters rather than the linear filters.

Parameter selection for the nonlinear circuitry began with selection of a set to constrain the "worst case" ILS approach motions to remain within the hardware capabilities. Modification was then made to improve the fidelity of the cues in terms of time-history comparisons, and final modification based on subjective opinions of three participating pilots concluded the process. The parameter values selected are presented in table II.

It should be emphasized that the parameters presented for each washout were chosen for a particular airplane simulation and a particular motion base by the three participating pilots. These parameters would perhaps vary with a change in airplane, task, motion base, or even with a change in pilots. However, the values are presented

here as the results of an attempt to optimize subjectively for the stipulated simulation. Since the nonlinear washout acts adaptively on the airplane motions to constrain the base excursions, it intuitively follows, and recent experience has indicated, that changes in airplane, tasks, or pilots, which determine the inputs to the washout, do not necessarily imply changes in washout parameters for satisfactory performance to be maintained with the nonlinear washout. It is anticipated, however, that a change in motion-base characteristics would require changes in the parameters of the washout in order to achieve the optimal performance.

COMPARISON OF THE TWO WASHOUT CIRCUITRIES

The method of comparing the two washout circuitries was originally intended to consist of an analysis of variance based on objective-data results and also a comparison of subjective opinions. However, upon implementation of the linear washout, an analysis of variance was carried out comparing fixed-base operation against linear-washout operation. The results of this comparison are presented in reference 8, and the analysis of variance is included in a later section herein. Upon implementation of the nonlinear washout some time later, the objective-data base was extended to include nonlinear-washout operation, and a new analysis of variance was conducted.

Additionally, between the times of implementation of the two circuitries, a major change in the lateral handling characteristics of the Boeing 737 airplane simulator was made. The change arose as a result of a comparison of newly acquired flight data with simulated flight data and involved the addition of a β feedback term in the simulation equations of the yaw damper. Appendix C contains the equations of the yaw damper, both with and without the β feedback term.

Figure 5 presents the unmodified (without β feedback) 737 simulator response to the aileron pulse input of figure 2, along with the linear- and nonlinear-washout responses to the airplane motions. The responses of figure 2 are those of the modified simulator (with β feedback). The major result of the modification in terms of handling characteristics was that rolling to a desired bank angle became a much simpler task, as evidenced by a comparison of the roll rates presented in figures 2(a) and 5(a).

Since the objective data for the fixed-base and linear-washout operations had been obtained from the simulator without the β feedback term, the comparison data for nonlinear operations were also collected in this mode. Subjective data were solicited both without and with the β feedback term in the yaw-damper equations and are presented in a later section under these classifications.

TASK CONDITIONS AND DATA BASE

Figure 6 illustrates the ILS task, which consisted of the following: (1) a transition to the localizer beam, followed by (2) a transition to the glide slope, and (3) the ensuing approach down to about 76 m (250 ft). Three approach conditions were provided: the standard approach previously described, the standard approach with instantaneous encounter of a weather front (a 10 knot crosswind with moderate turbulence), and the standard approach with the occurrence of an engine failure. Instrumentation consisted of an attitude-direction indicator, vertical-speed indicator, a horizontal-situation indicator, altimeter, airspeed indicator (both calibrated and true), meters for angles of attack and sideslip, and a turn and bank indicator.

The approach conditions were flown under fixed-base conditions and under two moving-base conditions. Motion was restricted to five degrees of freedom because: (1) extreme hydraulic noise is induced by the heave motion of the synergistic base (all six actuators have to move alike to present a heave cue), and (2) only a small amount of vertical cue was available.

The small amount of vertical cue available is due to a combination of the position limits of the motion base and the short-period frequency of the 737 airplane in the landing-approach configuration. Since the position limits of the synergistic motion base change as the orientation of the base varies, the position limits used in determining the linear-washout parameters must be conservative. For the motions involved in this study, the vertical-position limits were chosen to be 0.457 m (1.5 ft). The low-frequency content of the normal acceleration of the airplane (less than 1 rad/sec, neglecting turbulence) is due to the low short-period frequency. (See table III.) The amount of vertical cue available for motion simulation is thus less than 0.05g (the product of amplitude and frequency squared). The participating pilots felt that the vertical cue available was not worth the noise distraction.

During the performance of the landing-approach task under the aforementioned conditions, root-mean-square (rms) data were collected over two regimes. A short-duration regime, intended to reflect the immediate effect of the weather front and the engine-failure conditions, and a longer duration regime, intended to evaluate total performance, were used. The regimes overlapped and were based on airplane range. (See fig. 6.) The rms values were obtained for glide-slope deviation, localizer deviation, pitch-command bar deviation, roll-command bar deviation, and speed-command bar deviation. The equations for the flight director used in this study are presented in appendix D.

Subjective data consisted of pilot comments solicited during objective-data collection from the three participating pilots, as well as subjective evaluation data from standard maneuvers about straight-and-level flights by seven pilots.

OBJECTIVE-DATA RESULTS

The objective-data results are presented in the form of two analyses of variance experiments: the first comparing fixed-base operation against linear-washout operation, and the second comparing fixed-base, linear-washout, and nonlinear-washout operations. Both experiments utilized the simulated 737 airplane without the β feedback term in the yaw damper.

Comparison of Fixed-Base Operation With Linear-Washout Operation

The design of this experiment consisted of the $2 \times 3 \times 3$ factorial design (ref. 9) shown in table IV. The fixed-effect factors involved are pilots, approach conditions, and linear motion against fixed-base operation. The results of the analyses of variance of the 10 separate rms measurements are shown in table V. Significance of the one-tailed F-tests is indicated by a single asterisk for the 5-percent level and by a double asterisk for the 1-percent level.

The results indicate significant differences in mean rms performances between pilots and also between approaches. No significant differences in mean rms performances are found between motion and fixed-base operation. The occasional significance of the two-factor interaction AC indicates that the differences between pilots varied with the approach condition over all motion conditions, or, alternately, the differences in performance between approaches varied from pilot to pilot, regardless of the motion condition, for some of the performance measures.

Comparison of Fixed-Base, Linear-Washout, and Nonlinear-Washout Operations

After implementation and parameter selection were completed for the nonlinear washout, the ILS task was repeated to expand the objective-data base to include the nonlinear washout. The expanded experiment consisted of the $3 \times 3 \times 3$ factorial design shown in table VI. The results of the 10 new analyses of variance of the rms measurements are shown in table VII. Significance of the one-tailed F-tests is indicated by a single asterisk for the 5-percent level and by a double asterisk for the 1-percent level. Again, the results indicate significant differences between pilots and approaches, and significance of the two-factor interaction AC, as shown in table V.

The now-occasional significance between motion conditions is not frequent enough to warrant any claims of differences, particularly in light of the possibility of heterogeneity of data. (The nonlinear data were collected separately and at a later date.) This conclusion can also be drawn concerning the significance of the interactions involving motion B.

Further, the occasional significances between motion conditions are not consistent across the performance measures. It might be expected that the significant differences indicated for the localizer measurements would be reflected also in the roll-command bar measurements. Likewise, significance of the pitch bar measurements for long durations might be expected to be accompanied by glide-slope and speed-measurement differences, and perhaps by the short-duration complement measurements also.

SUBJECTIVE-DATA RESULTS

Pilot comments obtained during this study fell purposefully into two categories: general comments from three pilots on the effectiveness of motion, and specific comments from seven pilots on the representation of motion cues for standard maneuvers by each washout method.

General Comments

The three pilots participating in the objective-data task shared the opinion that motion greatly increased the realism of the simulation and also increased the pilot workload. All three pilots preferred the nonlinear washout to the linear washout, although they preferred the linear washout to fixed-base operation.

Specific Comments

Seven pilots participated in a subjective evaluation of the linear- and nonlinear-washout methods by rating the motion cues presented by each method for throttle, column, wheel, and pedal inputs about a straight-and-level condition in a landing-approach mode. Each pilot determined his own evaluation inputs and also flew portions of the ILS landing approach. In addition to rating the motion for each type of control input, the pilots were asked to rate how well the overall motion came to representing that of an airplane (e.g., does it "feel" like an airplane). The initial rating categories were excellent, good, fair, poor, and unacceptable, but the pilots rather consistently used ratings halfway between two of the given categories.

The lateral ratings and the overall motion ratings were obtained for both of the lateral-handling characteristic cases: without the β feedback in the yaw damper, and with the β feedback in the yaw damper. The longitudinal-handling characteristics were not affected by this change. The subjective results of this evaluation with the β feedback in the yaw damper are also presented in reference 10.

Longitudinal inputs.- The results of the evaluations involving longitudinal inputs are presented in table VIII, with an open symbol representing the rating of the linear method

and a solid symbol representing the nonlinear-method rating. The first four pilots, represented by the triangular symbols, have had actual 737 cockpit experience.

Throttle inputs: Figure 7 presents typical time histories for a change in throttle setting. Inputs to the washouts from the simulated airplane, if ignoring the body-inertial transformations, are the longitudinal acceleration (scaled at one-half) $f_{s,x}$ and the pitch rate q_a. As figure 7 shows, very little difference exists between the linear and nonlinear responses for these inputs. The fundamental difference between the two pitch-rate filters is obscured in order to represent the decrease in $f_{s,x}$ at a time equal to 6 seconds.

The pilot ratings for throttle changes, as shown in table VIII, are the same for each method. (No change in a pilot's rating between linear and nonlinear washout is indicated by the open symbol appearing above the solid symbol.) Indeed, when given the methods back to back for throttle comparison, the pilots could not detect that a change had been made.

Column inputs: Time histories of an elevator doublet input are presented in figure 8. As with throttle inputs, the fundamental difference between the pitch-rate filters is obscured because of the coordination of pitch with longitudinal acceleration. The nonlinear response does contain more pitch rate and more pitch-angle change, resulting in better phasing of the $f_{s,x}$ cue. However, the differences are small, and four pilots rated the washout methods the same for this control (table VIII), whereas the other three rated the nonlinear method slightly higher.

Lateral inputs without β feedback.- The results of the evaluations of the lateral inputs for the airplane without β feedback are presented in the previous format (of table VIII) in table IX.

Wheel inputs: The pilots preferred to break the motion cues that accompany aileron inputs into roll cues and yaw cues for the purpose of individual cue evaluation. Figure 9 presents time histories for the roll cues by using ailerons to bank the airplane 20° for a 30° heading change with a return to a straight-and-level condition. Without β feedback in the yaw damper, the roll rate of the airplane is oscillatory, with the peak at 6 seconds being about one-half of the peak at 3 seconds. The linear-washout response for this case yields a second peak of p that is larger than the first peak and could give the pilot the impression of a net left bank, rather than a right bank. This anomalous rate cue is not present in the nonlinear-washout response.

All pilots rated the nonlinear roll cues to be at least one category higher (better) than the linear cues, and two pilot ratings are three categories higher. The poor side-force representation by both washouts, due to lack of sufficient y-travel of the base both to offset the misalinement of the gravity vector (due to the roll cue) and to present the side-force cue (refs. 4 and 8), was not noticed by any of the pilots.

Figure 10 presents the time histories of the yaw cues for the previous maneuver. At a time of 18 seconds, when the yaw rate of the airplane returns to zero, the linear washout presents an anomalous rate cue. The nonlinear response does not contain this anomalous cue. Three of the pilots rated the yaw cues of each washout to be approximately the same; one of these three gave each washout a rating of good, and the other two rated the nonlinear washout one-half category higher than the linear washout. The four other pilots rated the nonlinear washout somewhat higher than the linear washout, with one change of one category, and three changes of two categories.

Pedal inputs: Since little pedal control is used on the 737 airplane, the pilot ratings for roll and yaw cues are based mostly on wheel inputs. However, all the pilots conducted rudder maneuvers for each washout; no resulting changes were made in the roll and yaw ratings. The yaw time histories for a typical rudder input are shown in figure 11, and figure 12 presents the roll time histories for the same inputs.

Overall airplane feel: All seven pilots rated the nonlinear washout to be at least one category higher than the linear washout in terms of overall airplane feel.

Lateral inputs with β feedback.- The results of the evaluations of the lateral inputs for the simulated airplane with β feedback in the yaw damper (which more closely approximates the flight vehicle) are presented in table X.

Wheel inputs: As with the previous case, the motion cues resulting from lateral inputs are presented in terms of roll- and yaw-cue ratings. Figure 13 presents the roll-cue time histories for an aileron-induced bank of 20° for a 30° heading change with a return to straight and level. In this case, the anomalous roll rate of the linear washout is evident, and the subjective evaluations of all seven pilots reflect the fact that this motion was felt to be unnatural for an airplane. All pilots rated the nonlinear roll cues to be at least $1\frac{1}{2}$ categories higher than the linear cues, and three pilot ratings were $2\frac{1}{2}$ categories higher. Again, none of the pilots noticed the poor side-force representation of both washouts.

Figure 14 presents the yaw-cue time histories for the previous aileron maneuver. Again, the anomalous rate cue was present; the pilots particularly noticed a negative rate when the airplane rate r_a returned to zero during maneuvers of this type. This fact is reflected in the ratings of table X, in which the nonlinear-washout ratings are at least one category higher, and four ratings are two higher.

Pedal inputs: No changes were made in the roll- and yaw-cue ratings as a result of the rudder maneuvers conducted by each pilot. The yaw time histories for a typical rudder input are shown in figure 15, and the roll time histories for the same inputs are presented in figure 16.

Overall airplane feel: The nonlinear washout was rated by all the pilots to be at least $1\frac{1}{2}$ categories higher than the linear washout in terms of overall airplane feel, with each pilot noting that the roll representation had the most impact on how much the simulation felt like an airplane.

CONCLUDING REMARKS

The results of this study comparing a linear-washout method with a nonlinear method can be summarized with respect to the two types of data as follows:

Objective Data

The lack of significant differences in pilot performance for the various motion conditions (fixed base, linear washout, and nonlinear washout) for the two objective experiments seems to indicate that pilot performance as measured was not influenced by the motion cues presented in this study during instrument-landing-system (ILS) approaches.

Subjective Data

The subjective results of this study, however, indicate that motion increases realism and that the pilots prefer it to fixed-base operation. More significantly, the pilots rated the nonlinear washout as highly preferable to the linear washout, and they specifically objected to anomalous rotational rate cues in roll and yaw with the linear method. Since the pilots considered roll representation to be most important in terms of the overall airplane feel, the elimination of the objectionable anomalous rate cues is highly desirable.

Langley Research Center
National Aeronautics and Space Administration
Hampton, Va. 23665
April 14, 1976

APPENDIX A

DETAILED EQUATIONS FOR THE LINEAR-WASHOUT CIRCUIT

The following is a block-by-block list of equations corresponding to figure 3:

Centroid transformation:

$$R_x = x_p + x_{p,c}$$

$$R_y = y_p + y_{p,c}$$

$$R_z = z_p + z_{p,c}$$

$$f_{s,x} = f_x - \left(q_a^2 + r_a^2\right)R_x + \left(q_a p_a - \dot{r}_a\right)R_y + \left(r_a p_a + \dot{q}_a\right)R_z$$

$$f_{s,y} = f_y + \left(p_a q_a + \dot{r}_a\right)R_x - \left(p_a^2 + r_a^2\right)R_y + \left(r_a q_a - \dot{p}_a\right)R_z$$

$$f_{z,c} = f_z + \left(p_a q_a - \dot{q}_a\right)R_x + \left(q_a r_a + \dot{p}_a\right)R_{\dot{y}} - \left(p_a^2 + q_a^2\right)R_z$$

Variation about 1g:

$$f_{s,z} = f_{z,c} + g$$

High-pass filter:

$$f_{c,z} = \frac{k_{z,1}f_{s,z} - 2\xi_{z,1}\omega_{n,z,1}\int f_{c,z}\,dt - \omega_{n,z,1}^2\iint f_{c,z}\,dt\,dt}{k_{z,2}}$$

Low-pass filter:

$$k_{\theta,2}\ddot{f}^*_{c,x} = k_{\theta,1}f_{s,x} - 2\xi_\theta\omega_{n,\theta}\dot{f}^*_{c,x} - \omega_{n,\theta}^2 f^*_{c,x}$$

$$k_{\phi,2}\ddot{f}^*_{c,y} = k_{\phi,1}f_{s,y} - 2\xi_\phi\omega_{n,\phi}\dot{f}^*_{c,y} - \omega_{n,\phi}^2 f^*_{c,y}$$

APPENDIX A

Body to inertial transformation, high-frequency components:

$$f'_{i,x} = f_{c,z}(\cos\phi \sin\theta \cos\psi + \sin\phi \sin\psi)$$

$$f'_{i,y} = f_{c,z}(\cos\phi \sin\theta \sin\psi - \sin\phi \cos\psi)$$

$$f'_{i,z} = f_{c,z}(\cos\phi \cos\theta)$$

Body to inertial transformation, low-frequency components:

$$f^*_{i,x} = f^*_{c,x}(\cos\theta \cos\psi) + f^*_{c,y}(\sin\phi \sin\theta \cos\psi - \cos\phi \sin\psi)$$
$$- g(\cos\phi \sin\theta \cos\psi + \sin\phi \sin\psi)$$

$$f^*_{i,y} = f^*_{c,x}(\cos\theta \sin\psi) + f^*_{c,y}(\sin\phi \sin\theta \sin\psi + \cos\phi \cos\psi)$$
$$- g(\cos\phi \sin\theta \sin\psi - \sin\phi \cos\psi)$$

Sum of low- and high-frequency components:

$$f_{i,x} = f'_{i,x} + f^*_{i,x}$$

$$f_{i,y} = f'_{i,y} + f^*_{i,y}$$

$$f_{i,z} = f'_{i,z}$$

Signal-shaping network:

$$\dot{\theta}_T = k_{q,T,1}k_{q,T,2}f^*_{i,x} + k_{q,T,1}\int f^*_{i,x}\,dt + k_{q,T,1}k_{q,T,3}\iint f^*_{i,x}\,dt\,dt$$

$$\dot{\phi}_T = -k_{p,T,1}k_{p,T,2}f^*_{i,y} - k_{p,T,1}\int f^*_{i,y}\,dt - k_{p,T,1}k_{p,T,3}\iint f^*_{i,y}\,dt\,dt$$

$$\dot{\psi}_T = k_{r,1}k_{r,2}f''_{i,z} + k_{r,1}\int f''_{i,z}\,dt + k_{r,1}k_{r,3}\iint f''_{i,z}\,dt\,dt$$

Inertial to body transformation:

$$p' = \dot{\phi}_T(\cos\theta \cos\psi) + \dot{\theta}_T(\cos\theta \sin\psi) - \dot{\psi}_T(\sin\theta)$$

$$q' = \dot{\phi}_T(\sin\phi \sin\theta \cos\psi - \cos\phi \sin\psi) + \dot{\theta}_T(\sin\phi \sin\theta \sin\psi + \cos\phi \cos\psi)$$
$$+ \dot{\psi}_T(\sin\phi \cos\theta)$$

$$r' = \dot{\phi}_T(\cos\phi \sin\theta \cos\psi + \sin\phi \sin\psi) + \dot{\theta}_T(\cos\phi \sin\theta \sin\psi - \sin\phi \cos\psi)$$
$$+ \dot{\psi}_T(\cos\phi \cos\theta)$$

Scale airplane angular rates:

$$p'' = k_p p_a$$

$$q'' = k_q q_a$$

$$r'' = k_r r_a$$

Sum of airplane and tilt rates:

$$p = p'' + p'$$

$$q = q'' + q'$$

$$r = r'' + r'$$

Transformation to Euler rates:

$$\dot{\phi} = p + q \sin\phi \tan\theta + r \cos\phi \tan\theta$$

$$\dot{\theta} = q \cos\phi - r \sin\phi$$

$$\dot{\psi} = (q \sin\phi + r \cos\phi) \sec\theta$$

Angular lead compensation:

$$\hat{\psi} = \psi + k_{\psi,l}\dot{\psi}$$

$$\hat{\theta} = \theta + k_{\theta,l}\dot{\theta}$$

$$\hat{\phi} = \phi + k_{\phi,l}\dot{\phi}$$

APPENDIX A

Translational lead compensation:

$$\hat{x} = x_d + A_1\ddot{x}_d + B_1\dot{x}_d$$

$$\hat{y} = y_d + A_2\ddot{y}_d + B_2\dot{y}_d$$

$$\hat{z} = z_d + A_3\ddot{z}_d + B_3\dot{z}_d$$

Translational washout:

$$\ddot{x}_d = f_{i,x} - a_1\dot{x}_d - b_1x_d$$

$$\ddot{y}_d = f_{i,y} - a_2\dot{y}_d - b_2y_d$$

$$\ddot{z}_d = f_{i,z} - a_3\dot{z}_d - b_3z_d$$

Limit prediction based on current position:

See reference 3 for equations and derivation.

APPENDIX B

COORDINATED ADAPTIVE WASHOUT

The following equations are those of the nonlinear washout and correspond to figure 4. The derivation of these equations may be found in reference 5.

Longitudinal filter equations:

$$\ddot{x} = p_{x,1} f_{i,x} - d_x \dot{x} - e_x x$$

$$\dot{\theta} = p_{x,2} f_{i,x} + p_{x,3} \dot{\theta}_a$$

$$\dot{p}''_{x,1} = K_{x,1}\left[\left(f_{i,x} - \ddot{x}\right)\frac{\partial \ddot{x}}{\partial p_{x,1}} - b_x x \frac{\partial x}{\partial p_{x,1}} - c_x \dot{x} \frac{\partial \dot{x}}{\partial p_{x,1}}\right] + \left[p'_{x,1}(o) - p_{x,1}\right] K_{c,1}$$

$$\dot{p}'_{x,1} = \begin{cases} \dot{p}''_{x,1} & \left(\dot{p}''_{x,1} > -0.06\right) \\ -0.06 & \left(\dot{p}''_{x,1} \leqq -0.06\right) \end{cases} \qquad p_{x,1} = \begin{cases} 1 & \left(p'_{x,1} > 1\right) \\ p'_{x,1} & \left(-0.1 \leqq p'_{x,1} \leqq 1\right) \\ -0.1 & \left(p'_{x,1} < -0.1\right) \end{cases}$$

$$\dot{p}''_{x,2} = K_{x,2}\left[\left(f_{i,x} - \ddot{x}\right)\left(\frac{\partial \ddot{x}}{\partial p_{x,2}} - \frac{\partial f_{i,x}}{\partial p_{x,2}}\right) + W_x\left(\dot{\theta}_a - \dot{\theta}\right)\frac{\partial \dot{\theta}}{\partial p_{x,2}} - b_x x \frac{\partial x}{\partial p_{x,2}} - c_x \dot{x} \frac{\partial \dot{x}}{\partial p_{x,2}}\right]$$

$$\dot{p}'_{x,2} = \begin{cases} 0.01 & \left(\dot{p}''_{x,2} > 0.01\right) \\ \dot{p}''_{x,2} & \left(-0.01 \leqq \dot{p}''_{x,2} \leqq 0.01\right) \\ -0.01 & \left(\dot{p}''_{x,2} < -0.01\right) \end{cases} \qquad p_{x,2} = \begin{cases} 0.05 & \left(p'_{x,2} > 0.05\right) \\ p'_{x,2} & \left(0.01 \leqq p'_{x,2} \leqq 0.05\right) \\ 0.01 & \left(p'_{x,2} < 0.01\right) \end{cases}$$

$$\dot{p}''_{x,3} = K_{x,3}\left[\left(f_{i,x} - \ddot{x}\right)\left(\frac{\partial \ddot{x}}{\partial p_{x,3}} - \frac{\partial f_{i,x}}{\partial p_{x,3}}\right) + W_x\left(\dot{\theta}_a - \dot{\theta}\right)\frac{\partial \dot{\theta}}{\partial p_{x,3}} - b_x x \frac{\partial x}{\partial p_{x,3}} - c_x \dot{x} \frac{\partial \dot{x}}{\partial p_{x,3}}\right]$$
$$+ \left[p''_{x,3}(o) - p_{x,3}\right] K_{c,2}$$

APPENDIX B

$$p_{x,3} = \begin{cases} 1 & \left(p''_{x,3} > 1\right) \\ p''_{x,3} & \left(0 \leq p''_{x,3} \leq 1\right) \\ 0 & \left(p''_{x,3} < 1\right) \end{cases}$$

$$\left(\frac{\partial \ddot{x}}{\partial p_{x,1}}\right) = f_{i,x} - d_x\left(\frac{\partial \dot{x}}{\partial p_{x,1}}\right) - e_x\left(\frac{\partial x}{\partial p_{x,1}}\right)$$

$$\left(\frac{\partial \ddot{x}}{\partial p_{x,2}}\right) = p_{x,1}\frac{\partial f_{i,x}}{\partial p_{x,2}} - d_x\left(\frac{\partial \dot{x}}{\partial p_{x,2}}\right) - e_x\left(\frac{\partial x}{\partial p_{x,2}}\right)$$

$$\left(\frac{\partial \ddot{x}}{\partial p_{x,3}}\right) = p_{x,1}\frac{\partial f_{i,x}}{\partial p_{x,3}} - d_x\left(\frac{\partial \dot{x}}{\partial p_{x,3}}\right) - e_x\left(\frac{\partial x}{\partial p_{x,3}}\right)$$

$$\left(\frac{\partial \dot{\theta}}{\partial p_{x,2}}\right) = f_{i,x} + p_{x,2}\frac{\partial f_{i,x}}{\partial p_{x,2}}$$

$$\left(\frac{\partial \dot{\theta}}{\partial p_{x,3}}\right) = p_{x,2}\frac{\partial f_{i,x}}{\partial p_{x,3}} + \dot{\theta}_a$$

$$\frac{\partial f_{i,x}}{\partial p_{x,2}} = \left[-f_{s,x}(\sin\theta\cos\psi) + f_{s,y}(\sin\phi\cos\theta\cos\psi) - g(\cos\phi\cos\theta\cos\psi)\right]\frac{\partial\theta}{\partial p_{x,2}}$$

$$\frac{\partial f_{i,x}}{\partial p_{x,3}} = \left[-f_{s,x}(\sin\theta\cos\psi) + f_{s,y}(\sin\phi\cos\theta\cos\psi) - g(\cos\phi\cos\theta\cos\psi)\right]\frac{\partial\theta}{\partial p_{x,3}}$$

$$f_{i,x} = S_x f_{s,x}(\cos\theta\cos\psi) + S_y f_{s,y}(\sin\phi\sin\theta\cos\psi - \cos\phi\sin\psi)$$
$$- g(\cos\phi\sin\theta\cos\psi + \sin\phi\sin\psi)$$

Lateral filter equations:

$$\ddot{y} = p_{y,1}f_{i,y} - d_y\dot{y} - e_y y$$

$$\dot{\phi} = -p_{y,2}f_{i,y} + p_{y,3}\dot{\phi}_a$$

APPENDIX B

$$\dot{p}''_{y,1} = K_{y,1}\left[\left(f_{i,y} - \ddot{y}\right)\frac{\partial \ddot{y}}{\partial p_{y,1}} - b_y y \frac{\partial y}{\partial p_{y,1}} - c_y \dot{y} \frac{\partial \dot{y}}{\partial p_{y,1}}\right] + \left[p'_{y,1}(o) - p_{y,1}\right]K_{c,3}$$

$$\dot{p}'_{y,1} = \begin{cases} \dot{p}''_{y,1} & \left(\dot{p}''_{y,1} > -0.06\right) \\ -0.06 & \left(\dot{p}''_{y,1} \leqq -0.06\right) \end{cases} \qquad p_{y,1} = \begin{cases} 0.8 & \left(p'_{y,1} > 0.8\right) \\ p'_{y,1} & \left(-0.1 \leqq p'_{y,1} \leqq 0.8\right) \\ -0.1 & \left(p'_{y,1} < -0.1\right) \end{cases}$$

$$\dot{p}''_{y,2} = K_{y,2}\left[\left(f_{i,y} - \ddot{y}\right)\left(\frac{\partial \ddot{y}}{\partial p_{y,2}} - \frac{\partial f_{i,y}}{\partial p_{y,2}}\right) + W_y\left(\dot{\phi}_a - \dot{\phi}\right)\frac{\partial \dot{\phi}}{\partial p_{y,2}} - b_y y \frac{\partial y}{\partial p_{y,2}} - c_y \dot{y} \frac{\partial \dot{y}}{\partial p_{y,2}}\right]$$

$$\dot{p}'_{y,2} = \begin{cases} 0.1 & \left(\dot{p}''_{y,2} > 0.1\right) \\ \dot{p}''_{y,2} & \left(-0.1 \leqq \dot{p}''_{y,2} \leqq 0.1\right) \\ -0.1 & \left(\dot{p}''_{y,2} < -0.1\right) \end{cases} \qquad p_{y,2} = \begin{cases} 0.01 & \left(p'_{y,2} > 0.01\right) \\ p'_{y,2} & \left(-0.01 \leqq p'_{y,2} \leqq 0.01\right) \\ -0.01 & \left(p'_{y,2} < -0.01\right) \end{cases}$$

$$\dot{p}''_{y,3} = K_{y,3}\left[\left(f_{i,y} - \ddot{y}\right)\left(\frac{\partial \ddot{y}}{\partial p_{y,3}} - \frac{\partial f_{i,y}}{\partial p_{y,3}}\right) + W_y\left(\dot{\phi}_a - \dot{\phi}\right)\frac{\partial \dot{\phi}}{\partial p_{y,3}} - b_y y \frac{\partial y}{\partial p_{y,3}} - c_y \dot{y} \frac{\partial \dot{y}}{\partial p_{y,3}}\right]$$

$$+ \left[p'_{y,3}(o) - p_{y,3}\right]K_{c,4}$$

$$\dot{p}'_{y,3} = \begin{cases} \dot{p}''_{y,3} & \left(\dot{p}''_{y,3} \geqq -0.2\right) \\ -0.2 & \left(\dot{p}''_{y,3} < -0.2\right) \end{cases} \qquad p_{y,3} = \begin{cases} 0.3 & \left(p'_{y,3} > 0.3\right) \\ p'_{y,3} & \left(0 \leqq p'_{y,3} \leqq 0.3\right) \\ 0 & \left(p'_{y,3} < 0\right) \end{cases}$$

$$\left(\frac{\partial \ddot{y}}{\partial p_{y,1}}\right) = f_{i,y} - d_y\left(\frac{\partial \dot{y}}{\partial p_{y,1}}\right) - e_y\left(\frac{\partial y}{\partial p_{y,1}}\right)$$

$$\left(\frac{\partial \ddot{y}}{\partial p_{y,2}}\right) = p_{y,1}\frac{\partial f_{i,y}}{\partial p_{y,2}} - d_y\left(\frac{\partial \dot{y}}{\partial p_{y,2}}\right) - e_y\left(\frac{\partial y}{\partial p_{y,2}}\right)$$

APPENDIX B

$$\left(\frac{\partial \dot{y}}{\partial p_{y,3}}\right) = p_{y,1}\frac{\partial f_{i,y}}{\partial p_{y,3}} - d_y\left(\frac{\partial y}{\partial p_{y,3}}\right) - e_y\left(\frac{\partial y}{\partial p_{y,3}}\right)$$

$$\left(\frac{\partial \dot{\phi}}{\partial p_{y,2}}\right) = -f_{i,y} - p_{y,2}\frac{\partial f_{i,y}}{\partial p_{y,2}}$$

$$\left(\frac{\partial \dot{\phi}}{\partial p_{y,3}}\right) = -p_{y,2}\frac{\partial f_{i,y}}{\partial p_{y,3}} + \dot{\phi}_a$$

$$\frac{\partial f_{i,y}}{\partial p_{y,2}} = \left[f_{s,y}(\cos\phi \sin\theta \sin\psi - \sin\phi \cos\psi) + g(\sin\phi \sin\theta \sin\psi + \cos\phi \cos\psi)\right]\frac{\partial \phi}{\partial p_{y,2}}$$

$$\frac{\partial f_{i,y}}{\partial p_{y,3}} = \left[f_{s,y}(\cos\phi \sin\theta \sin\psi - \sin\phi \cos\psi) + g(\sin\phi \sin\theta \sin\psi + \cos\phi \cos\psi)\right]\frac{\partial \phi}{\partial p_{y,3}}$$

$$f_{i,y} = S_x f_{s,x}(\cos\theta \sin\psi) + S_y f_{s,y}(\sin\phi \sin\theta \sin\psi + \cos\phi \sin\theta \sin\psi)$$

$$- g(\cos\phi \sin\theta \sin\psi - \sin\phi \cos\psi)$$

Yaw filter equations:

$$\dot{\psi} = p_\psi \dot{\psi}_a - e_\psi \psi$$

$$\dot{p}''_\psi = K_\psi\left[\left(\dot{\psi}_a - \dot{\psi}\right)\frac{\partial \dot{\psi}}{\partial p_\psi} - b_\psi \psi \frac{\partial \psi}{\partial p_\psi}\right] + \left[p'_\psi(o) - p_\psi\right]K_{c,5}$$

$$\dot{p}'_\psi = \begin{cases} \dot{p}''_\psi & \left(\dot{p}''_\psi > -0.4\right) \\ -0.4 & \left(\dot{p}''_\psi \leqq -0.4\right) \end{cases} \qquad p_\psi = \begin{cases} 1 & \left(p'_\psi > 1\right) \\ p'_\psi & \left(0 \leqq p'_\psi \leqq 1\right) \\ 0 & \left(p'_\psi < 0\right) \end{cases}$$

$$\left(\frac{\partial \dot{\psi}}{\partial p_\psi}\right) = \dot{\psi}_a - e_\psi\left(\frac{\partial \psi}{\partial p_\psi}\right)$$

APPENDIX C

THE YAW-DAMPER EQUATIONS

The following yaw-damper equations are used in this study:

Without β feedback:

$$y_1 = K_y r$$

$$y_2 = \frac{s}{(\tau s + 1)^2} y_1$$

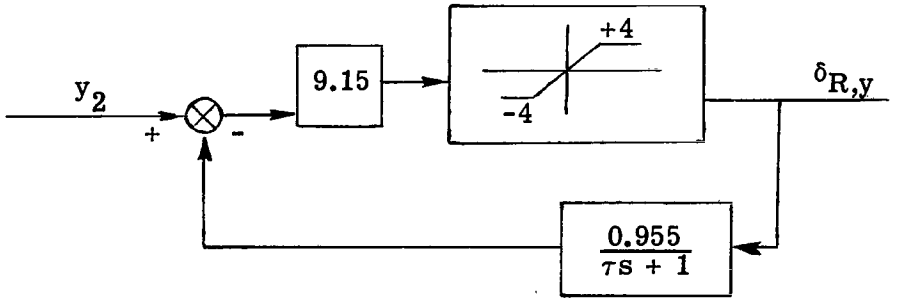

With β feedback:

$$y_1 = K_y\left(r - K_\beta \beta\right)$$

$$K_\beta = \begin{cases} 0 & \left(|\delta_a| \leqq 0.5\right) \\ 4 & \left(|\delta_a| > 0.5\right) \end{cases}$$

with y_2 and $\delta_{R,y}$ remaining as previously shown.

APPENDIX D

FLIGHT-DIRECTOR EQUATIONS

The following equations for the flight director are used in this study:

Input equations:

$$x_r = (x_\ell - x_o) \cos \psi_c + (y_\ell - y_o) \sin \psi_c$$

$$y_r = -(x_\ell - x_o) \sin \psi_c + (y_\ell - y_o) \cos \psi_c$$

$$R = \left(x_\ell^2 + y_\ell^2\right)^{1/2}$$

$$h_c = R \tan \gamma_c + h_o$$

$$\epsilon_h = h - h_c$$

$$\epsilon_\gamma = \tan^{-1}\left(\frac{\epsilon_h}{R}\right) \times \text{DPR}$$

$$\epsilon_\psi = \psi_a - \psi_c$$

$$\epsilon_y = \tan^{-1}\left(\frac{y_r}{R + y_b}\right) \times \text{DPR}$$

Pitch flight director:

$$G_1 = \begin{cases} 0.14(h - 50) & (h < 100) \\ h/15 & (h \geq 100) \end{cases}$$

G_1 limited to $[0, 100]$

$$S_1 = -(\theta_a + 2)$$

APPENDIX D

$$\dot{S}_2 = \frac{S_1 - S_2}{15} \qquad \text{(Initial condition: } S_2 = S_1\text{)}$$

$$\theta_c = G_1 \epsilon_\gamma - S_2$$

$$\theta_c \text{ limited to } [-12, 12]$$

$$\theta_s = \theta_c + S_1$$

Roll flight director:

$t - t_o \leqq 90$	$t - t_o > 90$
$L_y = 0.4$	$L_y = 0.12$
$L_\phi = 25$	$L_\phi = 15$
$K_0 = 2.8$	$K_0 = 3.8$
$K_1 = 2.833$	$K_1 = 3.5714$
$K_2 = 2.867$	$K_2 = 3.534$
$K_3 = 0.3333$	$K_3 = 0.7518$

$$\dot{\epsilon}_{y,l} = \frac{\epsilon_y - \epsilon_{y,l}}{\Delta t} \qquad \text{(Initial condition: } \epsilon_{y,l} = 0\text{)}$$

$$\dot{\epsilon}_{y,l} \text{ limited to } [-L_y, L_y]$$

$$\epsilon_{y,l} = \epsilon_{y,l} + \Delta t \dot{\epsilon}_{y,l}$$

$$\epsilon_{\psi,1} = K_0 \epsilon_\psi$$

$$\phi_f = \epsilon_\psi - 65\epsilon_{y,l} + 1.6\psi_a$$

APPENDIX D

$$\ddot{\phi}_1 = K_1\phi_f - K_2\dot{\phi}_1 - K_3\phi_1 \qquad \left(\text{Initial conditions: } \dot{\phi}_1 = 0 \text{ and } \phi_1 = 8.499\phi_f\right)$$

$$\phi_i = 21.2\epsilon_{y,\ell} + \epsilon_\psi - \dot{\phi}_1$$

ϕ_i limited to $[-30, 30]$

$$\phi_c = \phi_i - \epsilon_\psi$$

ϕ_c limited to $[-L_\phi, L_\phi]$

$$\phi_s = \phi_c - \phi_a$$

REFERENCES

1. Schmidt, Stanley F.; and Conrad, Bjorn: Motion Drive Signals for Piloted Flight Simulators. NASA CR-1601, 1970.

2. Schmidt, Stanley F.; and Conrad, Bjorn: A Study of Techniques for Calculating Motion Drive Signals for Flight Simulators. Rep. No. 71-28, Analytical Mechanics Associates, Inc., July 1971. (Available as NASA CR-114345.)

3. Parrish, Russell V.; Dieudonne, James E.; and Martin, Dennis J., Jr.: Motion Software for a Synergistic Six-Degree-of-Freedom Motion Base. NASA TN D-7350, 1973.

4. Parrish, Russell V.; Dieudonne, James E.; Martin, Dennis J., Jr.; and Bowles, Roland L.: Coordinated Adaptive Filters for Motion Simulators. Proceedings of the 1973 Summer Computer Simulation Conference, Simulation Councils, Inc., c.1973, pp. 295-300.

5. Parrish, Russell V.; Dieudonne, James E.; Bowles, Roland L.; and Martin, Dennis J., Jr.: Coordinated Adaptive Washout for Motion Simulators. J. Aircr., vol. 12, no. 1, Jan. 1975, pp. 44-50.

6. Dieudonne, James E.; Parrish, Russell V.; and Bardusch, Richard E.: An Actuator Extension Transformation for a Motion Simulator and an Inverse Transformation Applying Newton-Raphson's Method. NASA TN D-7067, 1972.

7. Parrish, Russell V.; Dieudonne, James E.; Martin, Dennis J., Jr.; and Copeland, James L.: Compensation Based on Linearized Analysis for a Six-Degree-of-Freedom Motion Simulator. NASA TN D-7349, 1973.

8. Parrish, Russell V.; and Martin, Dennis J., Jr.: Evaluation of a Linear Washout for Simulator Motion Cue Presentation During Landing Approach. NASA TN D-8036, 1975.

9. Steel, Robert G. D.; and Torrie, James H.: Principles and Procedures of Statistics. McGraw-Hill Book Co., Inc., 1960.

10. Parrish, R. V.; and Martin, D. J., Jr.: Empirical Comparison of a Linear and a Nonlinear Washout for Motion Simulators. AIAA Paper No. 75-106, Jan. 1975.

TABLE I.- LINEAR-WASHOUT PARAMETER VALUES

Variable	Value in SI units	Program value (U.S. units)
$k_{z,1}$	0	0
$\xi_{z,1}$	0.7	0.7
$\omega_{n,z,1}$, rad/sec	0.1	0.1
$k_{z,2}$	1.0	1.0
$k_{p,T,1}$, per m (per ft)	0.0003	0.001
$k_{p,T,2}$, sec	30.0	30.0
$k_{p,T,3}$, per sec	0.05	0.05
$k_{q,T,1}$, per m (per ft)	0.0003	0.001
$k_{q,T,2}$, sec	30.0	30.0
$k_{q,T,3}$, per sec	0.05	0.05
$k_{r,1}$, per m (per ft)	0.0012	0.004
$k_{r,2}$, sec	3.8	3.8
$k_{r,3}$, per sec	0.05	0.05
a_1, rad/sec	1.414	1.414
a_2, rad/sec	2.1	2.1
a_3, rad/sec	2.1	2.1
b_1, rad/sec	1.0	1.0
b_2, rad/sec	2.25	2.25
b_3, rad/sec	2.25	2.25
$\ddot{x}_l$, m/sec^2 (ft/sec^2)	5.8840	19.3044
$\ddot{y}_l$, m/sec^2 (ft/sec^2)	5.8840	19.3044
$\ddot{z}_l$, m/sec^2 (ft/sec^2)	7.8453	25.7392
A_1, sec^2	0.0069	0.0069
A_2, sec^2	0.0069	0.0069
A_3, sec^2	0.0069	0.0069

Variable	Value in SI units	Program value (U.S. units)
B_1, sec	0.14	0.14
B_2, sec	0.14	0.14
B_3, sec	0.14	0.14
$k_{\psi,l}$, sec	0.12	0.12
$k_{\theta,l}$, sec	0.12	0.12
$k_{\phi,l}$, sec	0	0
k_p	0.4	0.4
k_q	0.5	0.5
k_r	0.2	0.2
C_1, per sec	0.5	0.5
C_2, per sec	0.2	0.2
C_3, per sec	0.5	0.5
$k_{\theta,1}$	0.5	0.5
$k_{\theta,2}$	0.04	0.04
ξ_θ	0.14	0.14
$\omega_{n,\theta}$, rad/sec	1.0	1.0
$k_{\phi,1}$	0.04	0.04
$k_{\phi,2}$	0.04	0.04
ξ_ϕ	0.14	0.14
$\omega_{n,\phi}$, rad/sec	0.2	0.2
z_{neut}, m (ft)	0.6486	2.128
V_l, m/sec (ft/sec)	0.3048	1.0
x_{LF}	2.5	2.5
y_{LF}	2.5	2.5
z_{LF}	3.0	3.0

TABLE II.- NONLINEAR-WASHOUT PARAMETER VALUES

Variable	Value in SI units	Program value (U.S. units)
d_x, per sec	0.707	0.707
e_x, per sec^2	0.25	0.25
$K_{x,1}$, sec^3/m^2 (sec^3/ft^2)	0.51668	0.048
W_x, m^2/sec^2 (ft^2/sec^2)	0.00929	0.1
b_x, per sec^4	0.01	0.01
c_x, per sec^2	0.2	0.2
$K_{c,1}$, per sec	0.02	0.02
$K_{c,2}$, per sec	0.5	0.5
$K_{x,2}$, sec^6/m^4 (sec^6/ft^4)	0.005793	0.00005
$K_{x,3}$, sec^3/m^2 (sec^3/ft^2)	0.010764	0.001
$p'_{x,1}(o)$	1	1
$p'_{x,2}(o)$, sec/m (sec/ft)	0.16404	0.05
$p'_{x,3}(o)$	0.5	0.5
S_x	0.5	0.5
d_y, per sec	1.2727	1.2727
e_y, per sec^2	0.81	0.81
$K_{y,1}$, sec^3/m^2 (sec^3/ft^2)	0.51668	0.048
W_y, m^2/sec^2 (ft^2/sec^2)	0.00929	0.1
b_y, per sec^4	0.1	0.1
c_y, per sec^2	2	2
$K_{c,3}$, per sec	0.05	0.05
$K_{c,4}$, per sec	1.5	1.5
$K_{y,2}$, sec^6/m^4 (sec^6/ft^4)	0	0
$K_{y,3}$, sec^3/m^2 (sec^3/ft^2)	0.2691	0.025
$p'_{y,1}(o)$	0.8	0.8
$p'_{y,2}(o)$, sec/m (sec/ft)	0.032808	0.01
$p'_{y,3}(o)$	0.3	0.3
S_y	0.5	0.5
e_ψ, per sec	0.3	0.3
K_ψ, sec^2	100	100
b_ψ, per sec^2	1	1
$K_{c,5}$, per sec	0.1	0.1
$p'_\psi(o)$	1	1

TABLE III.- BOEING 737 FLIGHT CHARACTERISTICS

Weight, N (lb)	400 341 (90 000)
Center of gravity	$0.31\bar{c}$
Flap deflection, deg	40
Landing gear	Down
Damping ratio for –	
Short period	0.562
Long period	0.089
Dutch roll	0.039
Period, sec, for –	
Short period	6.30
Long period	44.3
Dutch roll	5.12

TABLE IV.- RANDOMIZED COMPLETE BLOCK DESIGN FOR OBJECTIVE DATA

Pilot	Motion	Approach conditions		
		Standard	Weather front	Engine out
1	No	5 runs	5 runs	5 runs
	Yes	5 runs	5 runs	5 runs
2	No	5 runs	5 runs	5 runs
	Yes	5 runs	5 runs	5 runs
3	No	5 runs	5 runs	5 runs
	Yes	5 runs	5 runs	5 runs

Source	Degrees of freedom
Replicates	4
Pilots, A	2
Motion, B	1
Approach, C	2
AB	2
AC	4
BC	2
ABC	4
Error	68

TABLE V.- COMPUTED F-VALUES FOR THE ANALYSES OF VARIANCE FOR TWO MOTION CONDITIONS

Factors	Degrees of freedom	Root-mean-square performance measures									
		Deviation of –									
		Localizer		Glide slope		Speed		Pitch bar		Roll bar	
		Short duration	Long duration	Short duration	Long duration	Short duration	Long duration	Short duration	Long duration	Short duration	Long duration
Pilots, A	2	0.0578	0.0619	**11.56	**25.89	**11.08	**13.18	**15.24	**34.50	**5.343	**7.635
Motion, B	1	0.1463	0.1065	0.0199	0.0186	0.6034	0.0610	0.6817	0.1202	0.2363	3.850
Approaches, C . .	2	**42.55	**36.31	**9.414	**5.574	0.2739	*3.399	*3.943	1.5999	**132.0	**152.2
Replicates	4	0.7615	0.4040	0.6267	0.4790	0.3059	0.2240	1.126	0.9488	1.802	0.7457
AB	2	0.0346	0.3428	0.0334	0.2791	0.0845	0.0689	1.037	1.549	2.392	1.311
AC	4	0.4077	0.5740	*2.902	2.429	**3.734	**3.940	2.192	1.683	**5.259	**9.056
BC	2	0.0718	0.0415	0.5605	1.731	1.518	1.101	0.4292	0.8435	1.906	1.963
ABC	4	0.4217	0.6464	0.2776	0.7830	0.6870	0.2644	0.1638	0.5340	1.105	0.4287
Error	68	--------	--------	--------	--------	--------	--------	--------	--------	---------	---------

*Indicates 5-percent significance level.

**Indicates 1-percent significance level.

TABLE VI.- RANDOMIZED COMPLETE BLOCK DESIGN FOR OBJECTIVE DATA INCLUDING NONLINEAR WASHOUT

Pilot	Motion	Approach conditions		
		Standard	Weather front	Engine out
1	No Linear Nonlinear	5 runs ↓	5 runs ↓	5 runs ↓
2	No Linear Nonlinear	5 runs ↓	5 runs ↓	5 runs ↓
3	No Linear Nonlinear	5 runs ↓	5 runs ↓	5 runs ↓

Source	Degrees of freedom
Replicates	4
Pilots, A	2
Approach, B	2
Motion, C	2
AB	4
AC	4
BC	4
ABC	8
Error	104
Total	134

TABLE VII.- COMPUTED F-VALUES FOR THE ANALYSES OF VARIANCE FOR THREE MOTION CONDITIONS

Factors	Degrees of freedom	Localizer		Glide slope		Speed		Pitch bar		Roll bar	
		Short duration	Long duration	Short duration	Long duration	Short duration	Long duration	Short duration	Long duration	Short duration	Long duration
Pilots, A	2	**5.089	**6.172	**21.57	**36.44	**16.22	**20.90	**79.54	**49.78	**8.043	**5.136
Motion, B	2	**6.493	**11.33	0.3925	*3.896	2.333	0.5585	0.6096	**5.617	1.104	2.583
Approaches, C . .	2	**42.23	**43.06	**17.35	**13.78	0.2270	**6.219	**8.872	**6.806	**193.1	**204.1
Replicates	4	0.0881	0.4534	0.2849	0.5830	0.3592	0.7069	0.3855	0.5184	0.0999	0.2394
AB	4	**5.392	**6.059	0.9902	*2.805	0.1112	0.1797	1.495	*2.861	1.191	*2.501
AC	4	**6.987	**8.804	**3.654	2.143	**4.235	*2.885	*2.693	1.237	**11.28	**14.94
BC	4	**4.819	**7.075	0.5791	1.320	0.9356	0.6806	0.6905	1.381	0.9834	1.609
ABC	8	**6.216	**8.832	0.5219	1.304	1.034	1.691	0.2964	0.7259	1.043	1.799
Error	104	--------	--------	--------	--------	--------	--------	--------	--------	---------	---------

*Indicates 5-percent significance level.

**Indicates 1-percent significance level.

TABLE VIII.- PILOT RATINGS OF LONGITUDINAL MOTION CUES
FOR LINEAR- AND NONLINEAR-WASHOUT METHODS

Input	Pilot rating								
	Excellent	Half-way	Good	Half-way	Fair	Half-way	Poor	Half-way	Unacceptable
Throttle			▷△▽⬡○□ ▶▲▼⬢●■		◁ ◀				
Column	△ ▲	⬡ ◀⬢	▷▽ ◁▶▼●■	○	□				

Pilot	Linear washout	Nonlinear washout	
1	△	▲	737 cockpit experience
2	▽	▼	
3	▷	▶	
4	◁	◀	
5	□	■	
6	⬡	⬢	
7	○	●	

TABLE IX.- PILOT RATINGS OF MOTION CUES FOR AIRPLANE MODEL WITHOUT β FEEDBACK

Input		Pilot rating								
		Excellent	Half-way	Good	Half-way	Fair	Half-way	Poor	Half-way	Unacceptable
Wheel and pedal	Roll		◀▲⬢	▶▼■●	◁	△○		□	▽⬡	▷
	Yaw			△ ▶▼▲⬢■	◀●	◁⬡○		▷▽□		
Overall airplane feel			◀▲	●▼⬢■	▶△	○◁	⬡	▽□		▷

Pilot	Linear washout	Nonlinear washout	
1	△	▲	737 cockpit experience
2	▽	▼	
3	▷	▶	
4	◁	◀	
5	□	■	
6	⬡	⬢	
7	○	●	

TABLE X.- PILOT RATINGS OF MOTION CUES FOR AIRPLANE MODEL WITH β FEEDBACK

Input		Pilot rating								
		Excellent	Half-way	Good	Half-way	Fair	Half-way	Poor	Half-way	Unacceptable
Wheel and pedal	Roll	●	▶◀▲▼⬢	■	▷	◁○		△▽⬡□		
	Yaw		▼●	▶◀▲⬢■	○	◁▽		▷△⬡□		
Overall airplane feel		●	▶◀▲	▼⬢■	○	▷◁	⬡	△▽□		

Pilot	Linear washout	Nonlinear washout	
1	△	▲	737 cockpit experience
2	▽	▼	
3	▷	▶	
4	◁	◀	
5	□	■	
6	⬡	⬢	
7	○	●	

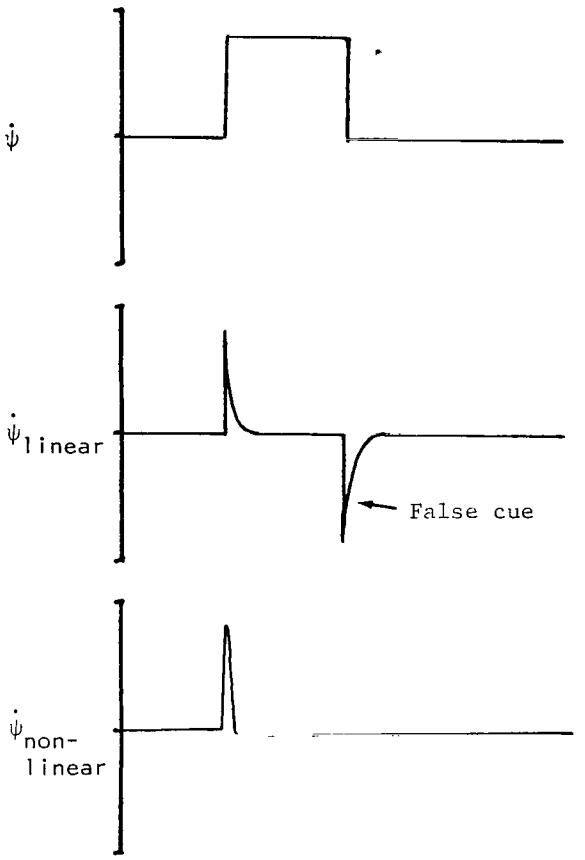

Figure 1.- Response of first-order linear and nonlinear filters to a pulse input.

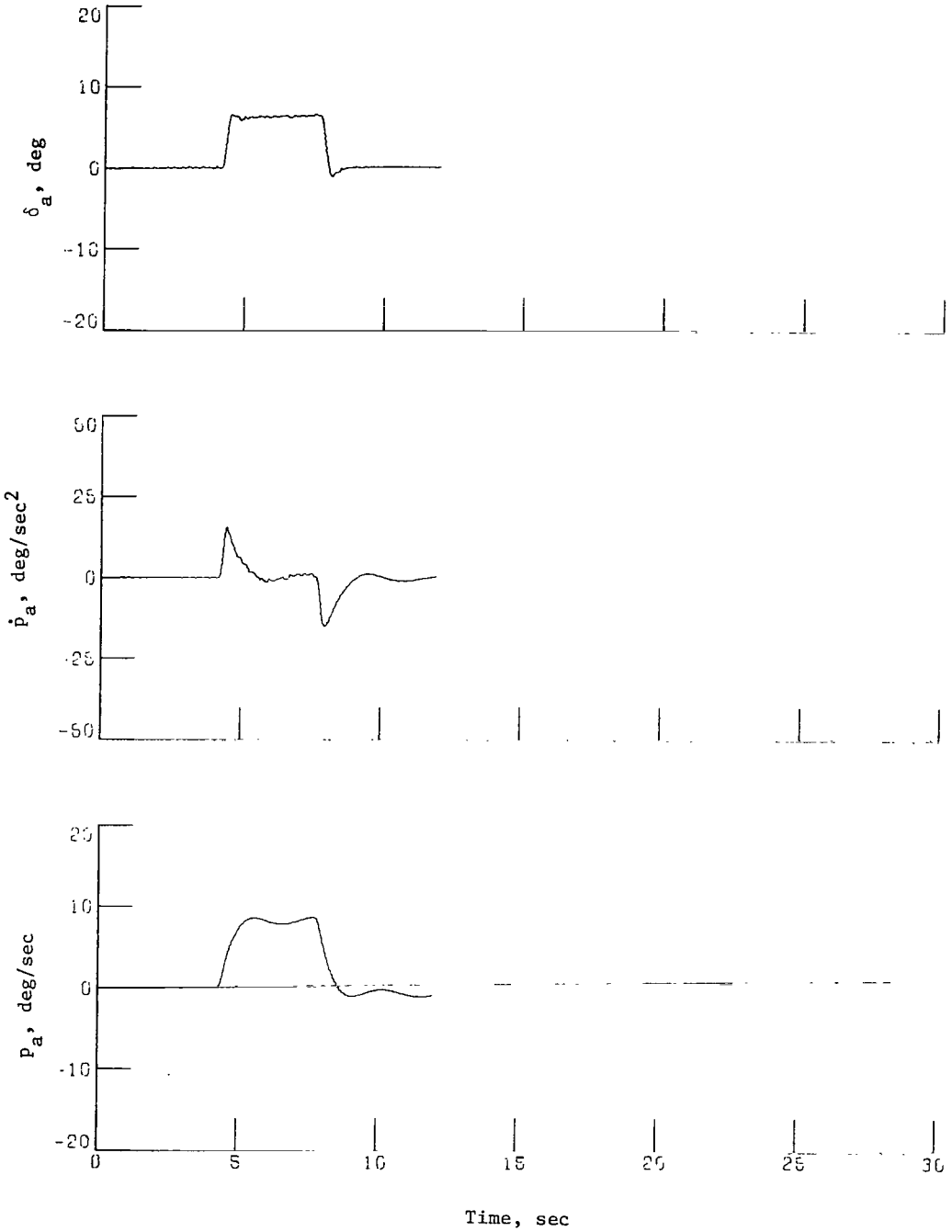

(a) 737 response.

Figure 2.- Time histories for an aileron pulse input.

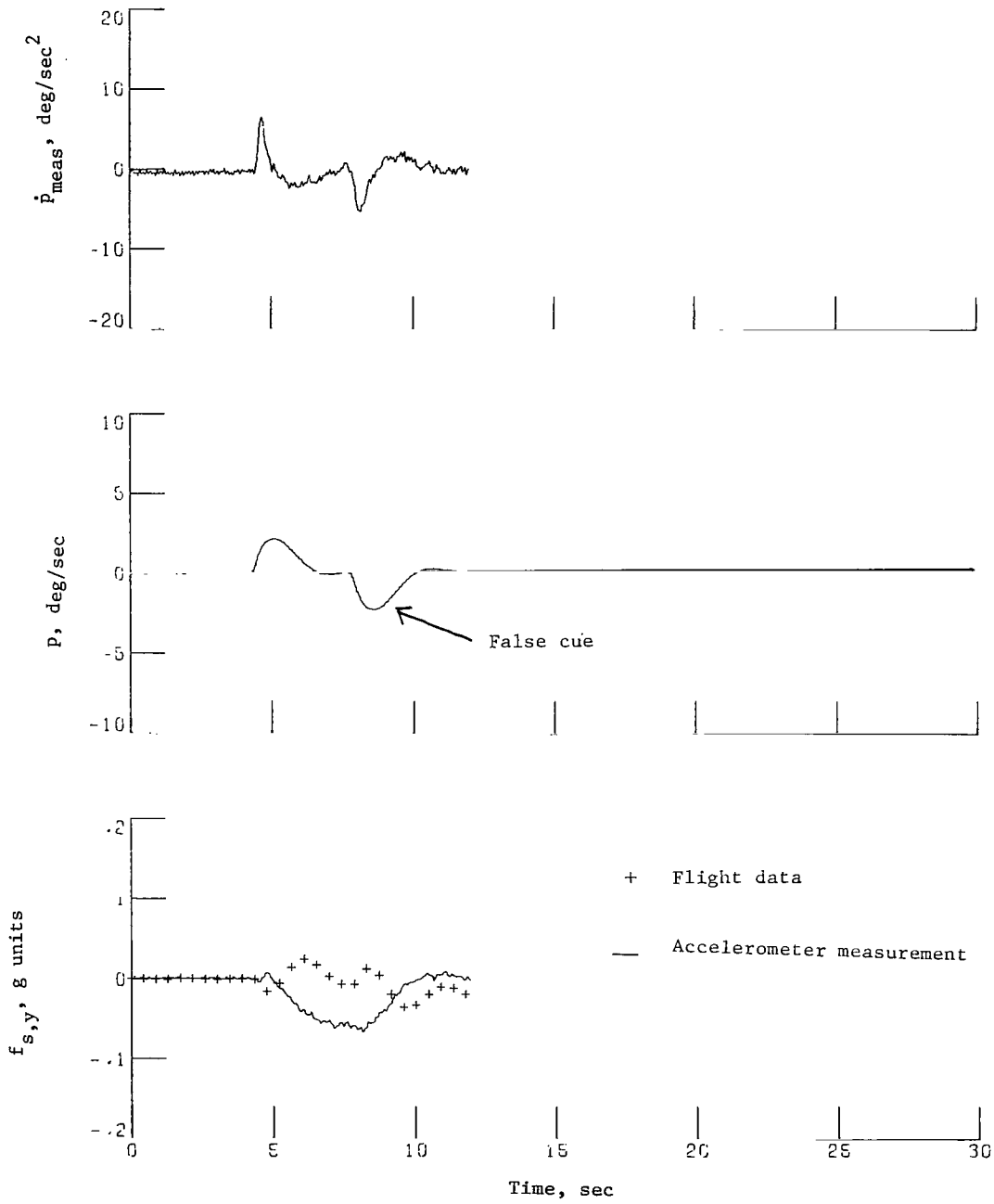

(b) Linear-washout response.

Figure 2.- Continued.

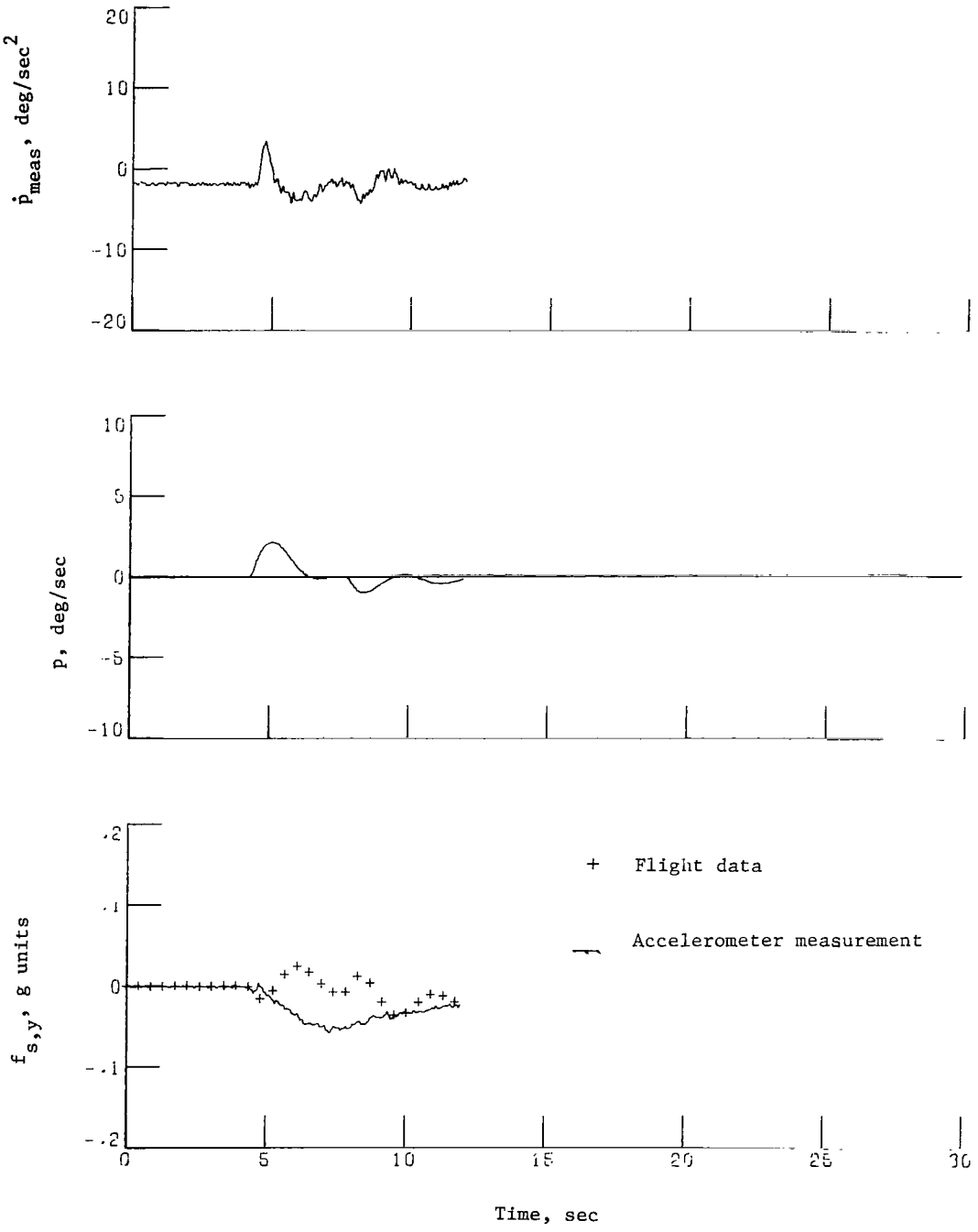

(c) Nonlinear-washout response.

Figure 2.- Concluded.

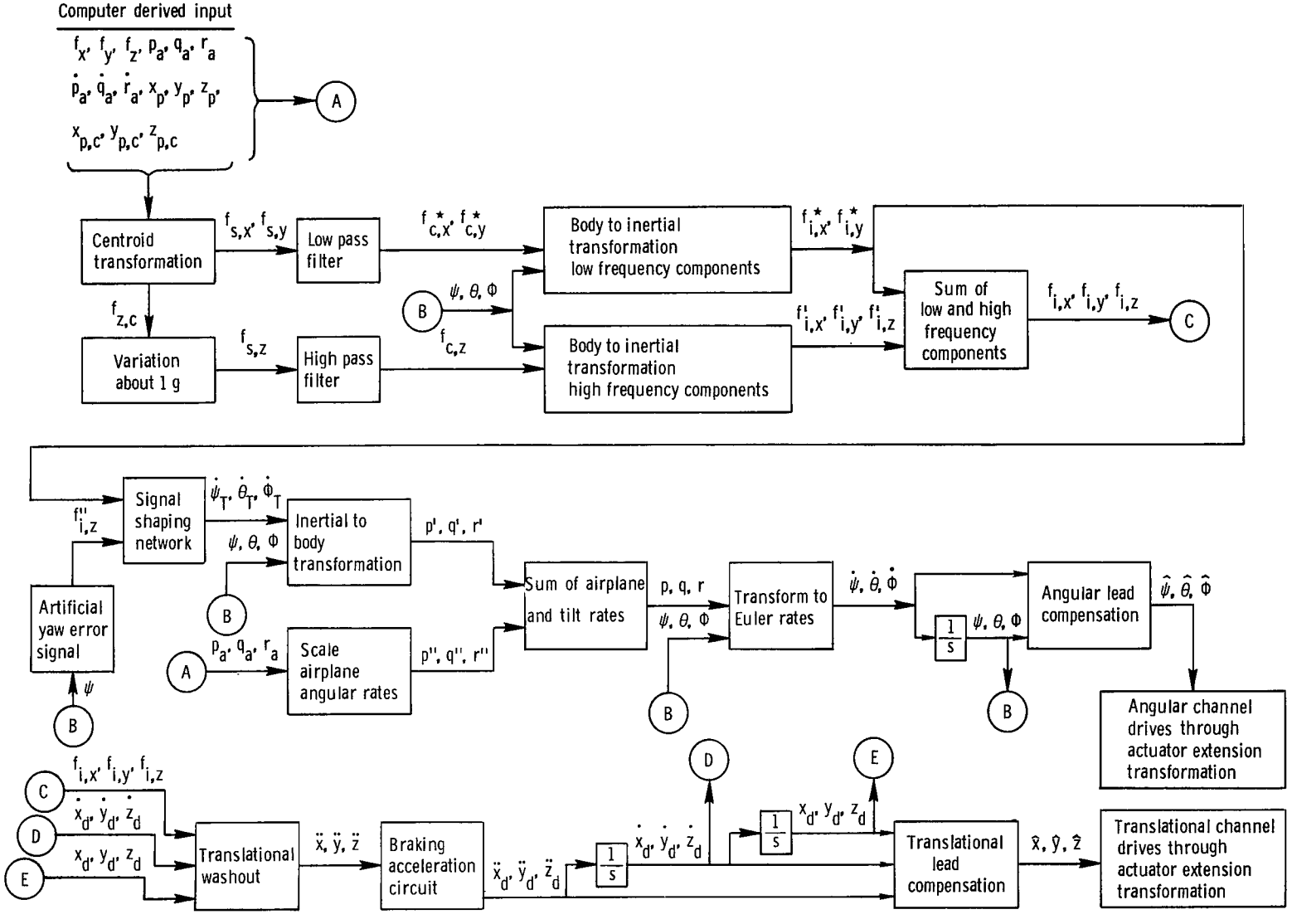

(a) Complete diagram.

Figure 3.- Detailed block diagram of washout circuitry.

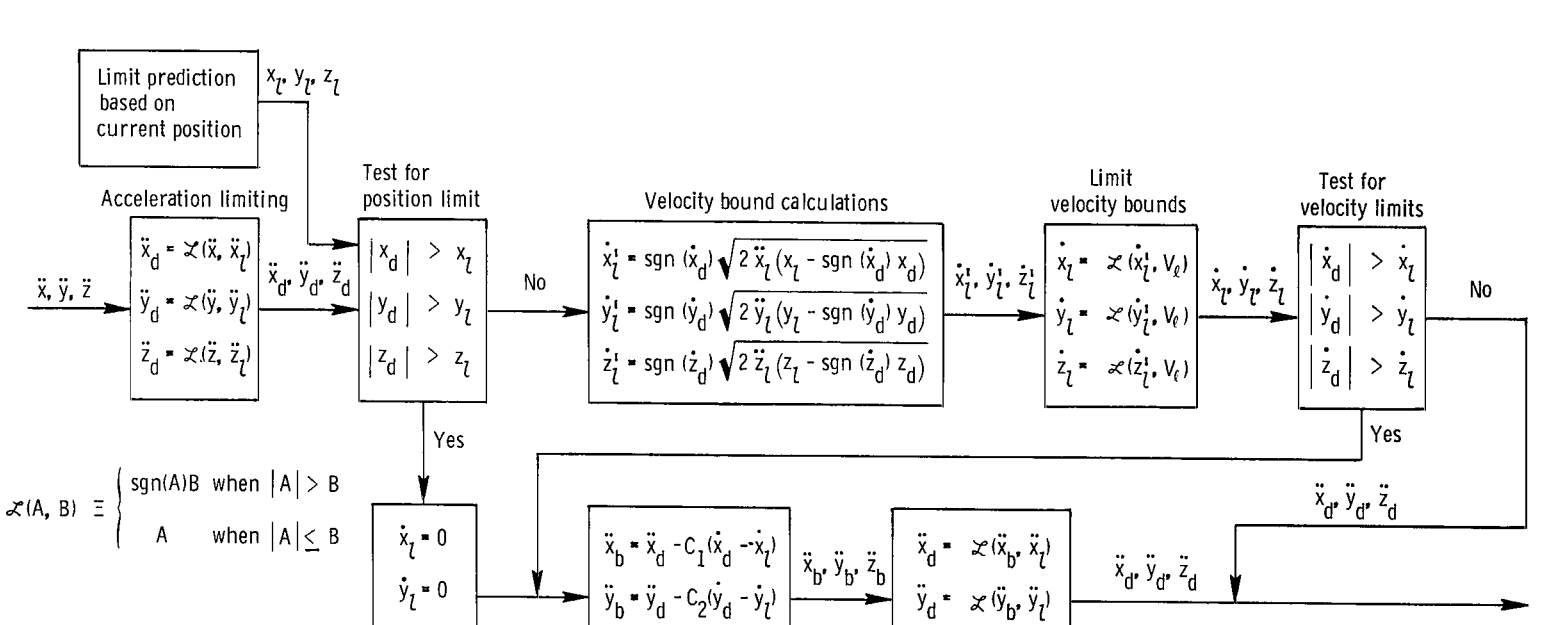

(b) Braking-acceleration circuit.

Figure 3.- Concluded.

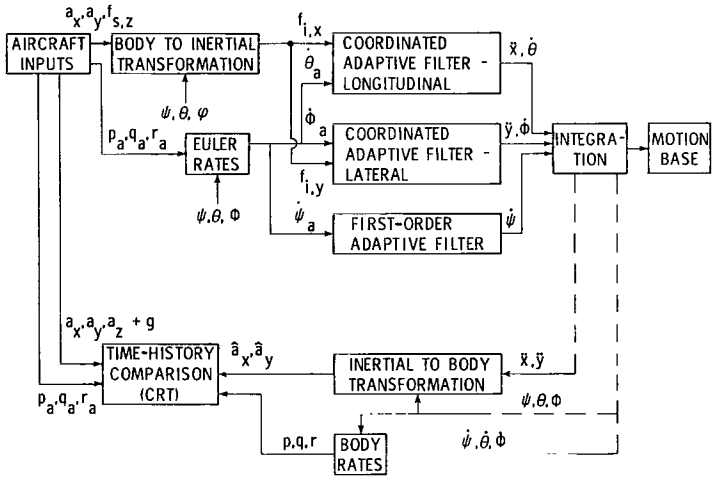

Figure 4.- Block diagram of coordinated adaptive washout.

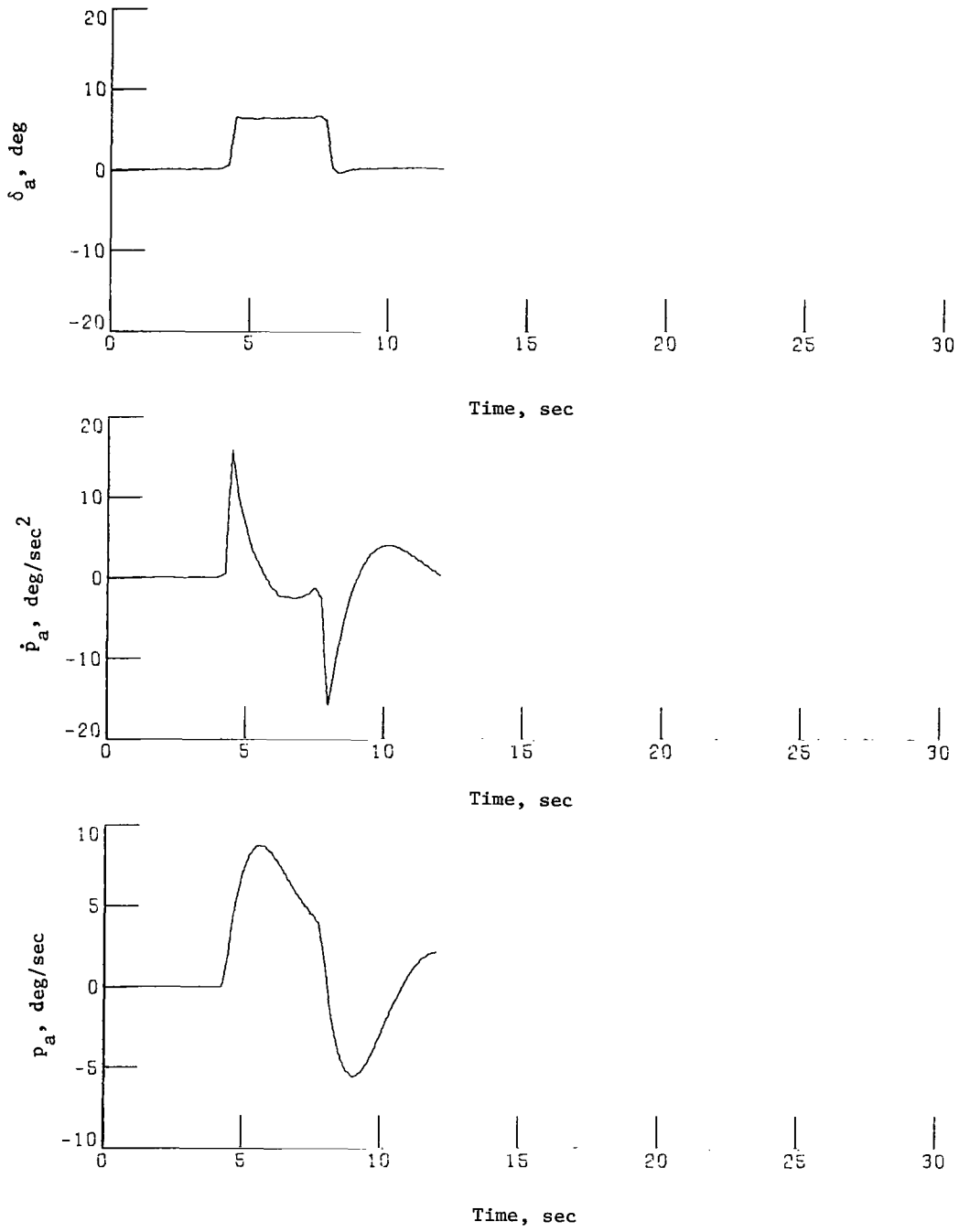

(a) 737 response without β feedback.

Figure 5.- Time histories for an aileron pulse input.

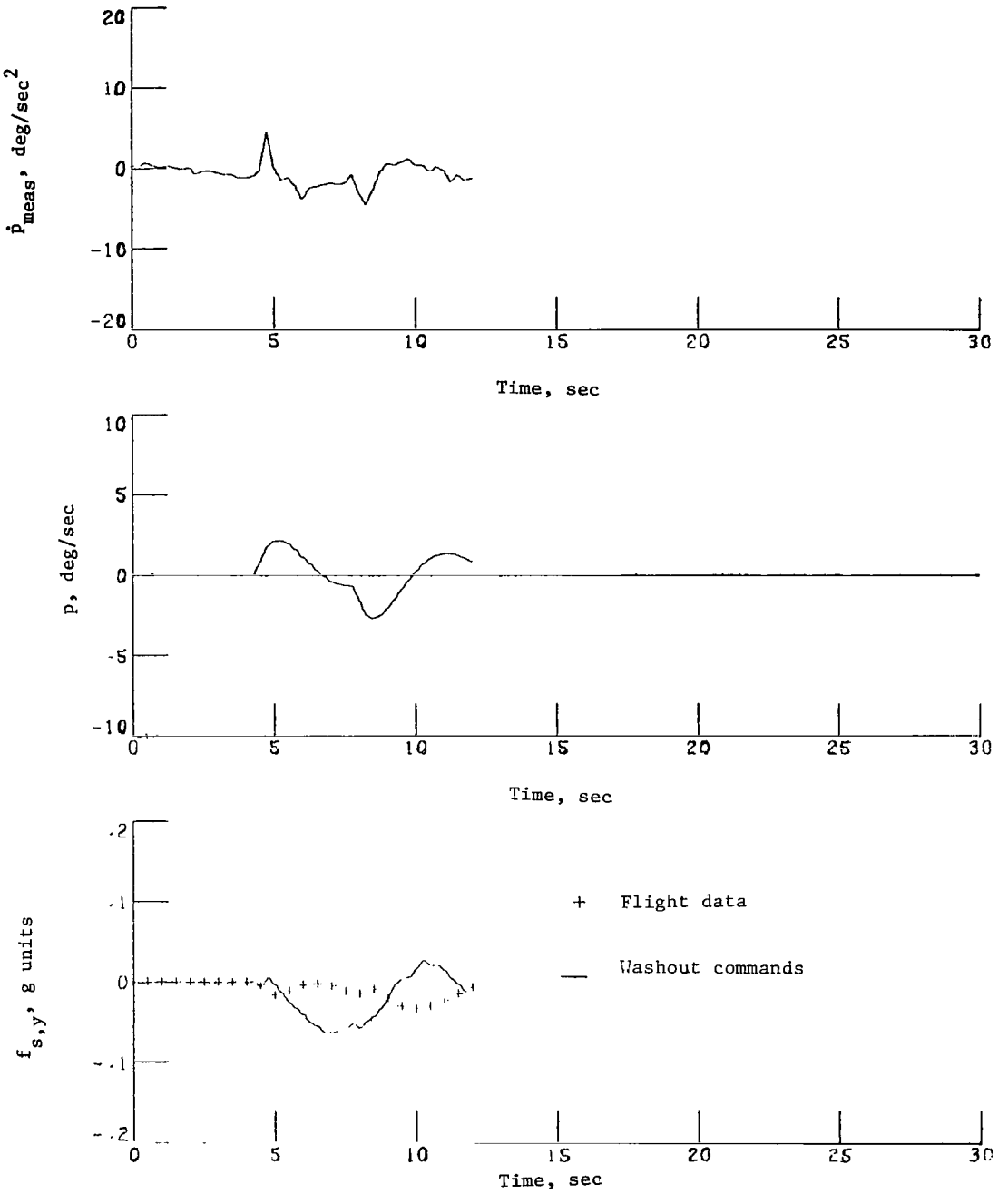

(b) Linear-washout response.

Figure 5.- Continued.

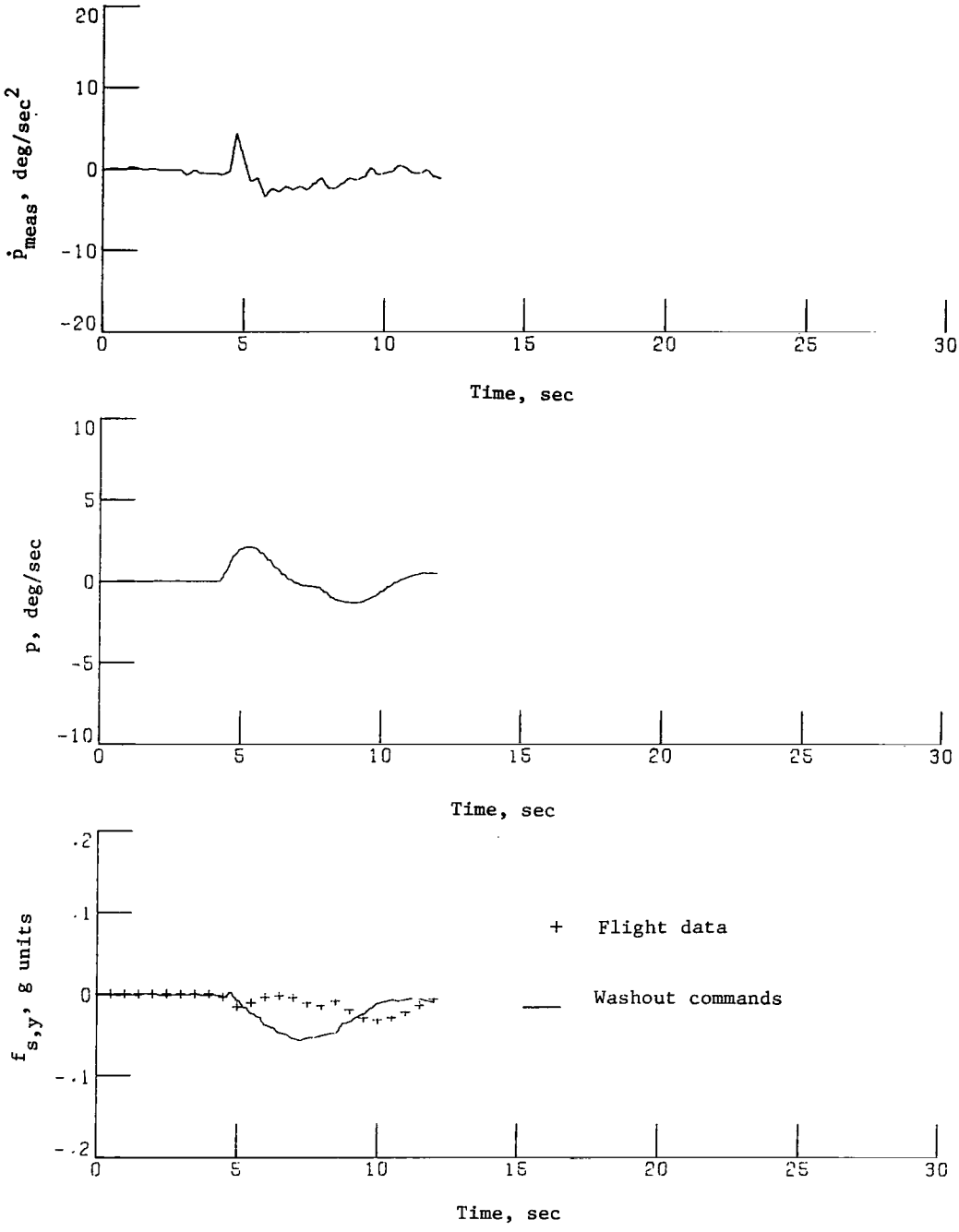

(c) Nonlinear-washout response.

Figure 5.- Concluded.

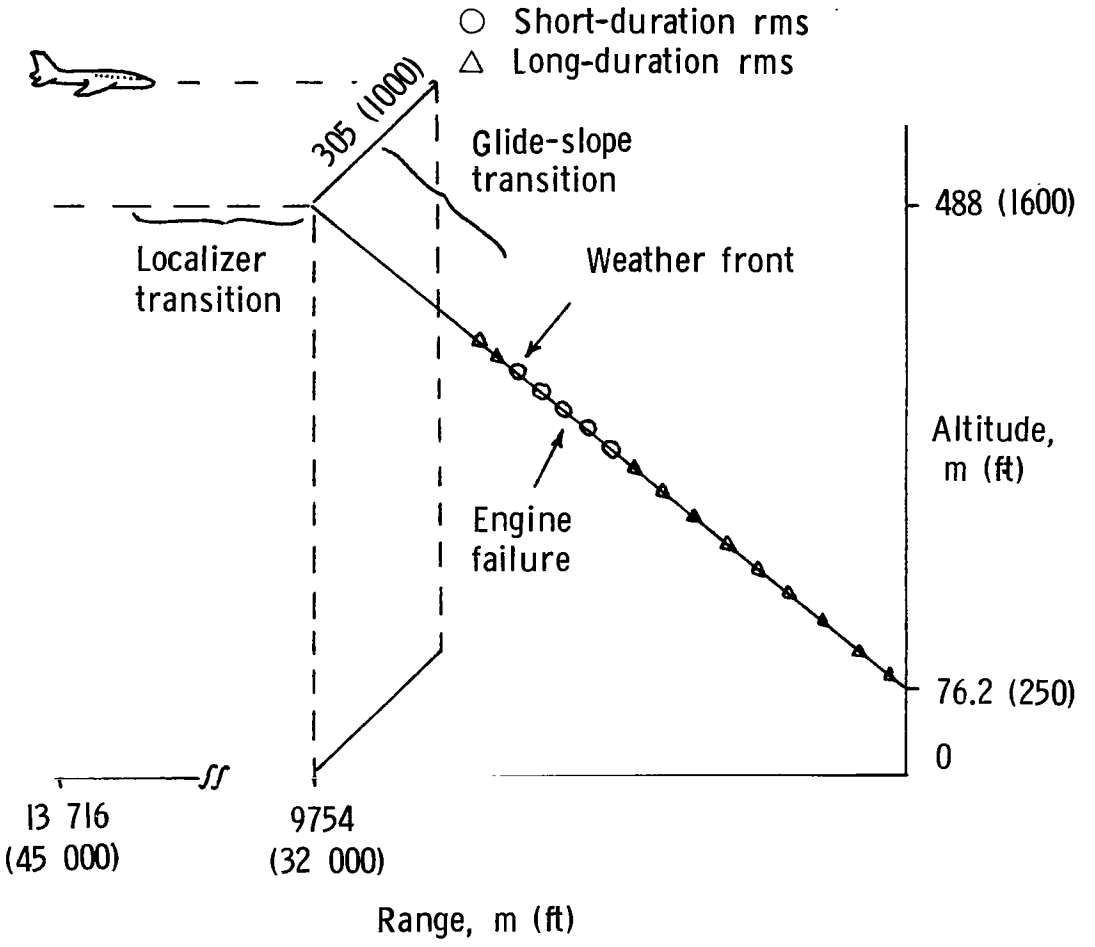

Figure 6.- Approach conditions.

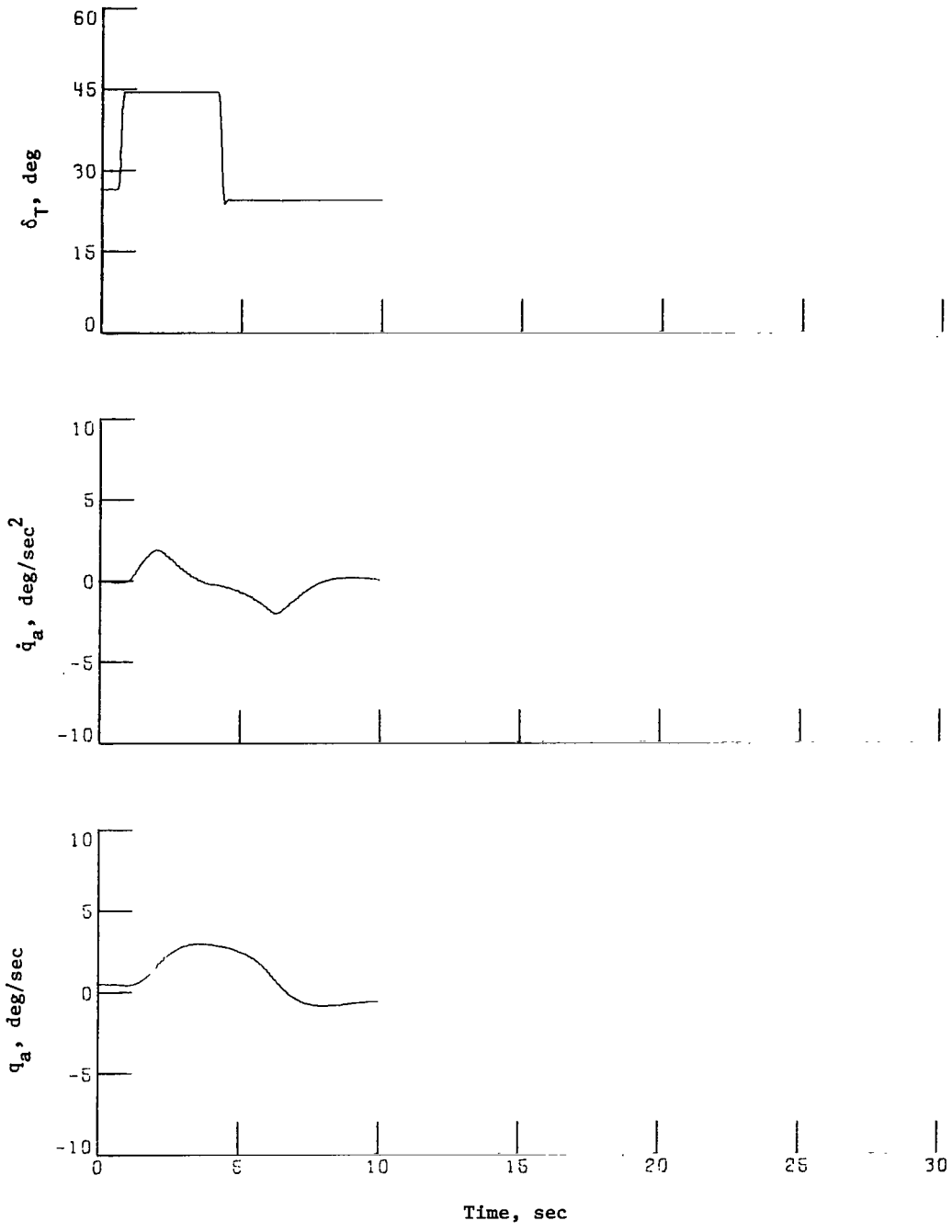

(a) 737 response.

Figure 7.- Time histories for a throttle input.

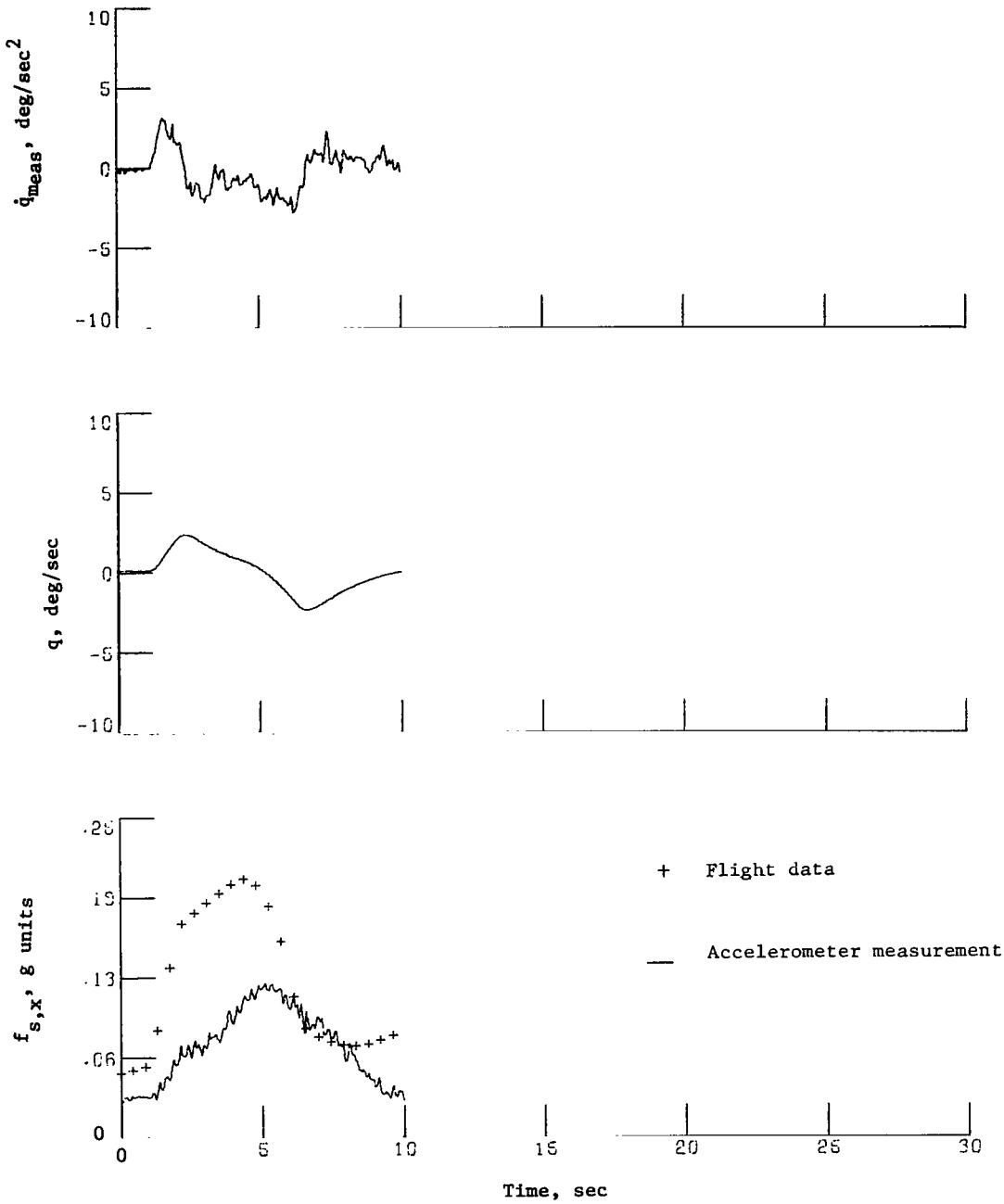

(b) Linear-washout response.

Figure 7.- Continued.

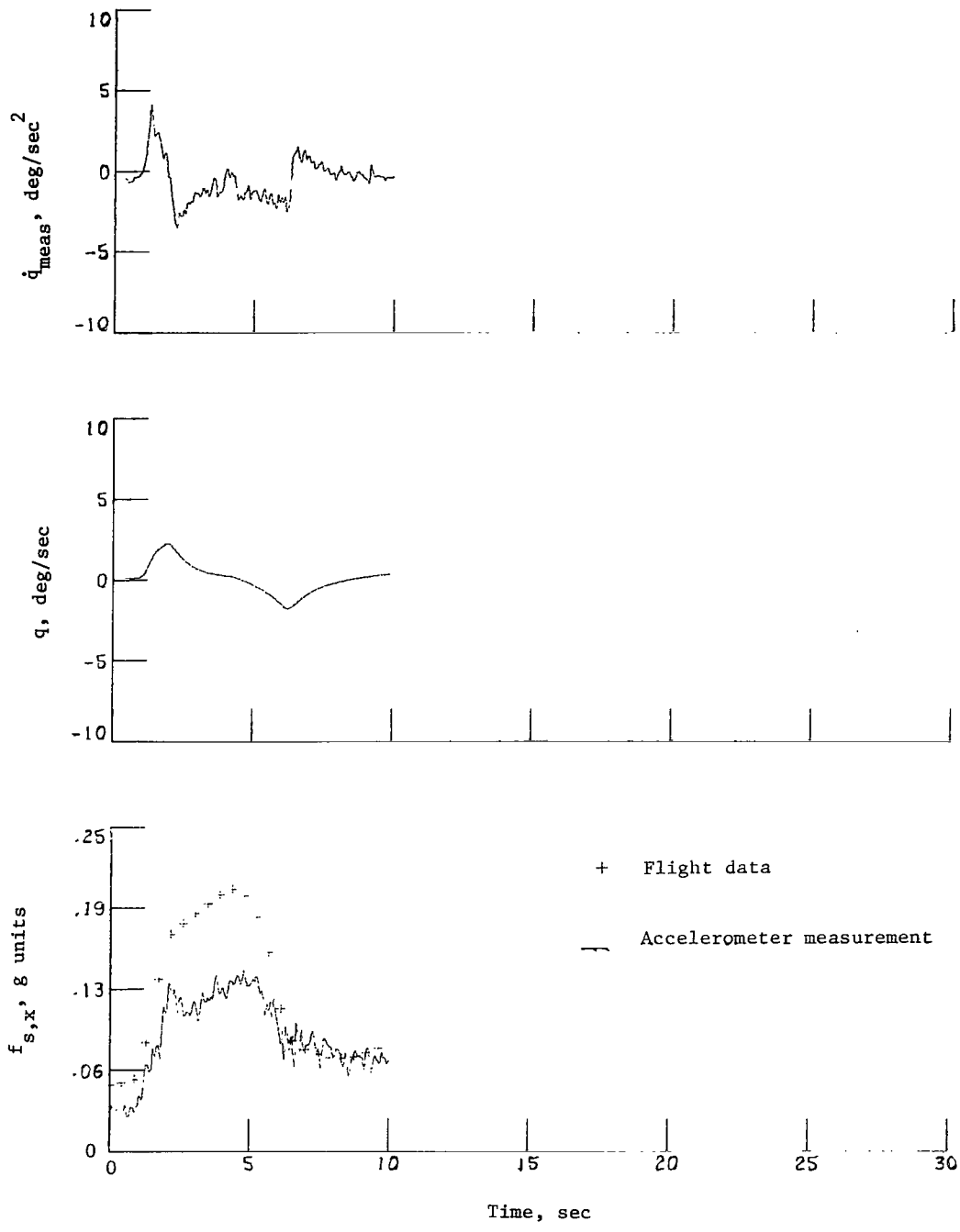

(c) Nonlinear-washout response.

Figure 7.- Concluded.

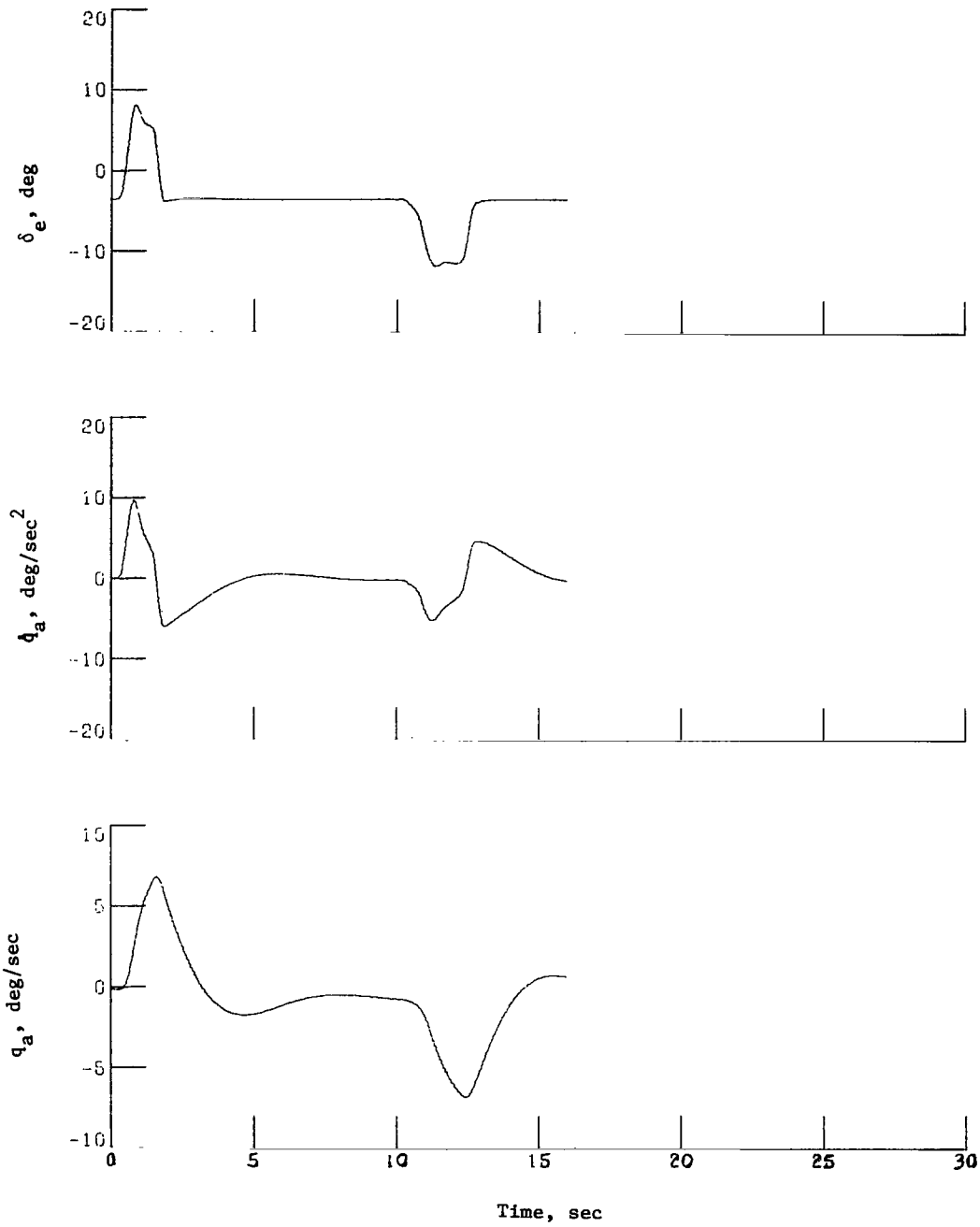

(a) 737 response.

Figure 8.- Time histories for an elevator input.

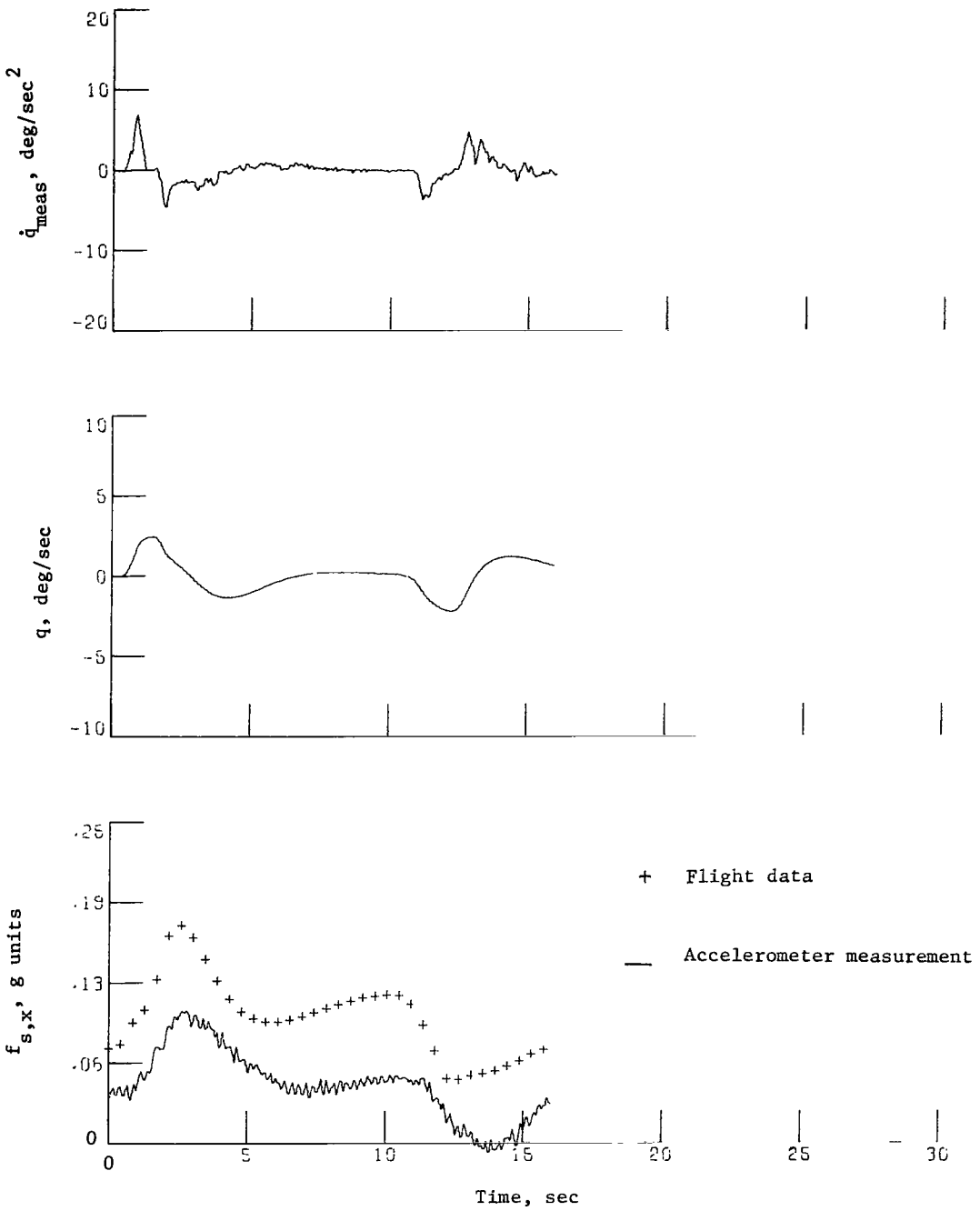

(b) Linear-washout response.

Figure 8.- Continued.

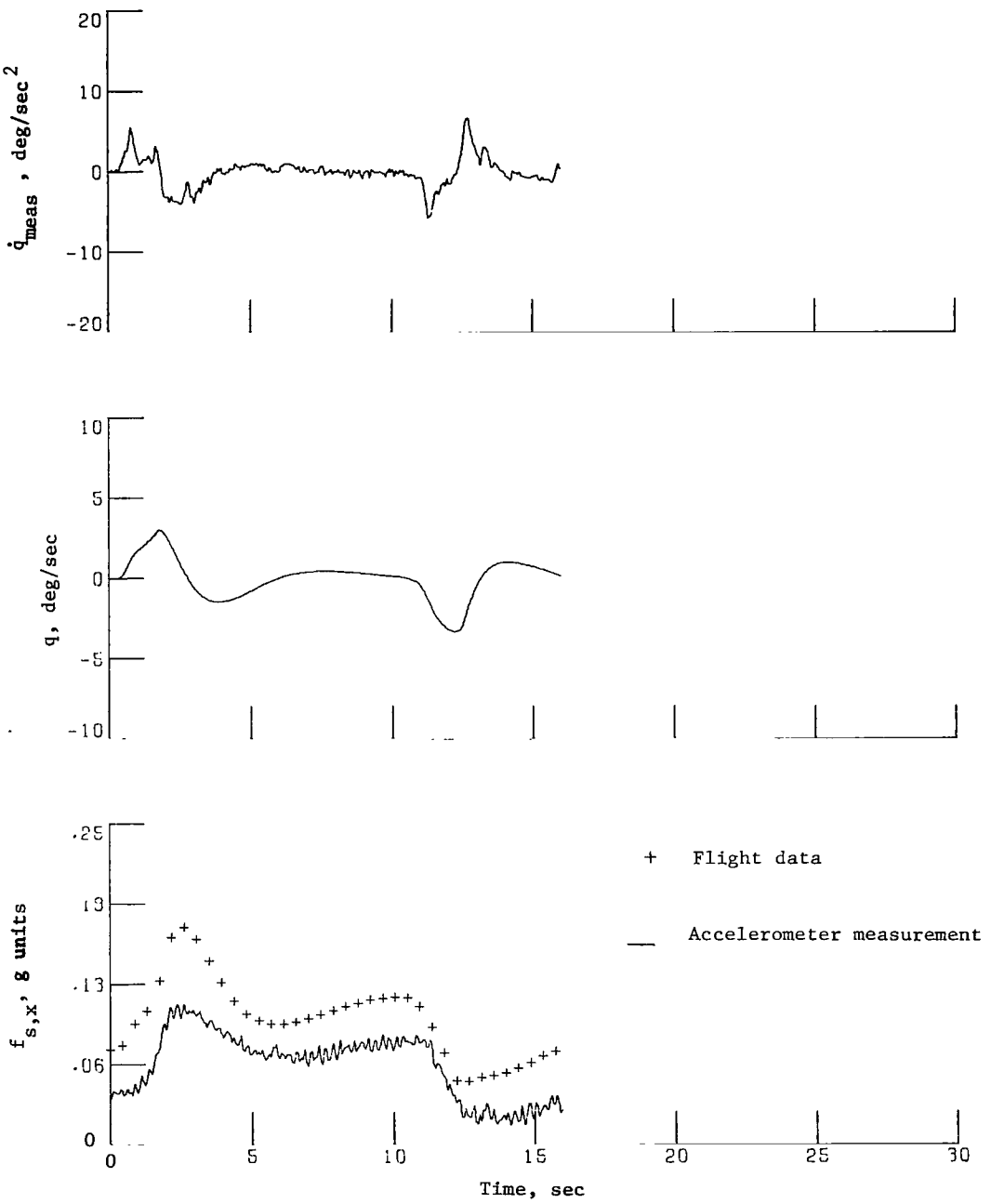

(c) Nonlinear-washout response.

Figure 8.- Concluded.

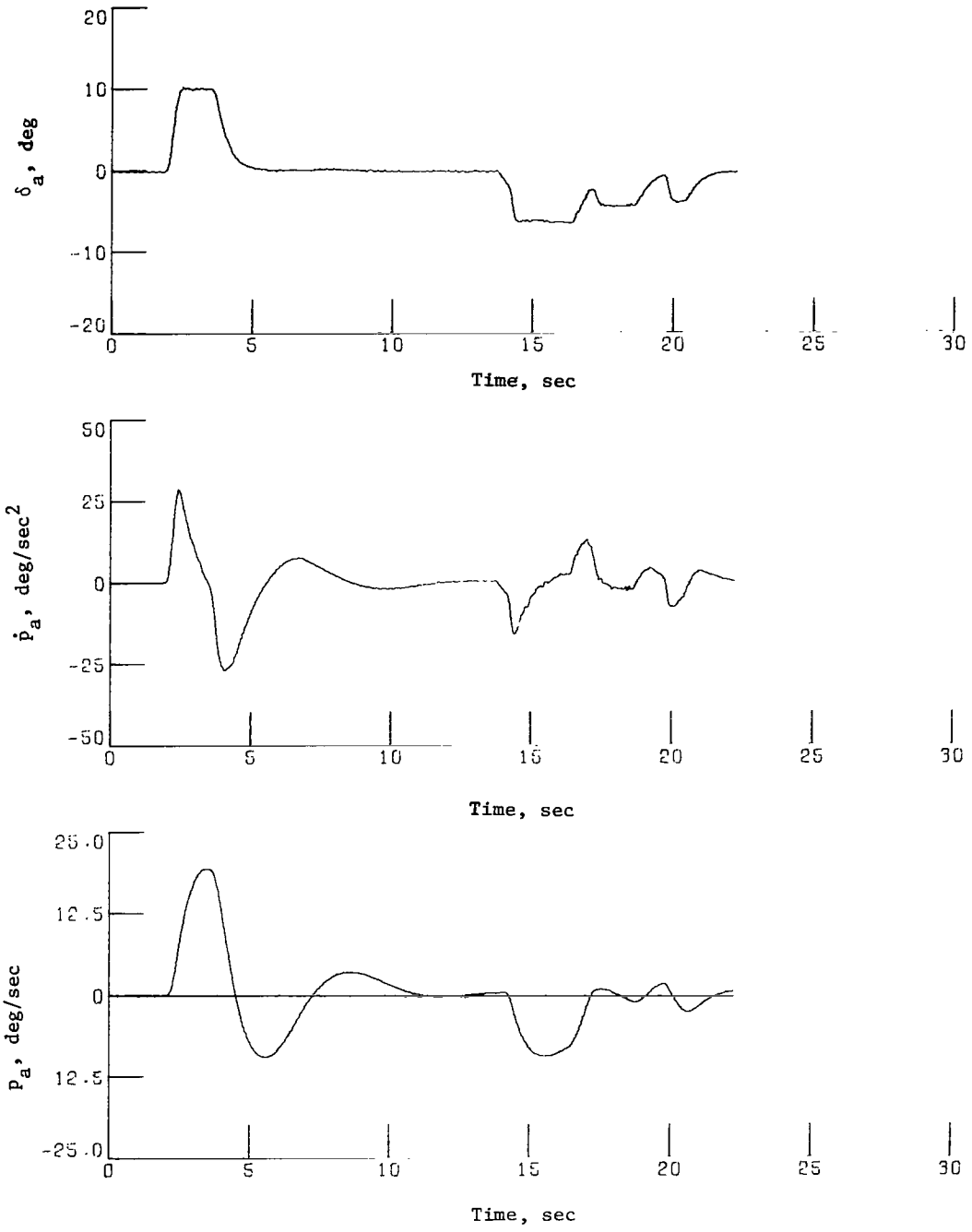

(a) 737 response without β feedback.

Figure 9.- Time histories of roll cues for aileron inputs.

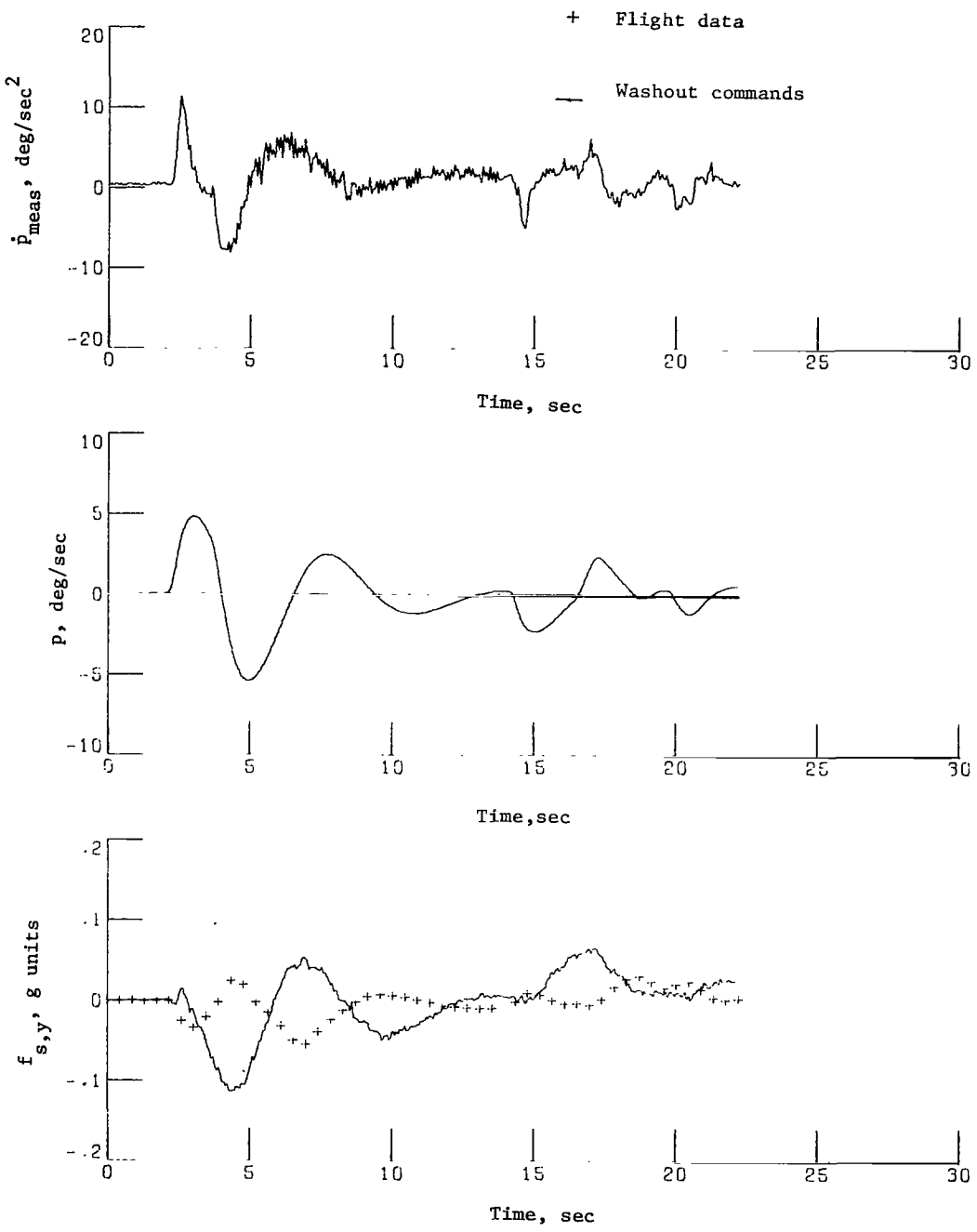

(b) Linear-washout response.

Figure 9.- Continued.

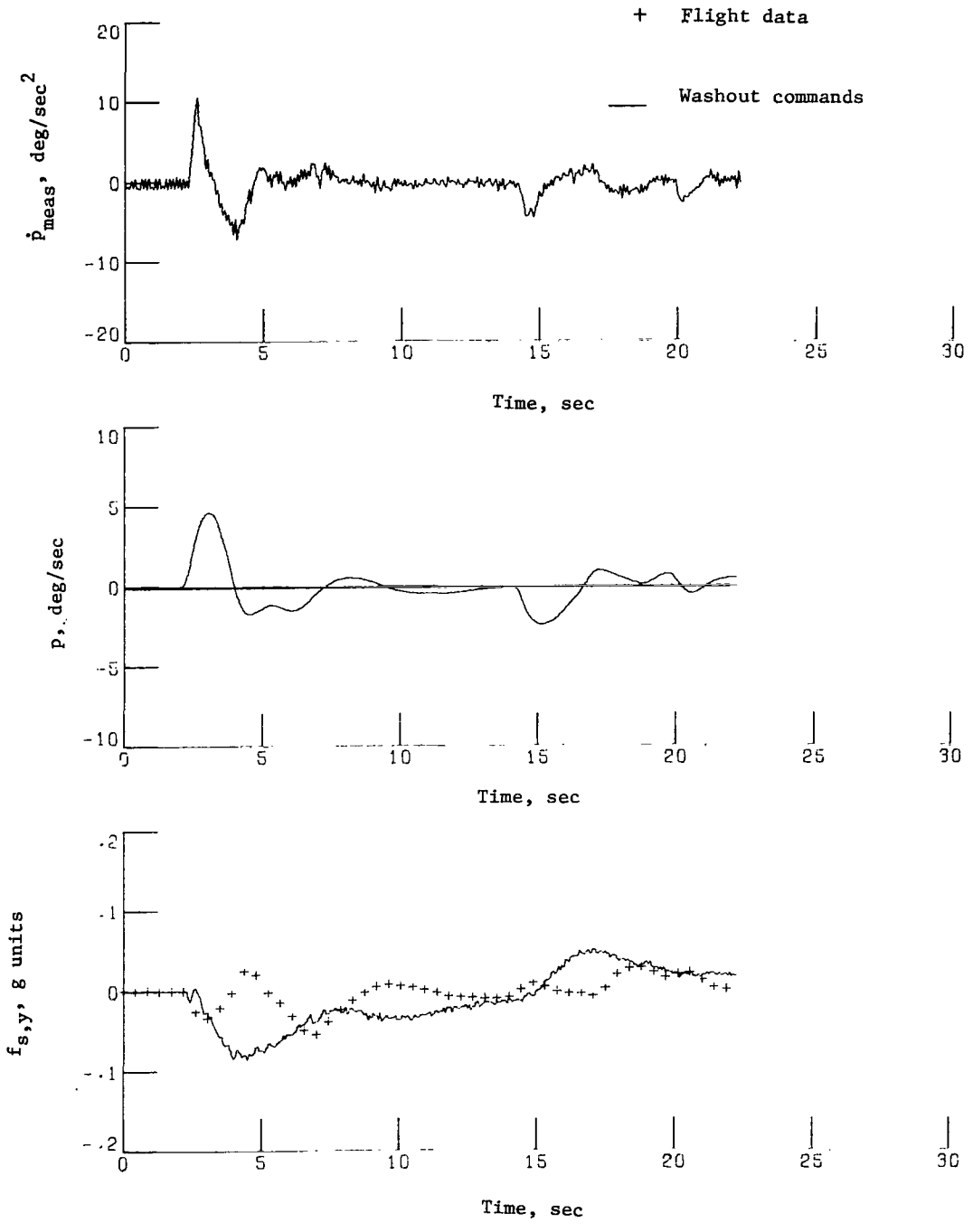

(c) Nonlinear-washout response.

Figure 9.- Concluded.

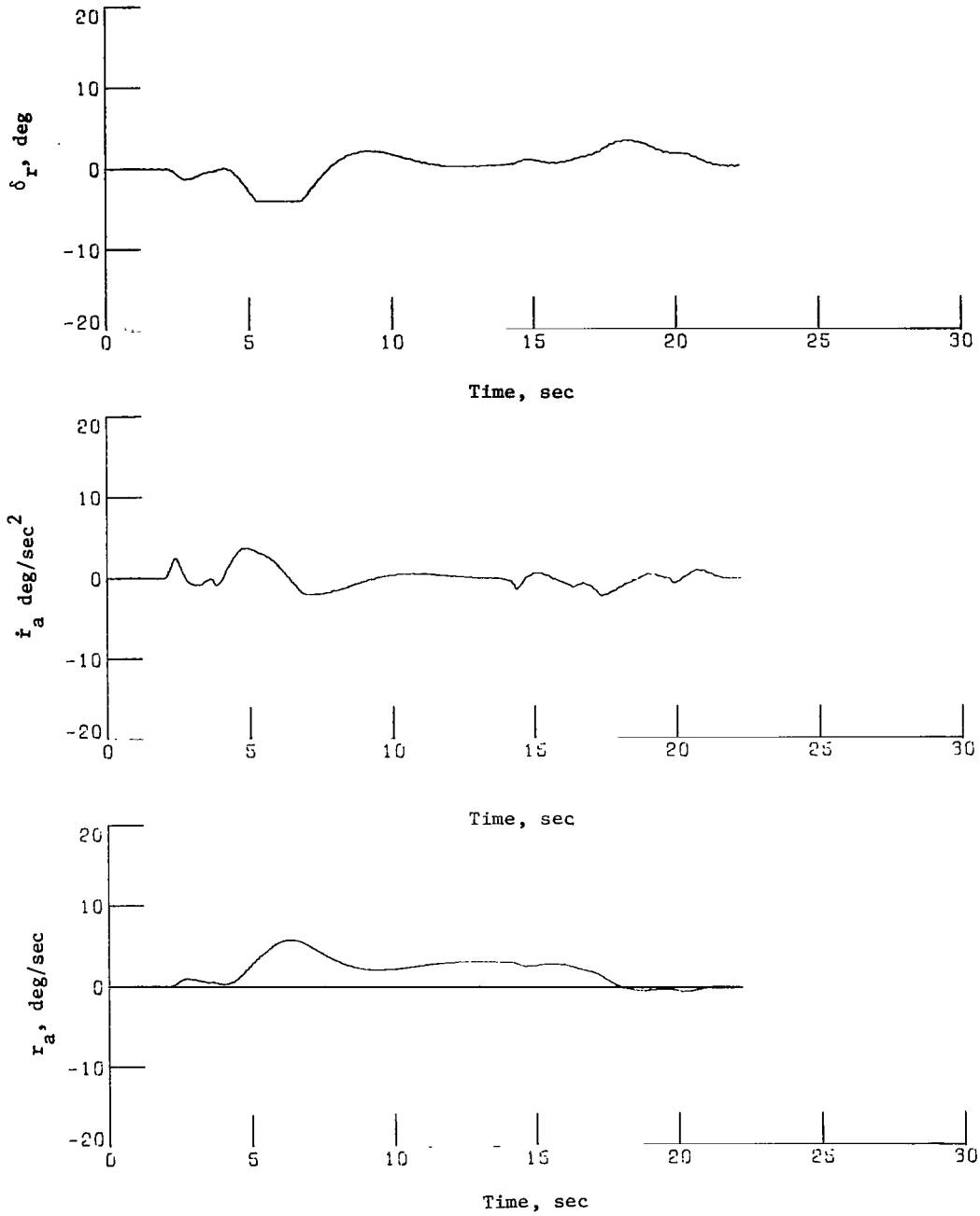

(a) 737 response without β feedback.

Figure 10.- Time histories of yaw cues for aileron inputs.

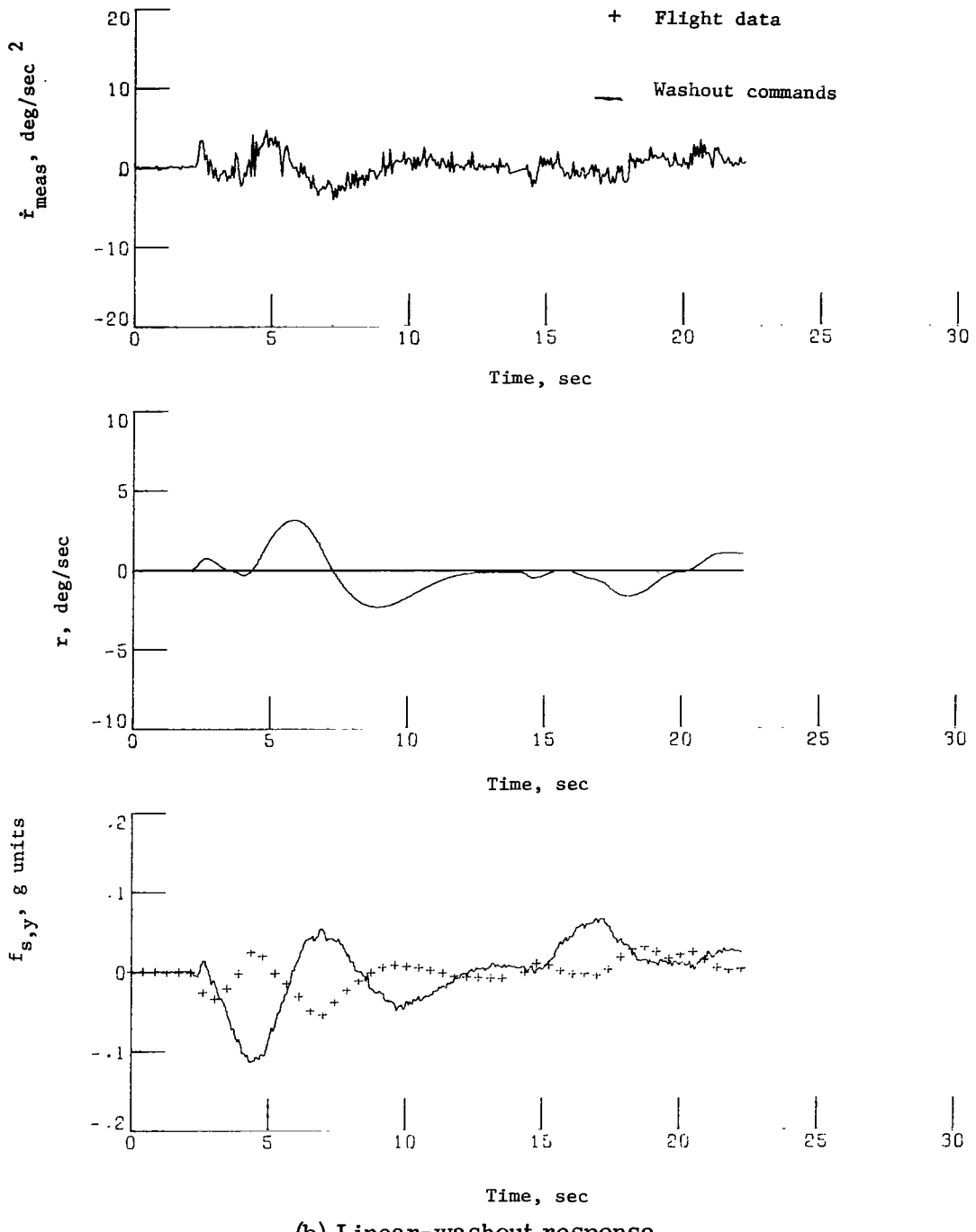

(b) Linear-washout response.

Figure 10.- Continued.

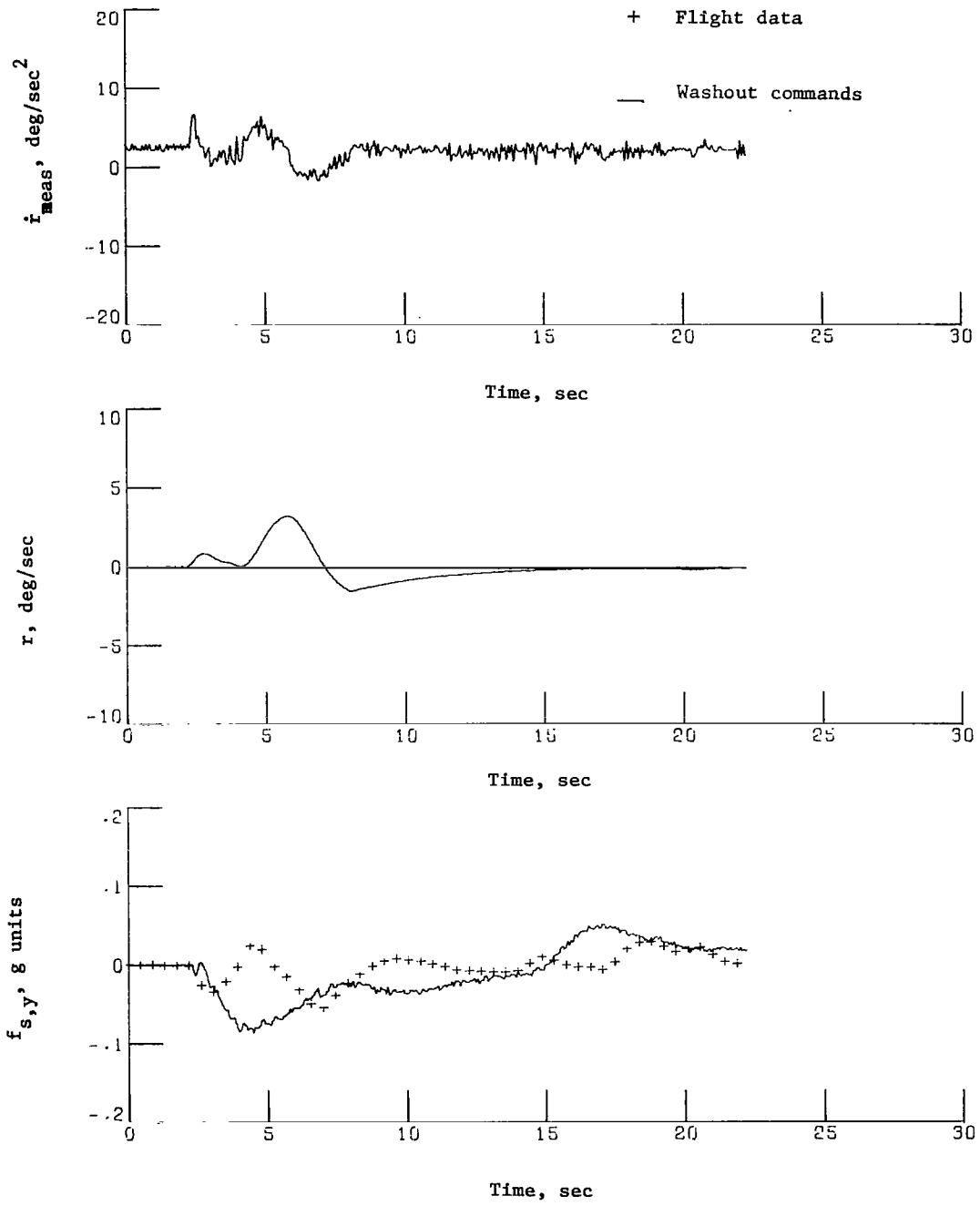

(c) Nonlinear-washout response.

Figure 10.- Concluded.

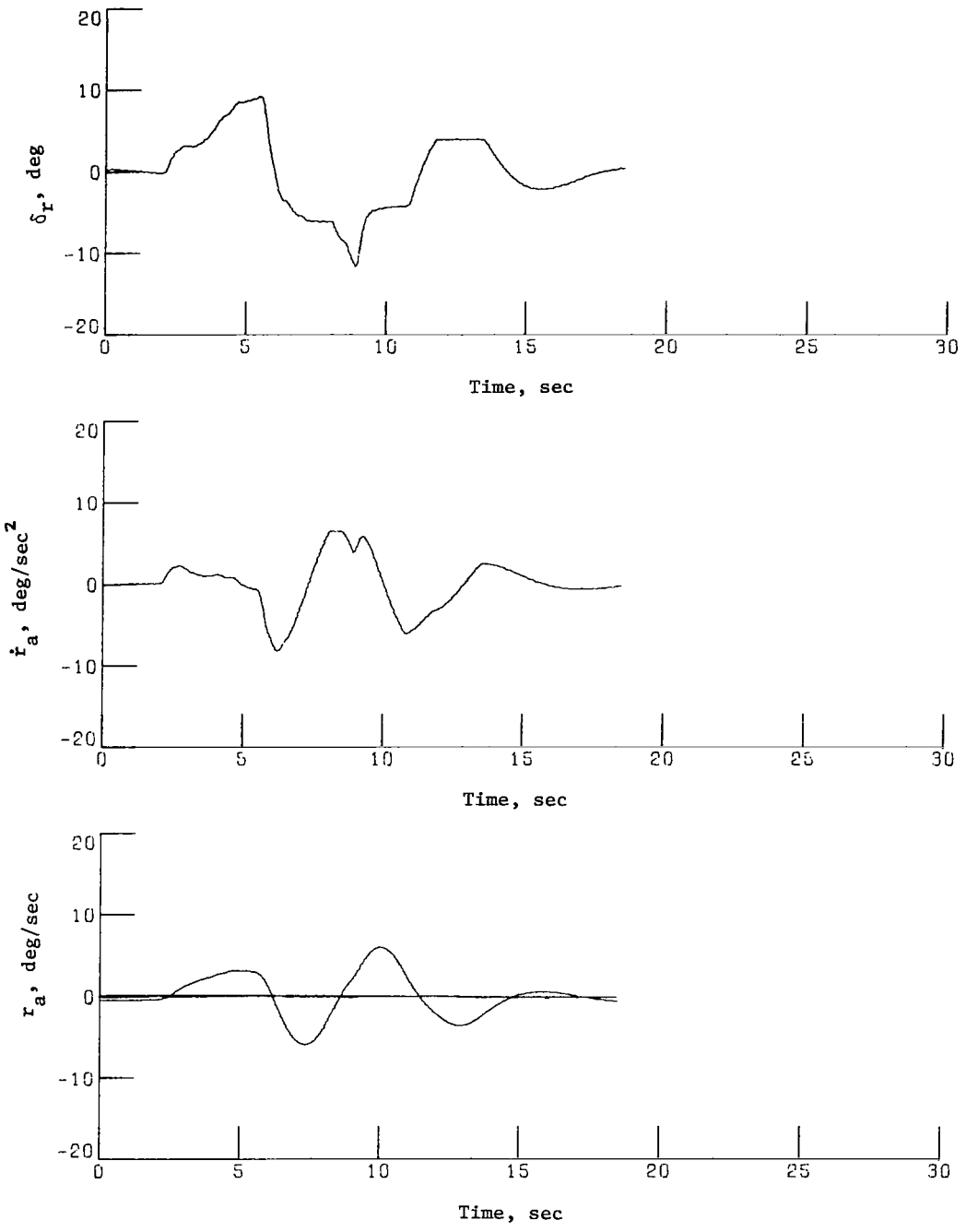

(a) 737 response without β feedback.

Figure 11.- Time histories of yaw cues for rudder inputs.

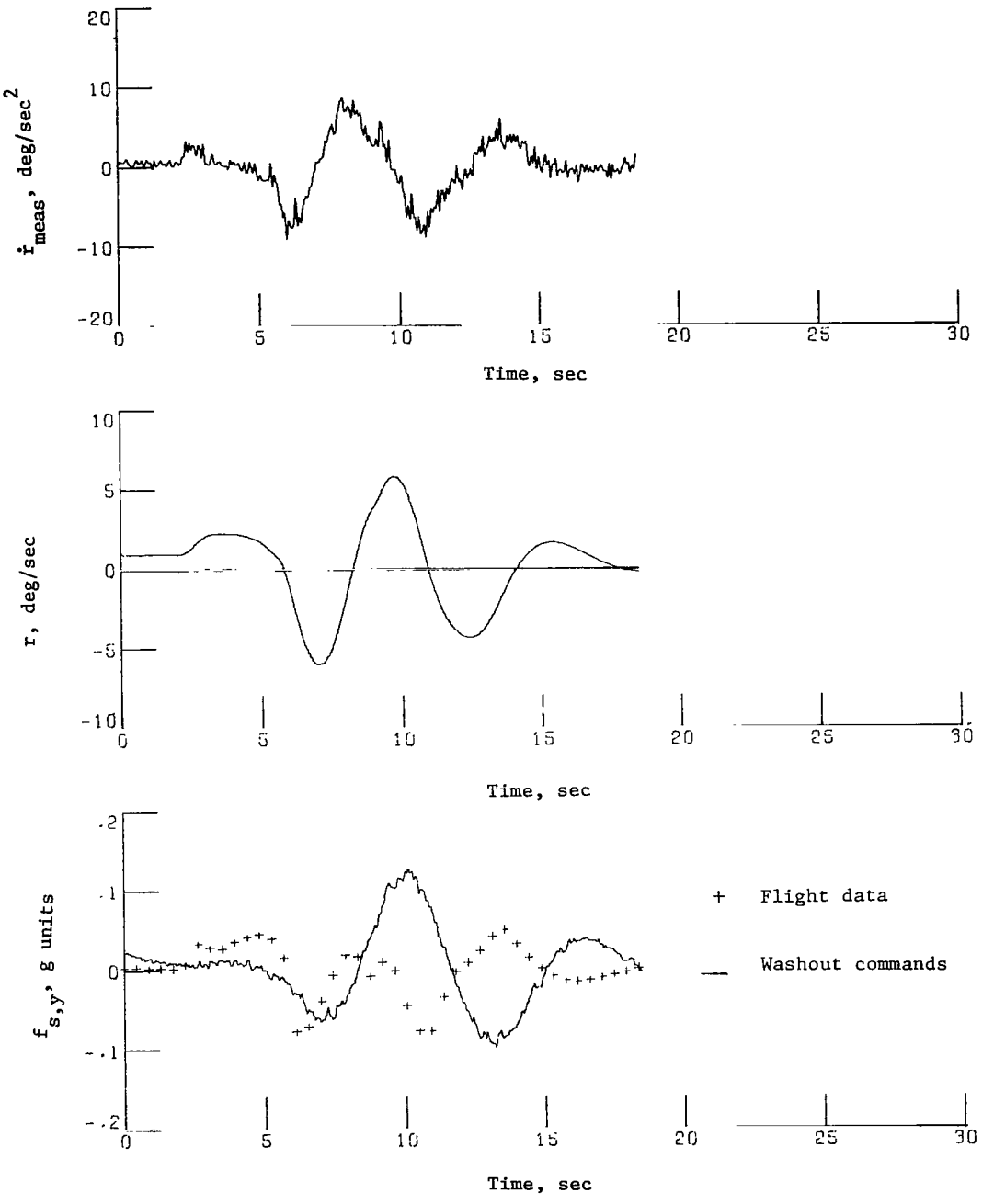

(b) Linear-washout response.

Figure 11.- Continued.

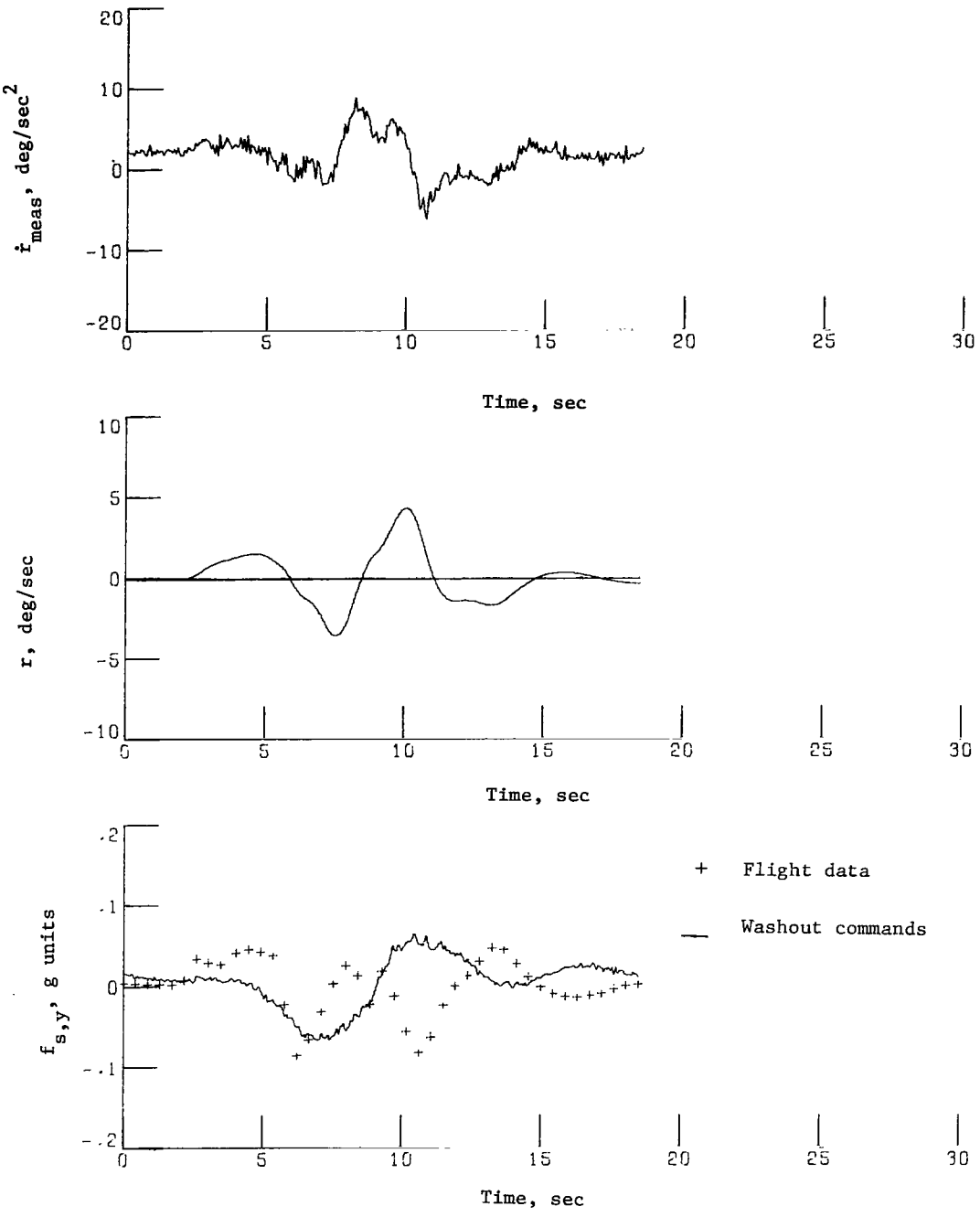

(c) Nonlinear-washout response.

Figure 11.- Concluded.

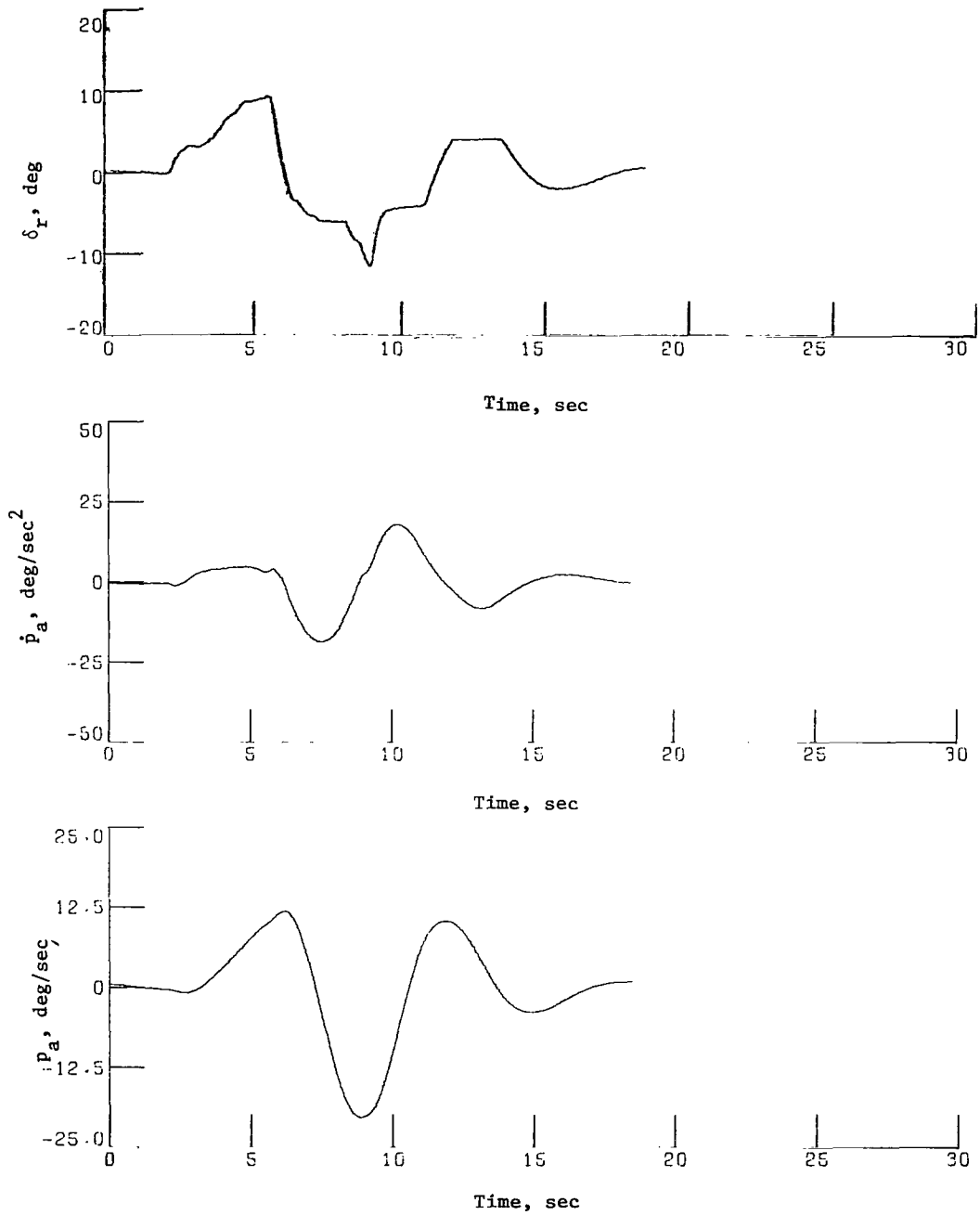

(a) 737 response without β feedback.

Figure 12.- Time histories of roll cues for rudder inputs.

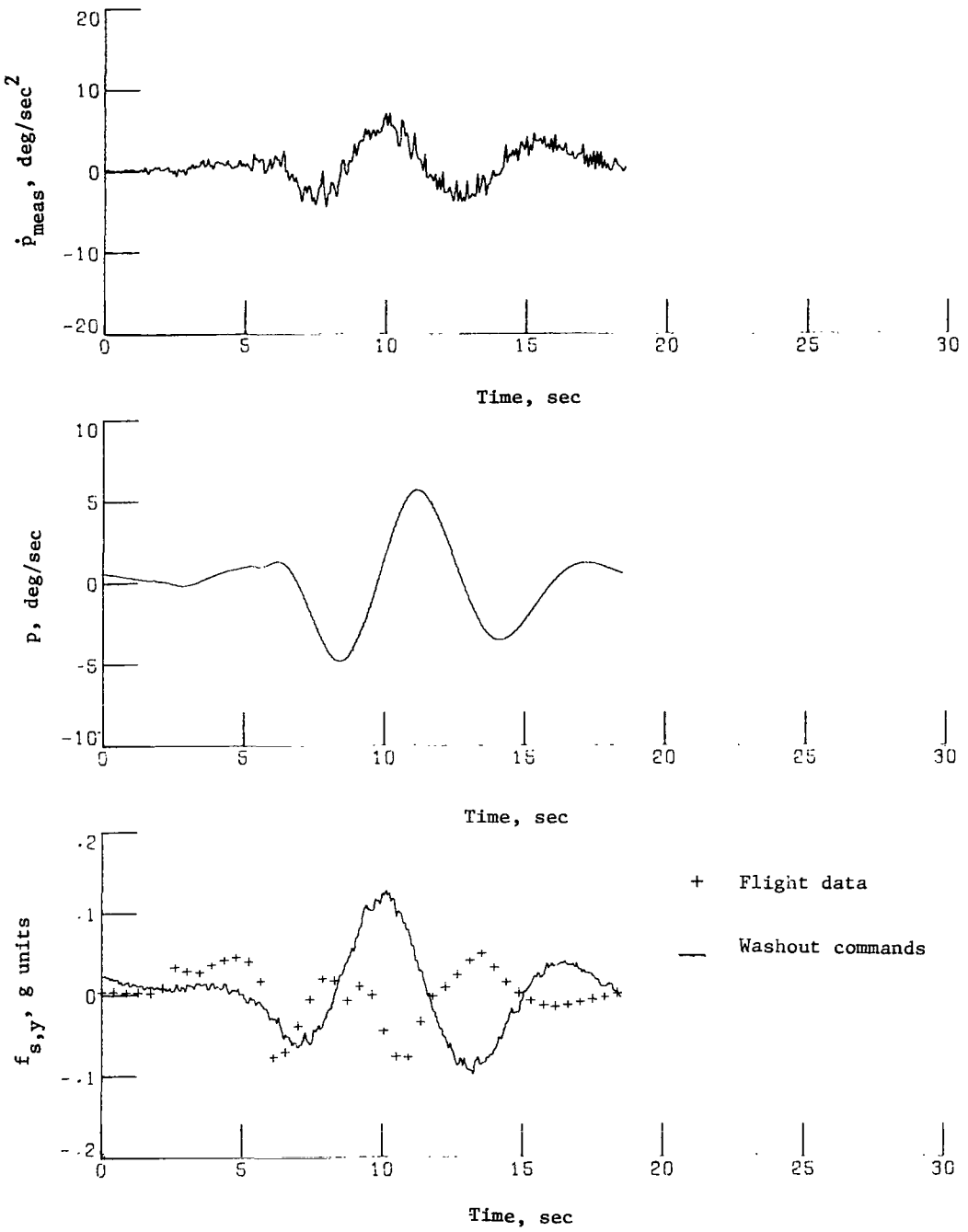

(b) Linear-washout response.

Figure 12.- Continued.

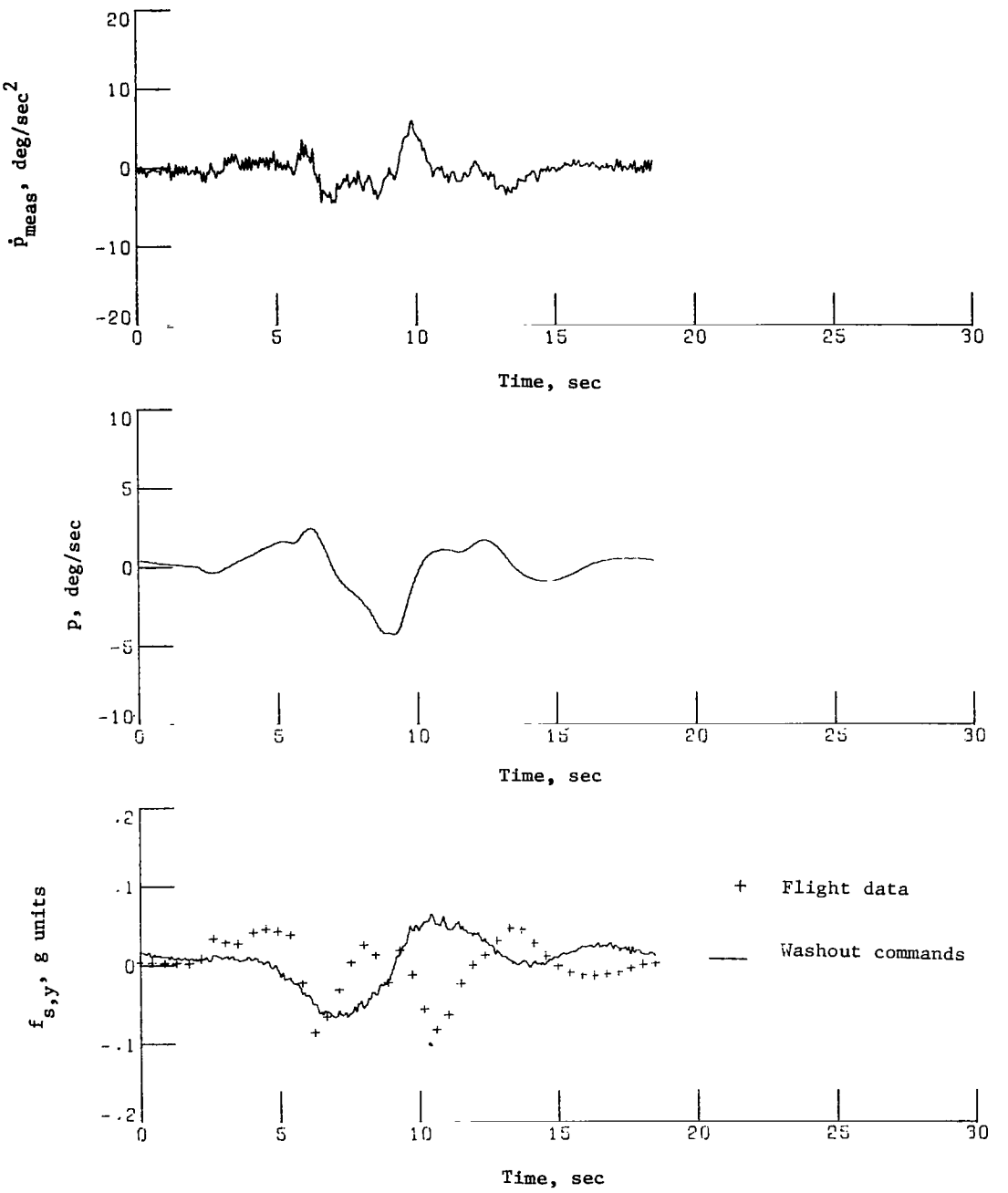

(c) Nonlinear-washout response.

Figure 12.- Concluded.

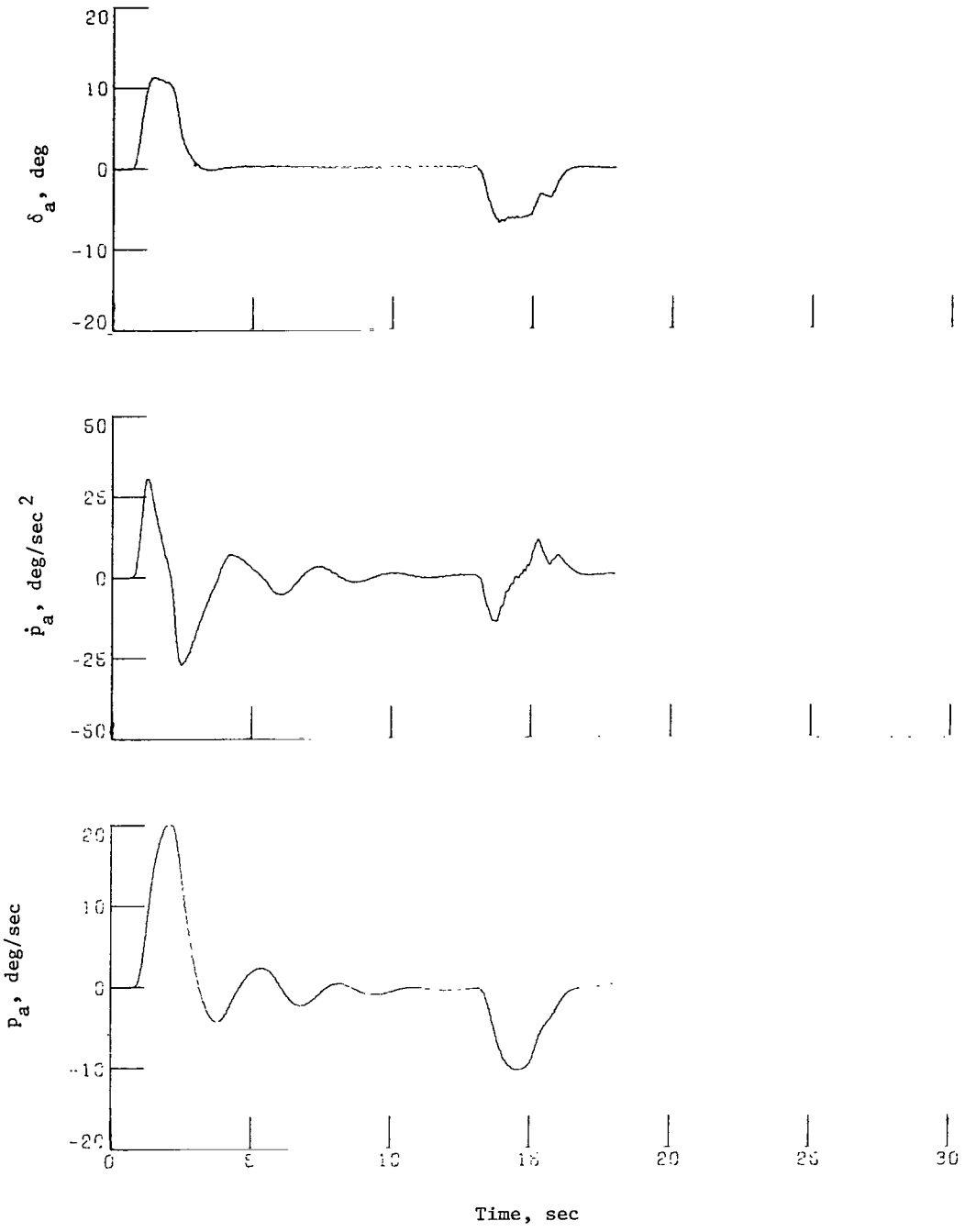

(a) 737 response.

Figure 13.- Time histories of roll cues for aileron inputs.

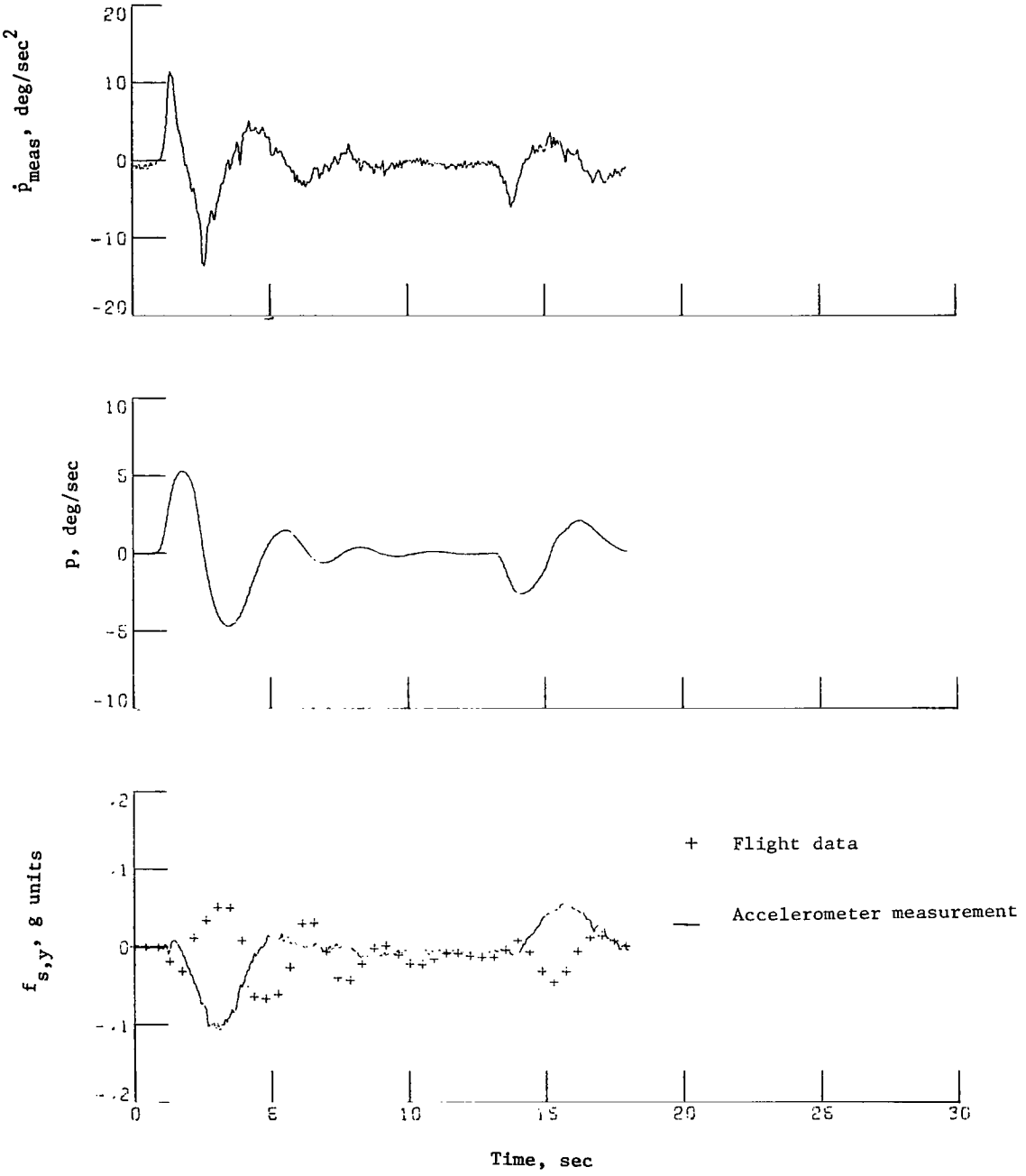

(b) Linear-washout response.

Figure 13.- Continued.

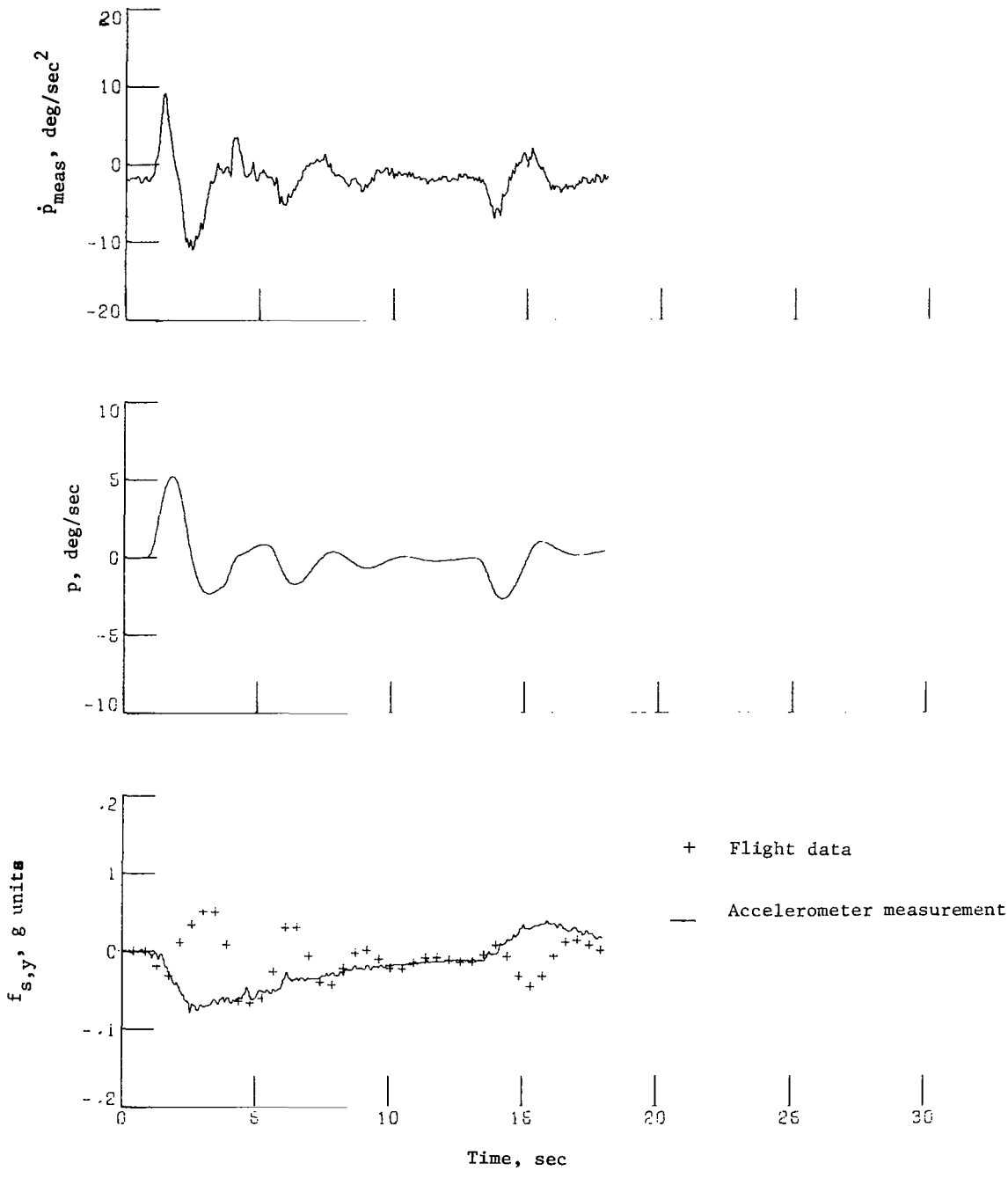

(c) Nonlinear-washout response.

Figure 13.- Concluded.

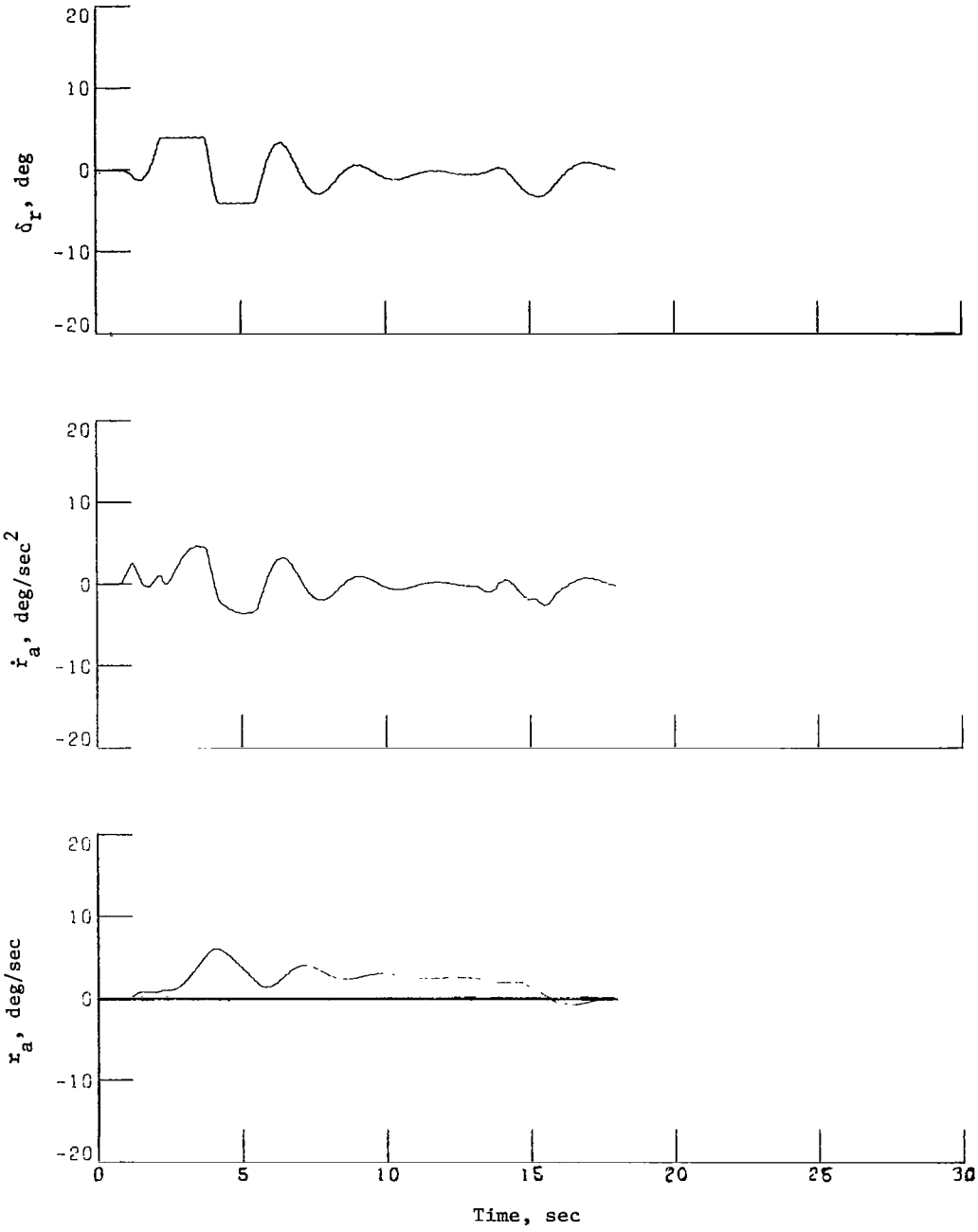

(a) 737 response.

Figure 14.- Time histories of yaw cues for aileron inputs.

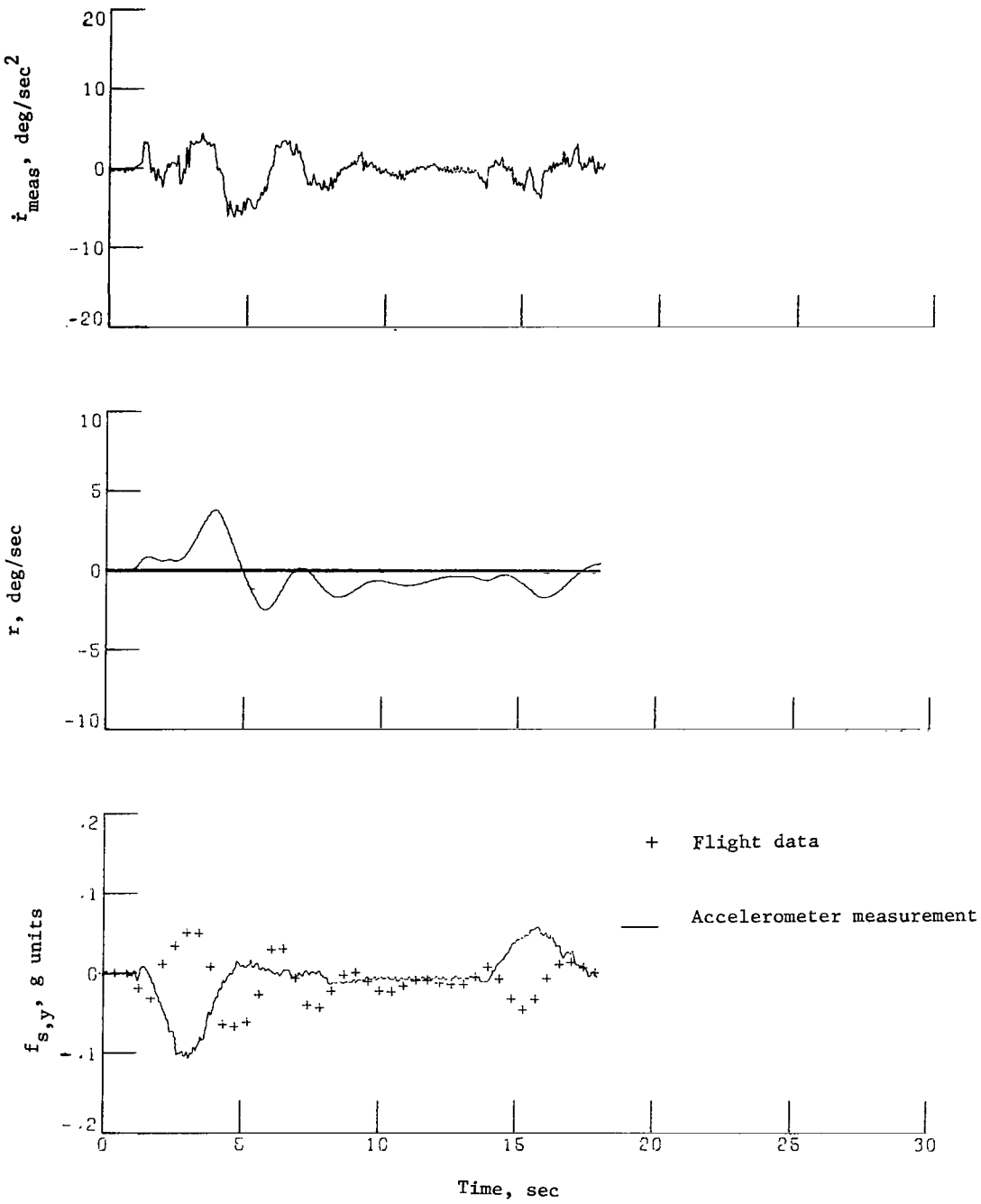

(b) Linear-washout response.

Figure 14.- Continued.

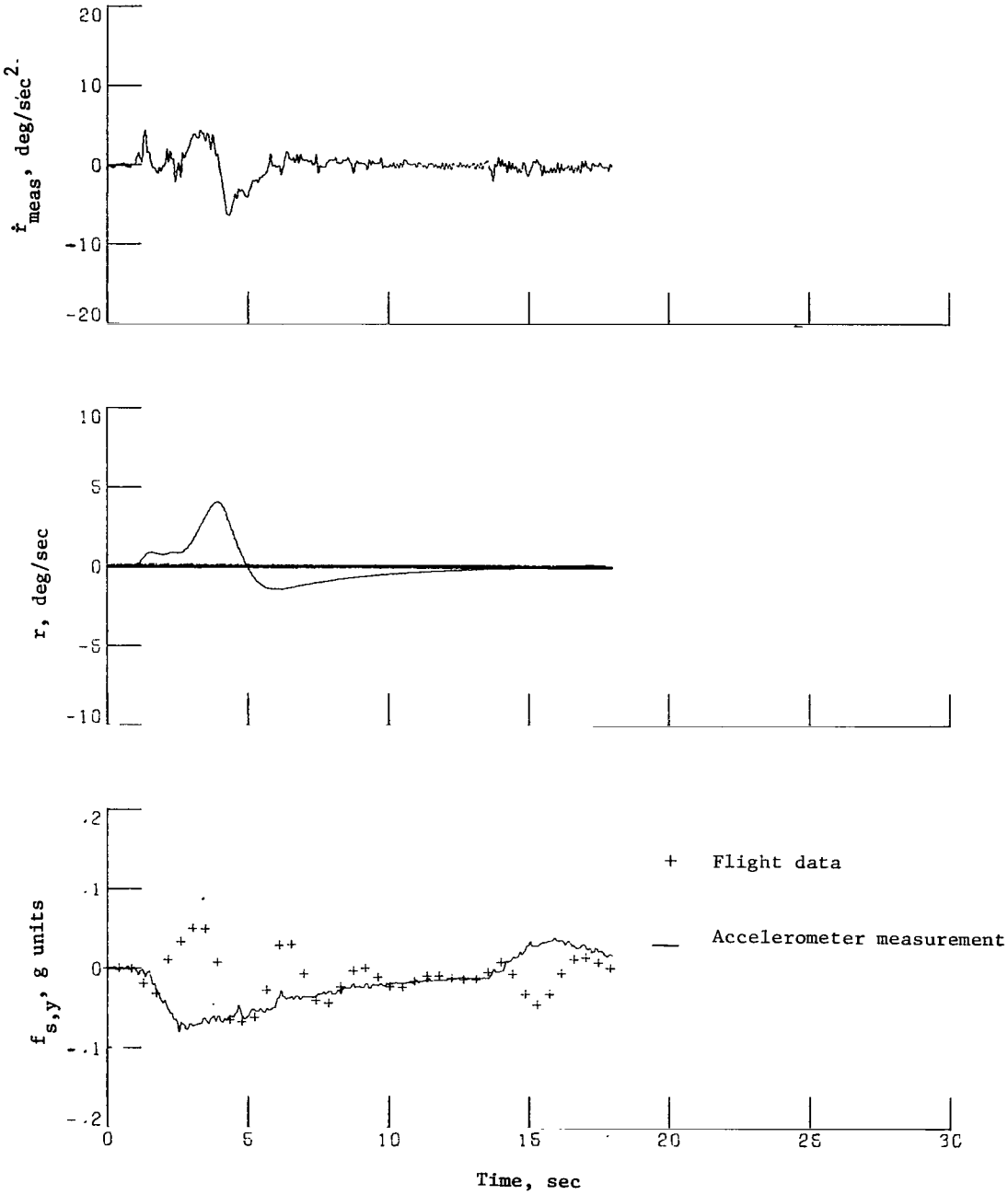

(c) Nonlinear-washout response.

Figure 14.- Concluded.

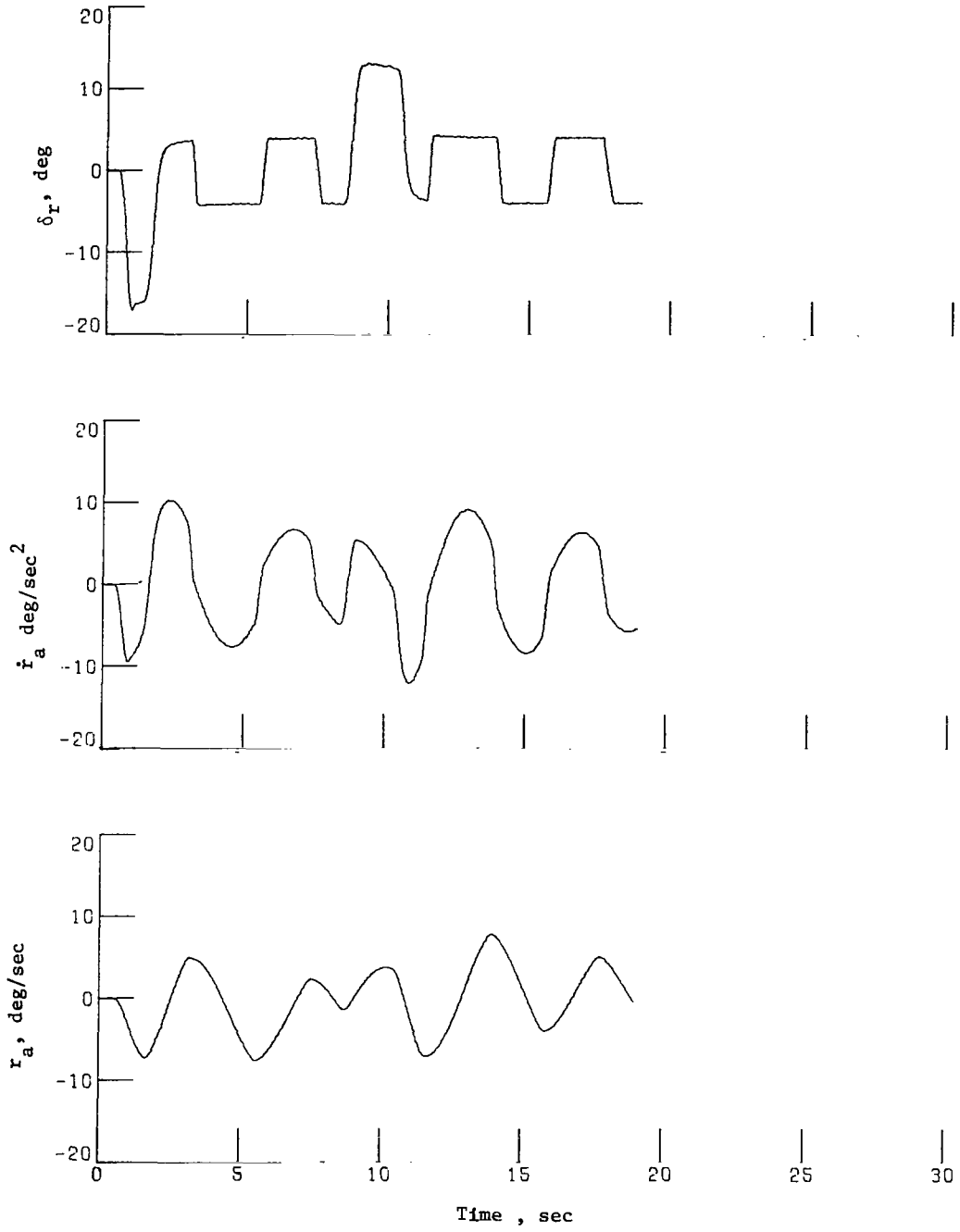

(a) 737 response.

Figure 15.- Time histories of yaw cues for rudder inputs.

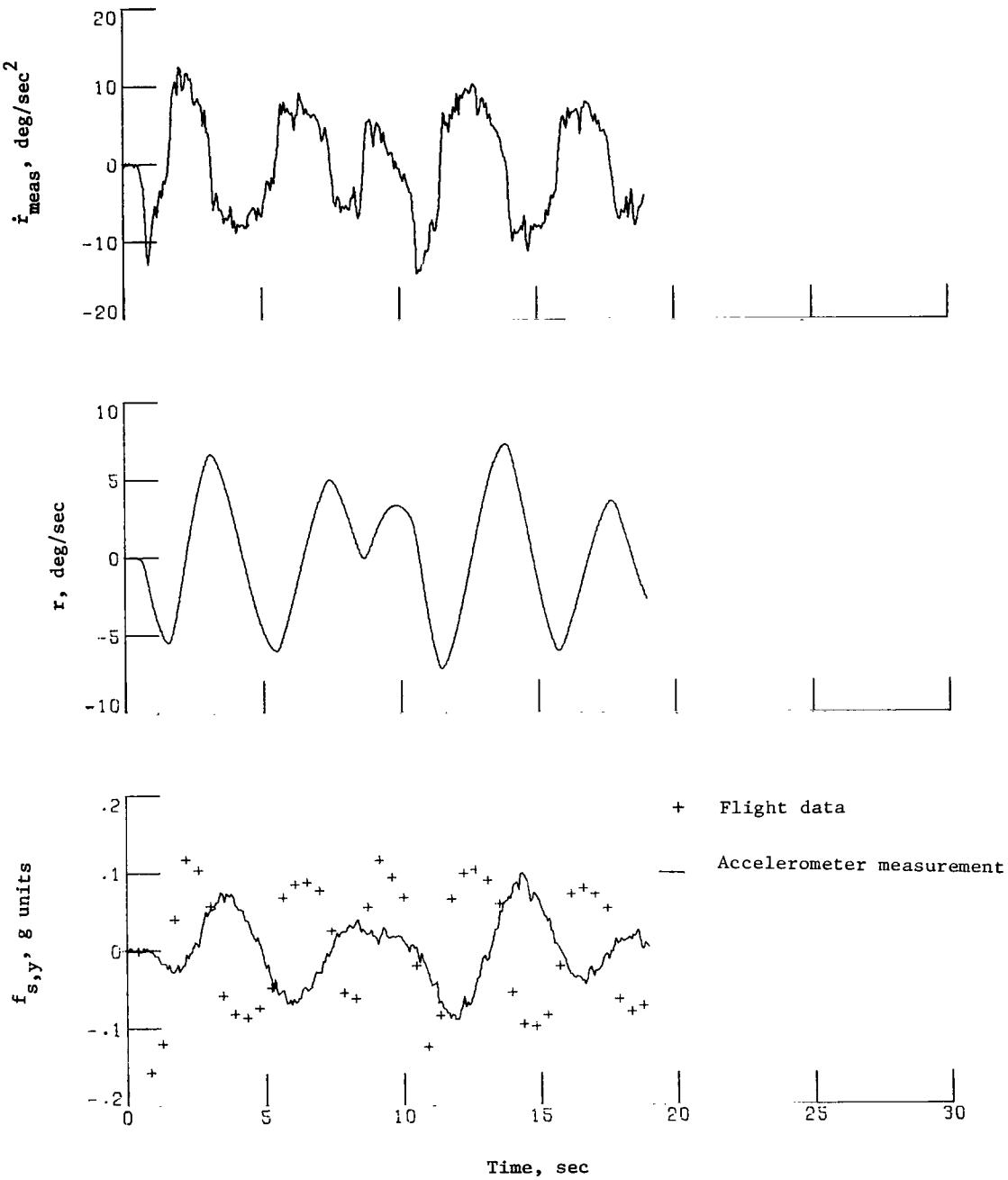

(b) Linear-washout response.

Figure 15.- Continued.

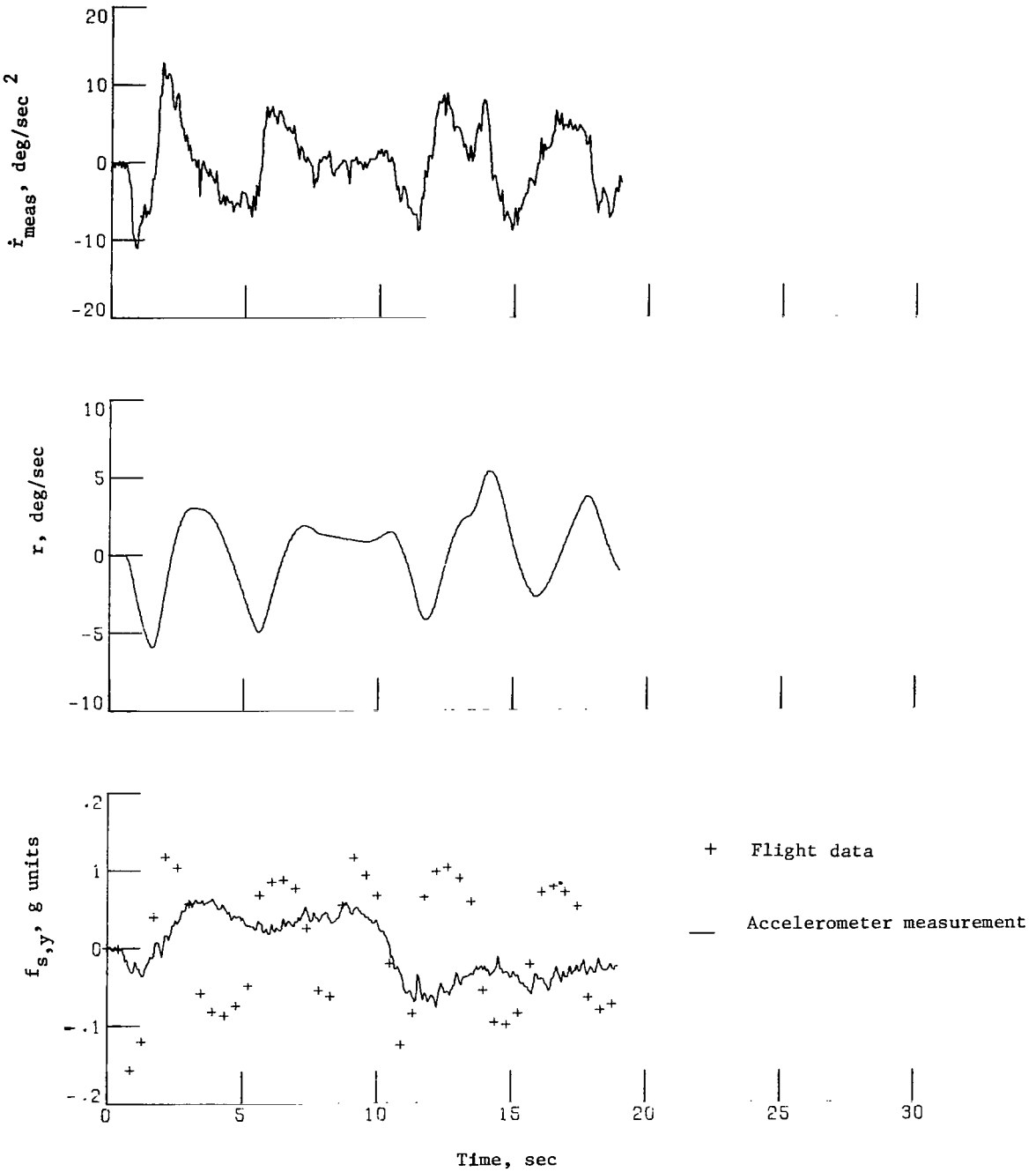

(c) Nonlinear-washout response.

Figure 15.- Concluded.

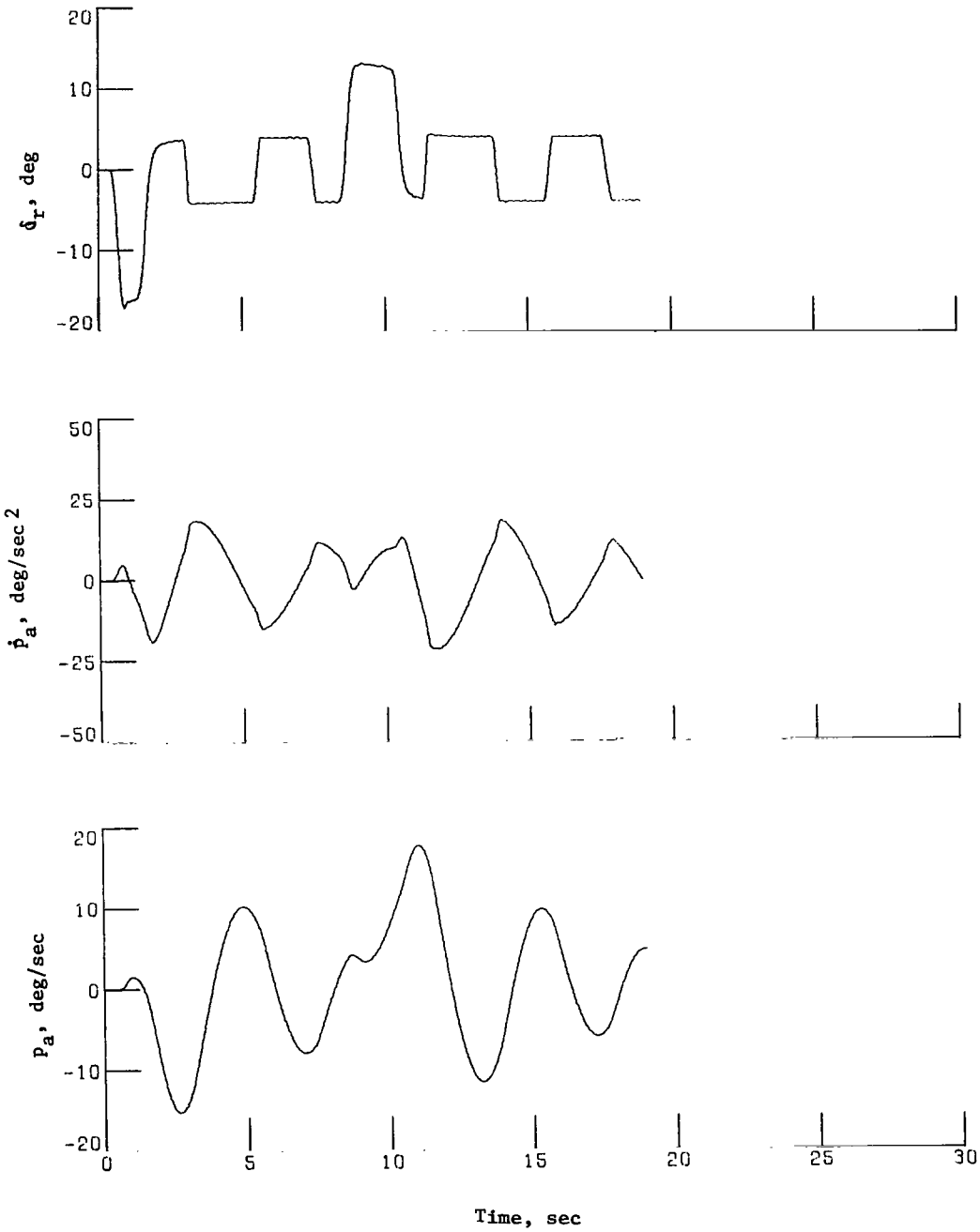

(a) 737 response.

Figure 16.- Time histories of roll cues for rudder inputs.

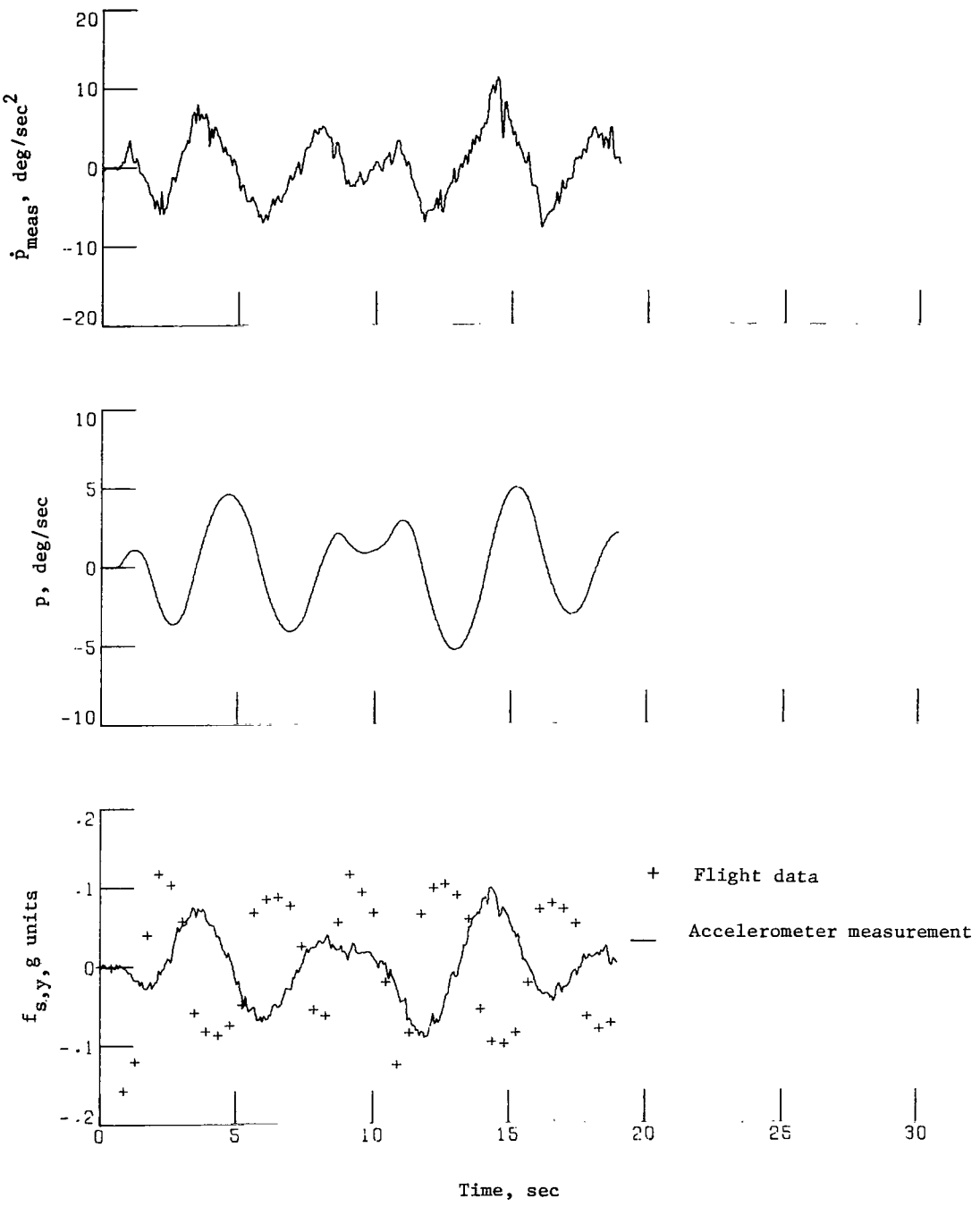

(b) Linear-washout response.

Figure 16.- Continued.

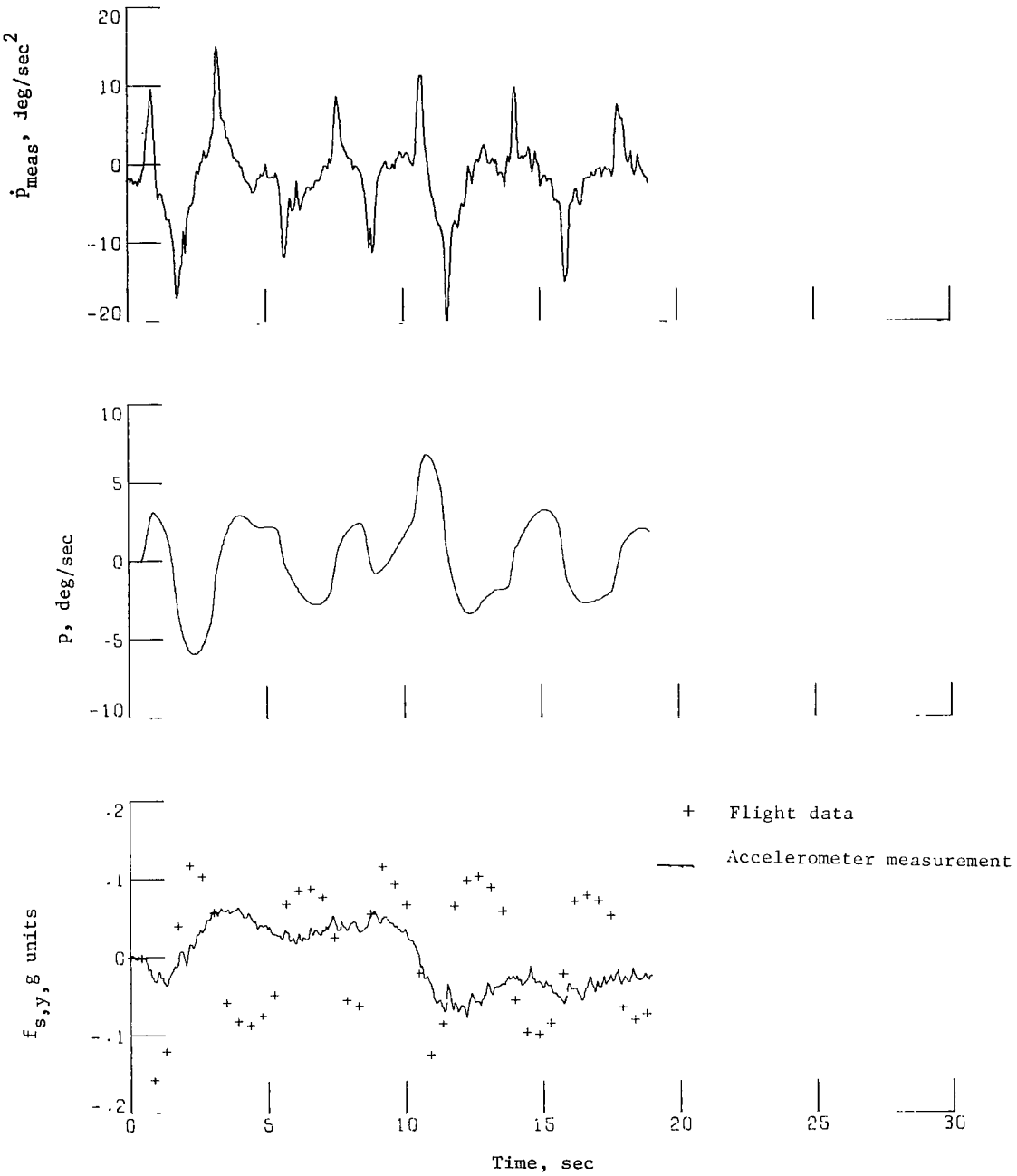

(c) Nonlinear-washout response.

Figure 16.- Concluded.

NATIONAL AERONAUTICS AND SPACE ADMINISTRATION
WASHINGTON, D.C. 20546

OFFICIAL BUSINESS
PENALTY FOR PRIVATE USE $300

SPECIAL FOURTH-CLASS RATE
BOOK

POSTAGE AND FEES PAID
NATIONAL AERONAUTICS AND
SPACE ADMINISTRATION
451

U.S.MAIL

566 001 C1 U A 760604 S00903DS
DEPT OF THE AIR FORCE
AF WEAPONS LABORATORY
ATTN: TECHNICAL LIBRARY (SUL)
KIRTLAND AFB NM 87117

If Undeliverable (Section 158
Postal Manual) Do Not Return

"The aeronautical and space activities of the United States shall be conducted so as to contribute . . . to the expansion of human knowledge of phenomena in the atmosphere and space. The Administration shall provide for the widest practicable and appropriate dissemination of information concerning its activities and the results thereof."

—NATIONAL AERONAUTICS AND SPACE ACT OF 1958

NASA SCIENTIFIC AND TECHNICAL PUBLICATIONS

TECHNICAL REPORTS: Scientific and technical information considered important, complete, and a lasting contribution to existing knowledge.

TECHNICAL NOTES: Information less broad in scope but nevertheless of importance as a contribution to existing knowledge.

TECHNICAL MEMORANDUMS: Information receiving limited distribution because of preliminary data, security classification, or other reasons. Also includes conference proceedings with either limited or unlimited distribution.

CONTRACTOR REPORTS: Scientific and technical information generated under a NASA contract or grant and considered an important contribution to existing knowledge.

TECHNICAL TRANSLATIONS: Information published in a foreign language considered to merit NASA distribution in English.

SPECIAL PUBLICATIONS: Information derived from or of value to NASA activities. Publications include final reports of major projects, monographs, data compilations, handbooks, sourcebooks, and special bibliographies.

TECHNOLOGY UTILIZATION PUBLICATIONS: Information on technology used by NASA that may be of particular interest in commercial and other non-aerospace applications. Publications include Tech Briefs, Technology Utilization Reports and Technology Surveys.

Details on the availability of these publications may be obtained from:

SCIENTIFIC AND TECHNICAL INFORMATION OFFICE

NATIONAL AERONAUTICS AND SPACE ADMINISTRATION

Washington, D.C. 20546